VOLUME 33 JANUARY 1955 NUMBER 1

Canadian Journal of Technology

Editor: G. A. LEDINGHAM

Published by THE NATIONAL RESEARCH COUNCIL
OTTAWA CANADA

CANADIAN JOURNAL OF TECHNOLOGY

(*Formerly Section F, Canadian Journal of Research*)

Under the authority of the Chairman of the Committee of the Privy Council on Scientific and Industrial Research, the National Research Council issues THE CANADIAN JOURNAL OF TECHNOLOGY and six other journals devoted to the publication of the results of original scientific research. Matters of general policy concerning these journals are the responsibility of a joint Editorial Board consisting of: members representing the National Research Council of Canada; the Editors of the Journals; and members representing the Royal Society of Canada and four other scientific societies.

The Chemical Institute of Canada has chosen the Canadian Journal of Technology and the Canadian Journal of Chemistry as its medium of publication for scientific papers.

Manuscripts for publication should be submitted to Dr. Léo Marion, Editor-in-Chief, Canadian Journal of Technology, National Research Council, Ottawa 2, Canada.
(For instructions on preparation of copy, see **Notes to Contributors** (inside back cover).)

Proof, correspondence concerning proof, and orders for reprints should be sent to the Manager, Editorial Office (Research Journals), Division of Administration, National Research Council, Ottawa 2, Canada.

Subscriptions, renewals, requests for single or back numbers, and all remittances should be sent to Division of Administration, National Research Council, Ottawa 2, Canada. Remittances should be made payable to the Receiver General of Canada, credit National Research Council.

The journals published, frequency of publication, and prices are:

Canadian Journal of Biochemistry and Physiology	Bimonthly	$3.00 a year
Canadian Journal of Botany	Bimonthly	$4.00 a year
Canadian Journal of Chemistry	Monthly	$5.00 a year
Canadian Journal of Microbiology*	Bimonthly	$3.00 a year
Canadian Journal of Physics	Monthly	$4.00 a year
Canadian Journal of Technology	Bimonthly	$3.00 a year
Canadian Journal of Zoology	Bimonthly	$3.00 a year

The price of single numbers of all journals is 75 cents.

*Volume 1 will combine three numbers published in 1954 with six published in 1955 and will be available at the regular annual subscription rate of $3.00.

Contents

Printed in Canada *by* University of Toronto Press

CANADIAN JOURNAL OF TECHNOLOGY

Notes to Contributors

Manuscripts

(i) ***General.*** Manuscripts should be typewritten, double spaced, on paper 8½×11 in. **The original and one copy are to be submitted.** Tables and captions for the figures should be placed at the end of the manuscript. Every sheet of the manuscript should be numbered.

Style, arrangement, spelling, and abbreviations should conform to the usage of this journal. Names of all simple compounds, rather than their formulas, should be used in the text. Greek letters or unusual signs should be written plainly or explained by marginal notes. Superscripts and subscripts must be legible and carefully placed.

Manuscripts should be carefully checked before they are submitted; authors will be charged for changes made in the proof that are considered excessive.

(ii) ***Abstract.*** An abstract of not more than about 200 words, indicating the scope of the work and the principal findings, is required, except in Notes.

(iii) ***References.*** References should be listed **alphabetically by authors' names,** numbered, and typed after the text. The form of the citations should be that used in this journal; in references to papers in periodicals, inclusive page numbers should be given but titles should not. All citations should be checked with the original articles and each one referred to in the text by the key number.

(iv) ***Tables.*** Tables should be numbered in roman numerals and each table referred to in the text. Titles should always be given but should be brief; column headings should be brief and descriptive matter in the tables confined to a minimum. Vertical rules should be used only when they are essential. Numerous small tables should be avoided.

Illustrations

(i) ***General.*** All figures (including each figure of the plates) should be numbered consecutively from 1 up, in arabic numerals, and each figure referred to in the text. The author's name, title of the paper, and figure number should be written in the lower left corner of the sheets on which the illustrations appear. Captions should not be written on the illustrations (see Manuscript (i)).

(ii) ***Line Drawings.*** Drawings should be carefully made with India ink on white drawing paper, blue tracing linen, or co-ordinate paper ruled in blue only; any co-ordinate lines that are to appear in the reproduction should be ruled in black ink. Paper ruled in green, yellow, or red should not be used unless it is desired to have all the co-ordinate lines show. All lines should be of sufficient thickness to reproduce well. Decimal points, periods, and stippled dots should be solid black circles large enough to be reduced if necessary. Letters and numerals should be neatly made, preferably with a stencil (**do NOT use typewriting**) and be of such size that the smallest lettering will be not less than 1 mm. high when reproduced in a cut 3 in. wide.

Many drawings are made too large; originals should not be more than 2 or 3 times the size of the desired reproduction. In large drawings or groups of drawings the ratio of height to width should conform to that of a journal page but the height should be adjusted to make allowance for the caption.

The original drawings and one set of clear copies (e.g. small photographs) are to be submitted.

(iii) ***Photographs.*** Prints should be made on glossy paper, with strong contrasts. They should be trimmed so that essential features only are shown and mounted carefully, with rubber cement, on white cardboard with no space or only a very small space (less than 1 mm.) between them. In mounting, full use of the space available should be made (to reduce the number of cuts required) and the ratio of height to width should correspond to that of a journal page (4⅛×7⅛ in.); however, allowance must be made for the captions. Photographs or groups of photographs should not be more than 2 or 3 times the size of the desired reproduction.

Photographs are to be submitted in duplicate; if they are to be reproduced in groups one set should be mounted, the duplicate set unmounted.

Reprints

A total of 50 reprints of each paper, without covers, are supplied free. Additional reprints, with or without covers, may be purchased.

Charges for reprints are based on the number of printed pages, which may be calculated approximately by multiplying by 0.6 the number of manuscript pages (double-spaced typewritten sheets, 8½×11 in.) and including the space occupied by illustrations. An additional charge is made for illustrations that appear as coated inserts. The cost per page is given on the reprint requisition which accompanies the galley.

Any reprints required in addition to those requested on the author's reprint requisition form must be ordered officially as soon as the paper has been accepted for publication.

Canadian Journal of Technology

Issued by THE NATIONAL RESEARCH COUNCIL OF CANADA

VOLUME 33 JANUARY 1955 NUMBER 1

AN AUTOMATIC RECORDING ANALYTICAL BALANCE[1]

BY E. J. CAULE[2] AND G. MCCULLY[3]

ABSTRACT

The design, construction, and operation of an automatic recording balance unit is described. The controller-recorder may be attached to an analytical balance or to any other fine balance; it requires no mechanical changes in the balance and no connections to the beam or spring. It embodies no precision fitting, but is built up of standard parts and a few parts easily made in the laboratory. The restoring force for unbalances in weight is the force between a primary coil and a short-circuited secondary coil. The sensing element for unbalance consists of the same two coils, use being made of the dependence on distance apart of their mutual inductance. The short-circuited coil hangs from the balance.

In studies conducted in this laboratory on the high temperature oxidation of various steels in oxygen, an automatic recording balance became necessary. To record curves of weight-gain versus time, manual weighing with an ordinary analytical balance had to be performed at least every 20 min. for 24 hr. a day for several weeks, since the oxidation could not be interrupted or limited to the normal working hours of the day. The tedium and high cost of such a schedule led to the development of the recording balance described below.

Several recording balances based on analytical balances have been described in the scientific literature (1, 2, 6), but they have the obvious disadvantage of requiring extensive alterations to an analytical balance or the complete building of a balance. The plan adopted here was to find a balancing and recording system that could be attached quickly and easily to any analytical balance without ruining the balance for future use in the ordinary manner, that required no precision parts and could be built from stock parts, and that was electrical rather than optical or mechanical in the character of its sensing and restoring functions. A further aim was to make the automatic device attachable to balances of types other than analytical, such as spring and torsion balances. With the idea in mind that a battery of several or many steel-testing furnaces might be needed in the future, the balance was designed to indicate at a remote central station.

[1]*Manuscript received July 27, 1954.*
Contribution from the Division of Applied Chemistry, National Research Council, Ottawa, Canada. Issued as N.R.C. No. 3440.

[2]*Division of Applied Chemistry, N.R.C.*
[3]*Army Section, Division of Radio and Electrical Engineering—presently with Communications Branch, Division of Radio and Electrical Engineering, N.R.C.*

The system finally built fulfilled all the requirements listed above. It was composed mainly of standard electronic circuits of simple design, with the addition of several easily made parts.

There are two main principles involved in the operation of the instrument described here:

(1) A torque about the fulcrum of a standard balance due to a change in weight is counteracted by a torque due to the repulsion between two coils, one of which is fixed in position on the floor of the balance case and is supplied with 700 cycle power, while the other is hung from the balance arm immediately above the first coil and is short-circuited. By Lenz's Law the primary current and induced current are repulsive.

(2) The value of the mutual inductance between the two coils is used as an indication of distance between the coils and thus as a means of obtaining an indication of change of tilt of the balance corresponding to change in weight.

The apparatus embodying these two principles is a balanced a-c. bridge having the fixed coil in one arm; a change of position of the "floating" coil creates an unbalance signal across the bridge which after amplification is used to increase or, alternatively, decrease the power in the bridge circuit, thereby tending to restore balance. A small amount of power from a secondary winding of the power transformer supplying the bridge is rectified and used to activate a recorder. Thus, a record of current as a function of time is obtained which can be translated into a record of weight change versus time. The first principle has been used by Hodsman and Brooke (5) in the design of a manually operated "electromagnetic weight loader" to dispense with the use of milligram weights and riders. The second is used in many commercial instruments of various types which embody transducers.

A third feature of the present automatic balance is the "anti-hunting" arrangement used. The period of most balances is between 15 and 20 sec., while in comparison the time of response of most electrical circuits is practically zero. Consequently in the first models made, which had no "anti-hunting" system, the balance reached a state of steady "hunt" of about 4 mgm. amplitude. This condition was eliminated in the following manner. For a given increase in weight and thus a given momentary unbalance in the bridge, the restoring force is applied, not all at once, but rather, in small increments six seconds apart in time. A multivibrator trips a ratchet relay geared to a "helipot" resistor controlling the amplitude of the current supplied to the coils. Thus the current is increased in small steps corresponding to one gear-tooth at intervals separated by the period of the multivibrator. By changing series resistors, the amount of control the "helipot" exerts on the current can be varied and thus the size of the current steps can be increased or diminished. The state of balance is restored in small steps so gently that, probably because of the friction of the central knife-edge, there is very little "hunting" about any of the temporary rest-points thus obtained on the way to the zero-point.

Fig. 1 is a block diagram which illustrates the general features described so far. The phase discriminator distinguishes between mutual approach and

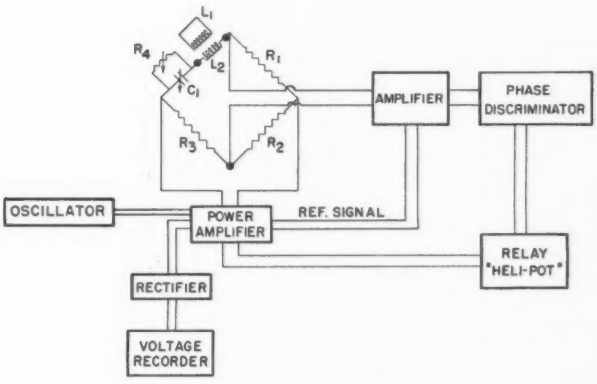

FIG. 1. Block diagram of complete circuit.

recession of the coils. It uses the fact that there is a difference in phase of 180° between the unbalance signals from the bridge for two different causes of unbalance. The phase difference is established by comparison of the unbalance signal with a constant reference voltage obtained from the power supply; the comparison is done by geometrical addition of the unbalance and reference voltages in a single tube.

The ratchet relay, of course, turns the "helipot" in only one direction; the balance thus takes care of only increases in weight or, alternatively, decreases. In the use for which the balance was planned, the oxidation of steel, only increases are found and so the unidirectional character is not a drawback; if both increases and decreases were expected an appropriate doubling of certain circuit elements could be easily made. In the present model the phase discriminator is so arranged that for approach of the coils to each other the error and reference signals are in phase and the voltages add directly. The resultant combined voltage, if above a certain level, adds to the multivibrator pulse to actuate the ratchet relay.

DETAILS OF CONSTRUCTION

The position of the coils with respect to the balance and load is shown in Fig. 2. The coils are of number 24 Formex covered copper wire. Their diameter is 10 cm. and their length along the axis 19 mm. for the bottom coil and 3 mm. for the top coil. The distance between the top edge of the lower coil and the bottom edge of the upper coil is usually 6 mm.; the spacing is not critical. The lower coil has a pyrex glass ring as a former and has seven layers of 25 turns each. The upper coil was wound on a glass former which, to save weight, was removed after the coil had been well "doped" with polystyrene cement; it has four layers of eight turns each. The two ends of the upper coil are soldered together. A simple copper tripod supports the short-circuited coil and between the tripod and the terminal knife-edge there is an aluminum counterweight of

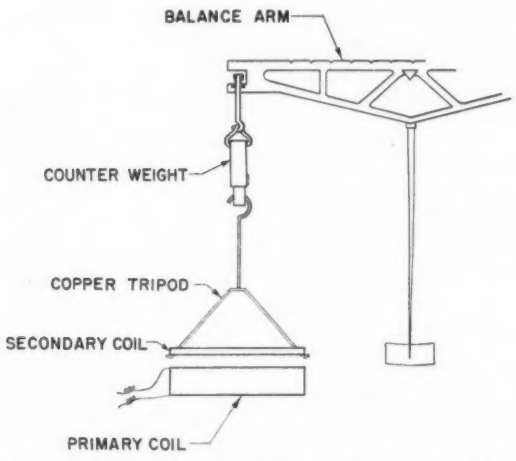

FIG. 2. Sketch showing arrangement of coils and support from balance arm.

slightly adjustable length. The lower coil is held in position on the floor of the balance case by a few strips of masking tape. A two-conductor Amphenol microphone connector is used to bring the leads to the lower coil through the wood of the balance case.

Figs. 3 and 4 show the details of the circuits suggested in Fig. 1. There are no unusual systems present and the components are all standard with the exception of the ratchet relay which was removed from some war surplus equipment and modified to suit the present need. It has a 24 v. d-c. coil of about 15 ohms resistance; the ratchet wheel has about 57 teeth. The modification consisted of introducing a small differential gear between the output shaft of the relay and the helipot gain control; the differential is connected to a handwheel on the panel front to allow the helipot to be reset to its original position when it has reached the end of its range. The differential gear system has another possible advantage; it offers a means of allowing two ratchet relays to operate the helipot, working in opposite directions, if it is desired to make the balance responsive to both positive and negative weight changes as explained above.

The bridge requires care in construction, since shielding is necessary as explained by Ferguson (4), whose principles were followed here. In the first model constructed the resistances were made in the laboratory and were quite satisfactory. They were wound bifilarly on bakelite cylinders, waxed, and suspended in tin cans as shields. A model constructed recently uses a bridge whose shielded components were bought from General Radio Corporation.

For all testing described below, the balance used was a Christian Becker Chainomatic balance. The recorder was a Leeds and Northrup Speedomax four-channel recorder with a chart speed of one inch per hour and a maximum scale reading of 100 mv.

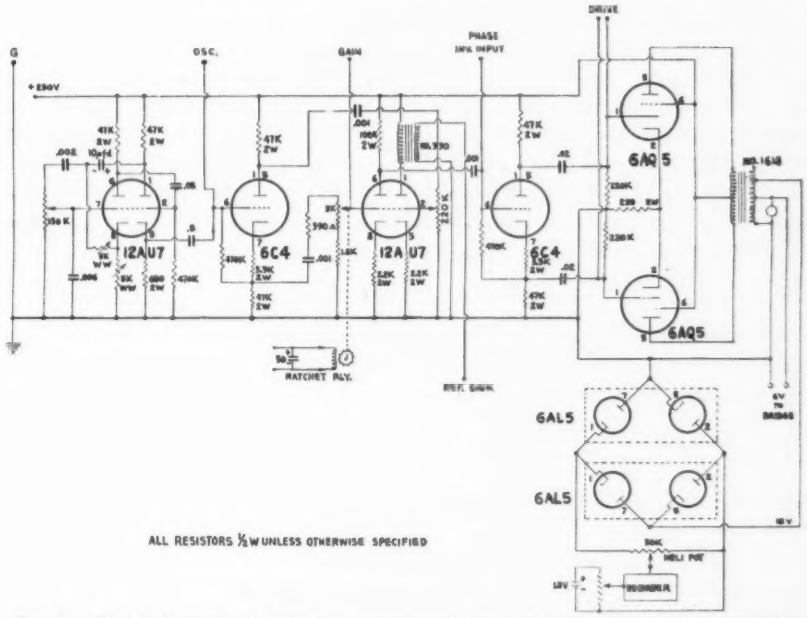

FIG. 3. Circuit diagram of oscillator, power amplifier, rectifier, and connections to bridge and recorder.

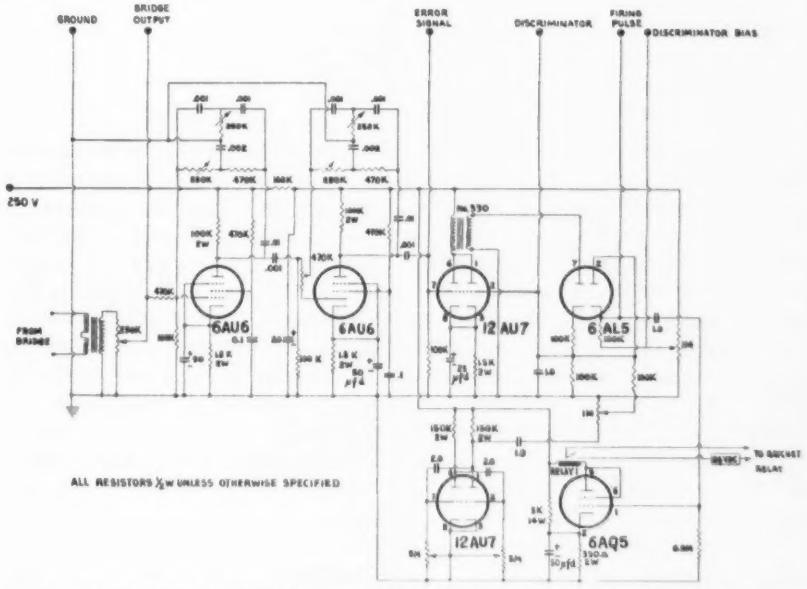

FIG. 4. Circuit diagram of tuned amplifier, phase discriminator, and multivibrator sections.

It is convenient at this point to explain that the balance was never operated below a certain minimum power level, below which the sensitivity would be too small to be useful. To avoid wasting chart space on this minimum voltage (which is essentially an additive constant to the varying voltage) an arrangement of a potentiometer resistor and a battery was put in the input line to the recorder by which the minimum voltage could be "bucked out". At the same time a pair of potentiometers was so arranged that the total range of voltage recorded by the Speedomax could be contracted or expanded as desired. These circuit elements are shown in Fig. 3.

THEORY AND PERFORMANCE

An expression for the force between two coils, one short-circuited as here, has been derived by Dr. A. F. Dunn of the Applied Physics Branch, Division of Physics, N.R.C. (3). It is:

$$[1] \qquad F = \left[M(m_2 - m_1) \frac{N_h}{Y_h} \cdot \frac{1}{L_c} \cdot \frac{1}{1+(R_c/\omega L_c)^2} \right] I^2$$

where the symbols have the following meanings:

F = force between coils,
M = mutual inductance between the coils,
m_2 = mutual inductance between smaller coil and end turn of helix,
m_1 = mutual inductance between smaller coil and other end turn of helix,
N_h = total number of turns in the helix,
Y_h = length of helix,
L_c = inductance of the short-circuited coil,
R_c = resistance of the short-circuited coil,
I = current flowing in the helix,
ω = frequency of the current in the helix.

This equation is useful as a guide to the design and operation of the apparatus. It is obvious that to get the maximum force with a given current, the expression in square brackets must be made as large as possible. Limitations on this aim are set by the necessity of getting a large unbalance signal from the bridge for a given slight movement in the relative position of the coils and also by the limitations of space in the balance case. These latter two considerations actually dictated the dimensions and the flat form of the coils; the design of the coils was thus largely on an experimental basis. The wire size, and thus the number of turns in the coils, was chosen for convenience in forming, for avoidance of heating effects, and for lightness in weight.

The variation of mutual inductance with relative position of the coils is shown in the first graph, Fig. 5. Since a given movement of the coils could be interpreted as a given weight change, it was possible to calculate the required sensitivity of the bridge from the required sensitivity of weight. Once the precision demanded of the bridge had been set, the amplification of the unbalance signal necessary to actuate the controller could be fixed. These steps were followed from data like those shown in Fig. 4.

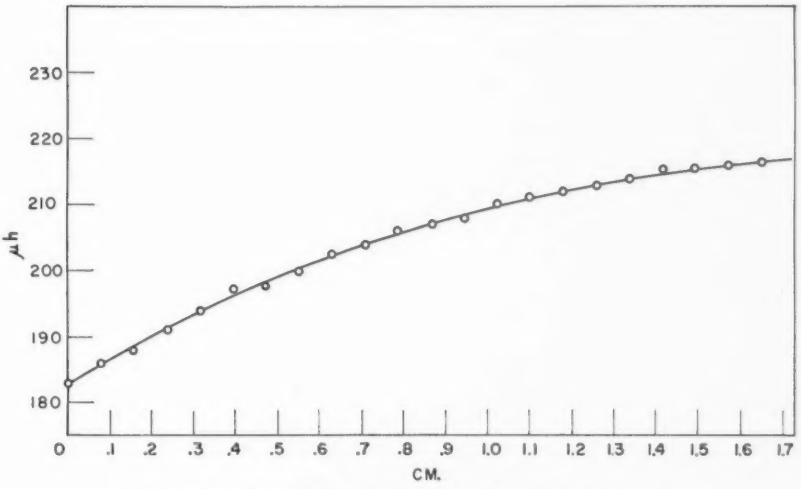

FIG. 5. Plot of mutual inductance versus distance between coils.

From the equation [1] shown above it can be seen that the effect of frequency is quite important. If the various other quantities in the equation are considered as constants, [1] can be reduced to:

$$[2] \qquad F = \frac{A}{B+(1/\omega^2)} \cdot I^2.$$

This equation can be transposed to this form:

$$[3] \qquad \frac{B+(1/\omega^2)}{A} = \frac{I^2}{F}.$$

The relationship between ω and I for a fixed value of force between the coils is seen to be complicated, but can be reviewed simply at a few points. As the frequency goes to zero, the current assumes very large values. As the frequency rises, the value of I drops. At high values of frequency, the current required takes on a constant value such that $I^2/F = B/A$.

The equation was tested experimentally as shown in Fig. 6 for a set of coils which were attached to a balance but were not provided with automatic control; instead, current from a signal generator whose frequency could be varied was applied to offset a given weight unbalance and the necessary voltage, rather than current, was read at various frequencies. The noticeable feature is the upswing in the experimental curve at higher values of frequency. This is probably due to the fact that the impedance of the circuit rises as the frequency increases, and consequently with a nearly constant current, the voltage rises. In any event it is clear that at the bottom of the dip in the curve, the force between coils is quite insensitive to frequency. It must also be noted that the values of A and B in equations [2] and [3] are quite dependent on the construction and material of the coils.

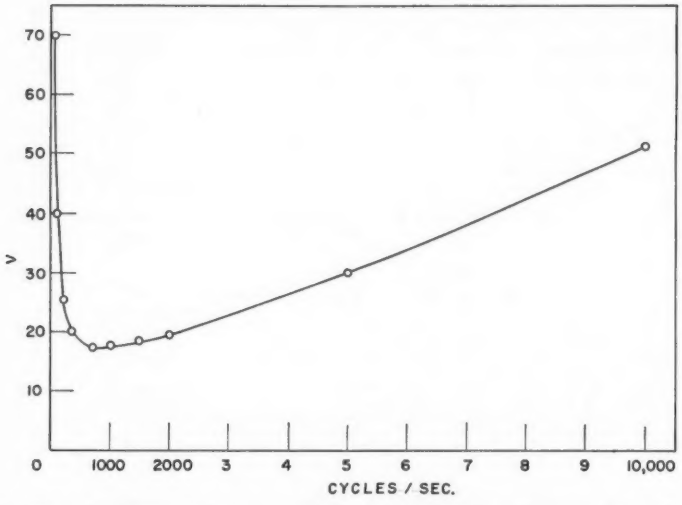

FIG. 6. Plot of voltage necessary to produce a force of 20 mgm. between test coils versus frequency.

The second major feature of equation [1] to be noted is that the force varies with the square of the current through the primary coil. The applicability of this law was tested by direct measurement of force and current. Fig. 7 shows a calibration curve taken from the chart record of the completely automatic instrument, which was allowed to balance itself at various loads applied by means of the chain of the Chainomatic balance. The plot of force against current squared is quite precisely linear. It is obvious that the line cannot in practice go through the origin of both axes since weight increments are measured from some point at which current is already flowing through the coils; with no current flowing the sensitivity would be zero. Thus the origin of weight is in this graph quite arbitrary.

The deviations from the line are an empirical measure of the sensitivity of the whole arrangement. The plot is the best line drawn by inspection of the points; the average deviation, without regard to sign, of the points is about $\frac{3}{4}$ mgm. The widest range used of weight increment corresponding to the whole range of the ratchet operated helipot was about 130 mgm., but the more usual range was, as shown here, 100 mgm.; the range could be contracted to as little as 20 mgm. At the same time the full scale of the recorder could always be used by means of the pair of potentiometers mentioned above which expand or contract the signal to the recorder. The use of ranges greater than 100 mgm. led to a great loss in sensitivity.

It has been found that the main limitation on sensitivity is neither the sensitivity of the bridge circuit, the stability of the amplifier, nor the resolution of the recorder, but is inherent in the use of the coils. A balance ordinarily swings in a gravitational field which is constant in the vertical direction; the restoring moment is due to the center of gravity which acquires a moment of

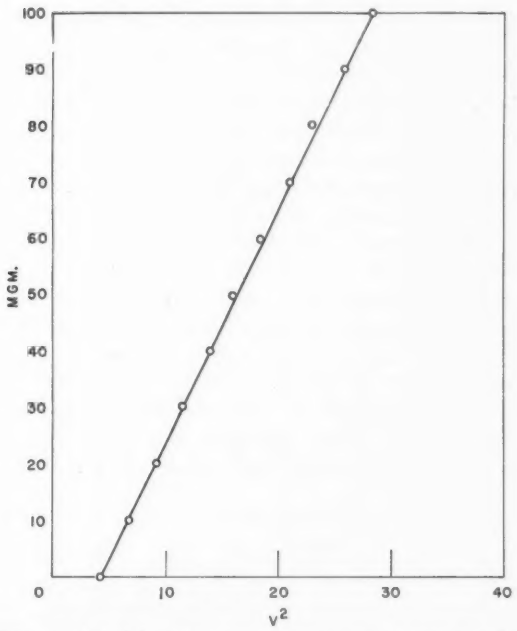

FIG. 7. Plot of force in mgm. versus square of output voltage.

force nearly linear in the distance either one of the pans is displaced. The short-circuited coil, however, is swinging in a strong magnetic field, and when it increases in weight moves into a yet stronger field. Thus its restoring moment adds to the restoring moment of the center of gravity. The balance thus loses sensitivity, because of lack of a homogeneous magnetic field about the power coil. This loss of sensitivity is shown in Fig. 8, where the number of divisions

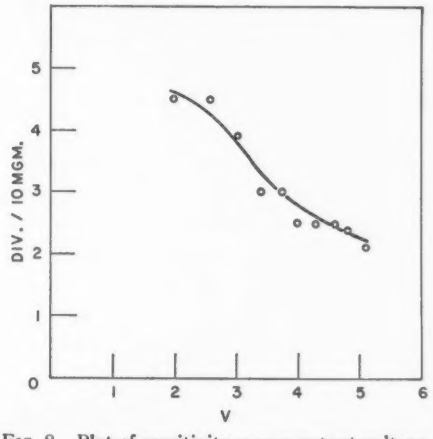

FIG. 8. Plot of sensitivity versus output voltage.

per milligram on the engraved scale on the analytical balance is plotted against the voltage applied across the coil. It could be offset, if desired, by increasing the bridge sensitivity.

As explained before, the speed of response of the controller has been deliberately kept low in order to avoid hunt. With the present period of six seconds between multivibrator pulses and with each step of the ratchet corresponding to, say, $\frac{2}{3}$ mgm., according to the range being used, the controller will follow exactly weight changes occurring at the rate of 1 mgm./9 sec. or 7 mgm./min. With appropriate changes in pulse rate and step size faster rates could undoubtedly be followed.

The stability of the recorder trace is to a large extent dependent on the avoidance of heat effects in the electronic equipment by the use of heavy-duty resistors in critical places, and on the good control to $\pm\frac{1}{2}$ v. of the 110 v. supply.

To test its performance after various calibrations the automatic balance was used to record the progress of several physical and chemical reactions which are accompanied by weight changes. One of these is shown in Fig. 9 to illustrate a typical use of the instrument. About one gram of calcium chloride

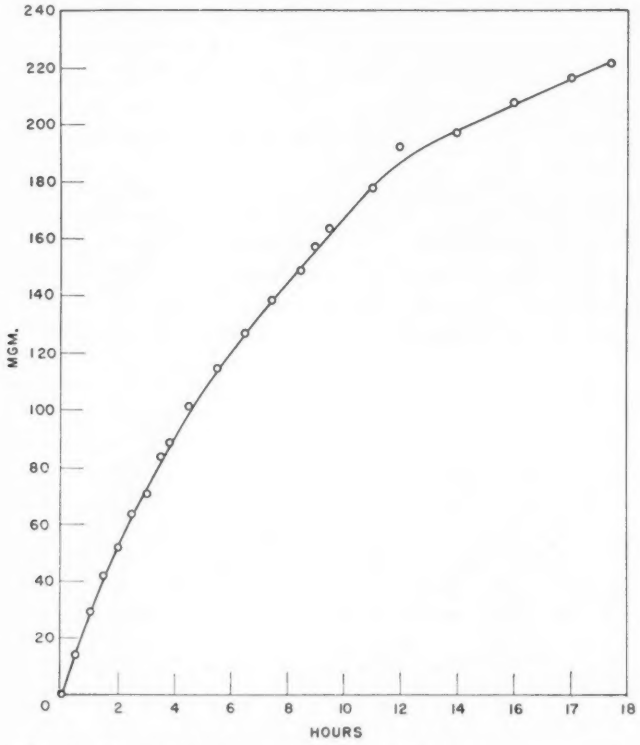

FIG. 9. Plot of weight increase of 1 gm. $CaCl_2$ crystals versus time.

granules was suspended from the balance on a watch glass. As the calcium chloride deliquesced the balance recorded the uptake of moisture. The total time of the experiment was about 20 hr. The experiment was crude since there was no control over the vapor pressure of water in the atmosphere.

Finally, the instrument was used in the work for which it was designed, the measurement of the oxidation rate of stainless steels. The experiments in this project last three weeks or more and consist sometimes of "dormant" periods of several days of no weight gain, followed by a half hour "burst" of very fast weight gained, followed again by a dormant period, and so on. The balance very satisfactorily meets the requirements of the project.

ACKNOWLEDGMENTS

The authors wish to express their thanks for co-operation and help to Mr. W. Brown of the Division of Electrical Engineering and Dr. A. F. Dunn of the Applied Physics Branch, Division of Physics, National Research Council, Ottawa. In particular, they would like to thank Mr. J. K. Waterman of the Division of Applied Chemistry, National Research Council, Ottawa, for aid in the design of circuits and for construction of the first and refinement of the second model.

REFERENCES

1. CHEVENARD, P., WACHE, X., and DE LA TULLAYE, R. Bull. soc. chim. France, 10: 41. 1944.
2. COUTTS, J. R. H., CROWTHER, E. M., KEEN, B. A., and ODEN, S. Proc. Roy. Soc. (London), A, 106: 33. 1924.
3. DUNN, A. F. Applied Physics Branch, Division of Physics, N.R.C. Private communication.
4. FERGUSON, J. G. Bell System Tech. J. 8: 560. 1929.
5. HODSMAN, G. F. and BROOKE, E. R. J. Sci. Instr. 28: 348. 1951.
6. VIEWEG, R. and GAST, T. Kunststoffe ver. Kunststoff-Tech. u.-Anwend. 34: 117. 1944.

AVERAGE INSOLATION IN CANADA DURING CLOUDLESS DAYS[1]

By C. L. Mateer[2]

ABSTRACT

Charts of the estimated insolation received in various parts of Canada on cloudless days have been prepared for the 15th day of each month, following the method used by Fritz in preparing such charts for the continental United States. In December, the charts show a strong latitudinal gradient of cloudless day insolation, with values ranging from about 150 langleys per day along the southern border to zero in the region of the polar night. In June, however, the amount of cloudless day insolation is about 750 langleys per day over most of Canada with lower values in regions of high atmospheric pollution and higher values in regions of greater elevation.

1. INTRODUCTION

The insolation[3] received each month in various parts of Canada is of interest to agricultural, engineering, meteorological, and other groups. For example, specific uses of insolation data include: studies of crop response to insolation and other meteorological factors; evaporation of water in irrigation and hydroelectric projects; design of outdoor artificial ice rinks; and maximum temperature forecasting. As a first step in the evaluation of the average insolation for all days, the present paper reports on the construction of charts of the estimated insolation on cloudless days. Preparation of charts of the average insolation, all days included, is now under way.

Charts of the average insolation over the United States on cloudless days have been prepared by Kimball (6) and Fritz (2). Because insolation data from the very limited number of solar radiation stations are insufficient for the direct construction of charts covering large geographical areas, the observed data are supplemented by computations based on the amount of water vapor present in the atmosphere. Although the method used here is very similar to that used by Fritz, it is described in some detail because of certain deviations from the Fritz technique.

2. COMPUTATIONS OF CLOUDLESS DAY INSOLATION

Fritz combined the equations of Klein (8) for radiation received on a horizontal surface and the atmospheric transmission values presented by Kimball (7) to construct an auxiliary chart which could be used to obtain the insolation at any given time and place. The basic equation (from Klein's work) used in the construction of this auxiliary chart was

$$[1] \qquad Q_m = [1.94 \,.\, (r_0/r)^2 \,.\, \cos\theta \,.\, (a''_m + 0.5 - 0.5a'_m)] - D_m$$

[1]*Manuscript received September 17, 1954.*
Contribution from Department of Transport, Canada, published by permission of the Controller of Meteorological Services.
[2]*Research Section, Meteorological Division, 315 Bloor Street West, Toronto 5, Ontario.*
[3]*Insolation is defined as the* incoming solar radiation *incident on a horizontal surface. This includes both the direct solar and the diffuse sky radiation.*

where

Q_m = insolation in langleys[4] per minute,
r_0 = mean distance between earth and sun,
r = actual distance between earth and sun,
θ = zenith angle of sun,
a'_m = fraction of solar energy transmitted through the moist, clean atmosphere considering depletion by scattering only,
a''_m = fraction of energy transmitted through the same atmosphere considering both scattering and absorption,
D_m = term including miscellaneous residual factors such as dust depletion, effect of ground reflection, etc.

The subscript "m" means that the symbol has a particular value for each optical "air mass" (where optical "air mass" is the path of light through the atmosphere referred to the vertical path as unity). The factor 1.94 is the solar constant in ly. per min.

At sea level, the air mass (m_s) is very nearly equal to sec θ for $\theta \leqslant 80°$. At a place where the pressure is p atmospheres, the air mass (m_p) is

[2] $$m_p = p\, m_s = p \sec \theta = p/\cos \theta.$$

Substituting from equation [2] for cos θ in equation [1],

[3] $$Q_m = [(r_0/r)^2 \cdot p \cdot F'_m] - D_m$$

where

[4] $$F'_m = 1.94(a''_m + 0.5 - 0.5\, a'_m)/m_p.$$

If we integrate equation [3] between sunrise and sunset, we obtain the total daily insolation

[5] $$Q = F - D$$

where Q is the total daily insolation, F is the integrated value of F'_m corrected for surface pressure and the actual distance between sun and earth, and D is the integrated value of D_m.

Because a'_m and a''_m depend only on the optical air mass (m_p) and the precipitable water vapor[5] (w), F'_m is a function of m_p and w only. Kimball (7) published a chart relating a'_m and a''_m to m_p and w and this chart was used, with equation [4], in the preparation of Fig. 1 (Fritz's Fig. 2).

For application to Fig. 1, values of the precipitable water vapor (w) on cloudless days were determined as follows: Let w' represent the monthly mean of precipitable water vapor in the atmosphere on all days. Values of w' for radiosonde stations in the continental United States have been computed by Shands (11); values for Alaskan radiosonde stations were computed from Ratner's (10) summary; values for radiosonde stations in northern Canada

[4] *1 langley (ly.) = 1 gm. cal. per sq. cm. = 3.68 B.t.u. per sq. ft.*

[5] *Precipitable water vapor is defined as the depth of liquid water which would result if all the water vapor in a vertical column of air extending to the top of the atmosphere were condensed and collected at the bottom.*

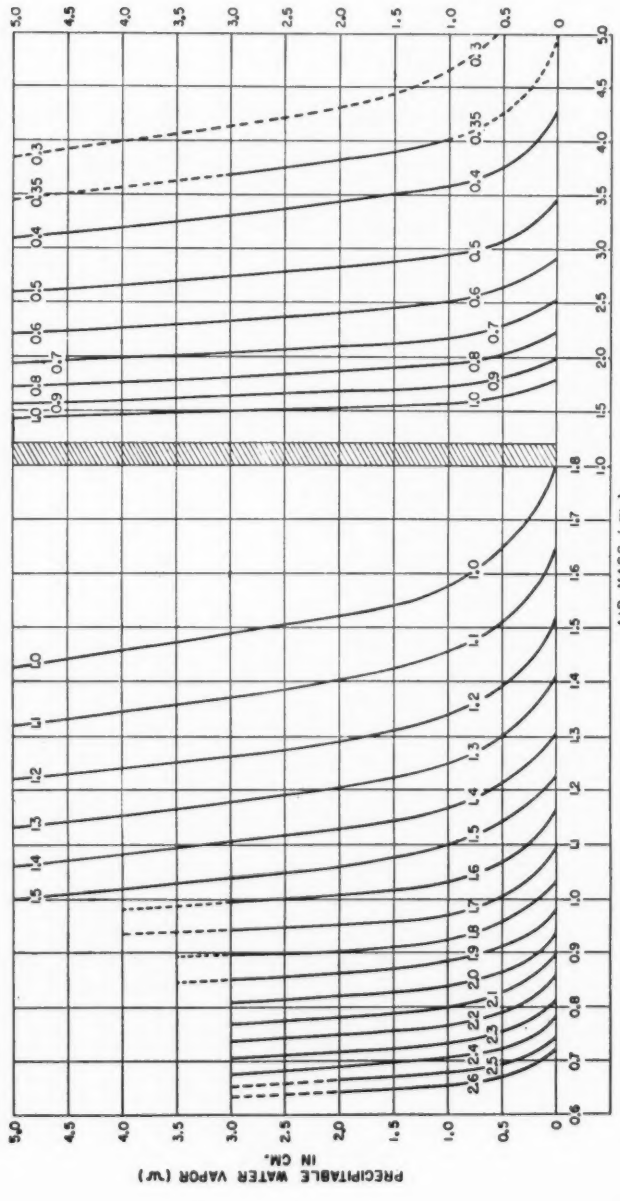

FIG. 1. Insolation in langleys per minute (figures inserted on curves) on a horizontal surface through a cloudless, dustless atmosphere as a function of w and m_p. Left-hand portion has been plotted with an expanded scale of abscissae. (After Fritz.)

were computed from the most recent records of the Meteorological Division (see also Henry and Armstrong (3)); and values for radiosonde stations in southern Canada from the recent summary of the Meteorological Division (12). Now, on the basis of European data, Humphreys (5) found that $w = 0.87w'$; Fritz found for Oakland (maritime climate) in January $w = 0.83w'$ and for Omaha (continental climate) in January $w = 0.86w'$. Consequently, Fritz used $w = 0.85w'$ in his computations and the same procedure is followed here. Values of w at radiation stations were obtained by interpolation of the data for the radiosonde stations.

Values of the solar zenith angle for each hour angle of daylight on the 15th day of each month were obtained from special charts based on the equation

$$\cos\theta = \sin\delta \sin\phi + \cos\delta \cos\phi \cos h \qquad [6]$$

where

δ = solar declination,
ϕ = latitude of radiosonde or radiation station,
h = solar hour angle.

Using these values of θ, the air mass (m_s) was read from a graph constructed from the data in the Smithsonian Meteorological Tables (Table 137, Sixth Rev. Ed. 1951) and the corrected air mass (m_p) was obtained from equation [2].

It was assumed that the monthly mean of w was representative of the 15th day of each month and that the diurnal variation of w was negligible. The values of w and m_p were used with Fig. 1 to obtain F'_m for each hour of daylight on the 15th day of each month. The hourly values were assumed to represent the average insolation during the 30 min. preceding and the 30 min. following the hour and were summed. This total was then multiplied by 60 $(r_0/r)^2 \cdot p$ to obtain the daily value of F. Tests with a planimeter revealed that this approximate method of integration was as accurate as the computation of F warranted.

In cases where $m_p > 4$, m_s does not equal sec θ nor does Kimball's chart (for a'_m and a''_m) extend beyond $m_p = 4$. In order to obtain an order of magnitude for the radiation in these cases, Kimball's data were extrapolated and charts similar to Fig. 1 were prepared for $m_p > 4$. In these computations, corrections were applied for average atmospheric refraction. The procedure here differs from that of Fritz who used observed values of insolation for those hours (when $m_p > 4$) on days when the radiation was high at stations in the appropriate latitudes.

The term F in equation [5] may now be considered as determined. It remains to determine "$-D$", the factor which includes the direct effect of dust, the indirect effect of surface albedo (see later), and errors introduced by the method of computaion of F.

3. TREATMENT OF OBSERVED INSOLATION DATA

Daily totals of insolation for several Alaskan, Canadian, and United States radiation stations have been published in the *Monthly Weather Review* to the

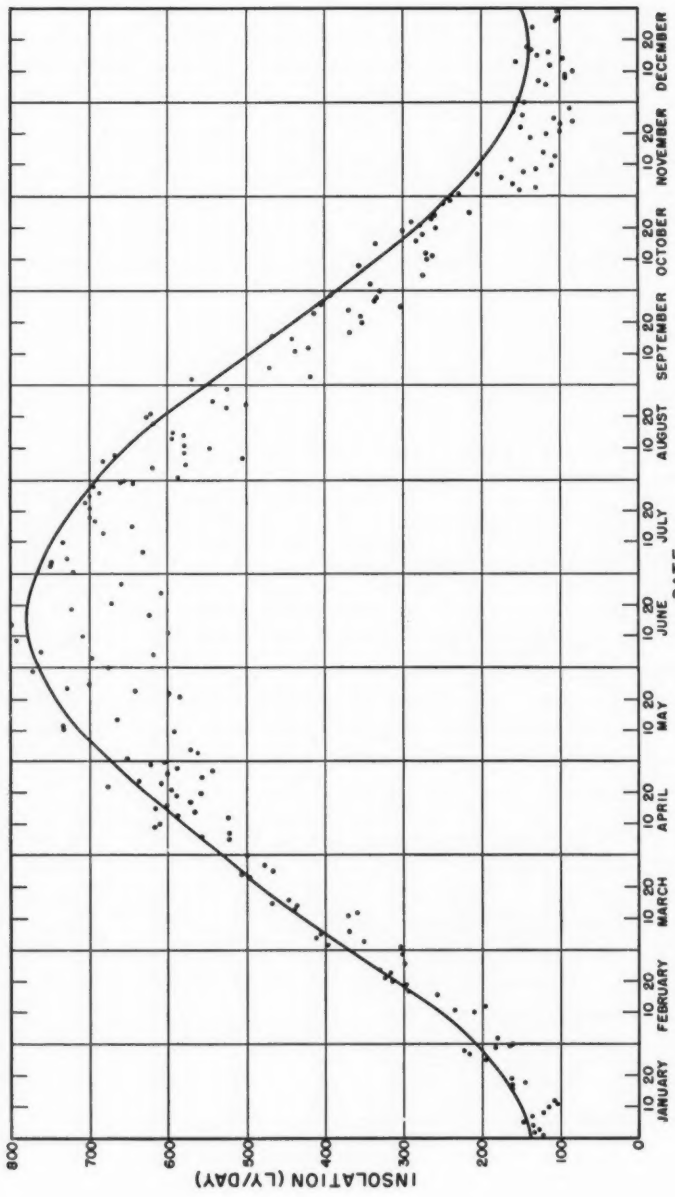

FIG. 2. Observed insolation at Winnipeg during 1952. The average cloudless day insolation is given by the curve drawn just below the very highest points.

end of 1949 and in the *National Summary of Climatological Data* (U.S. Weather Bureau) since then. Data for Canadian stations not published in these periodicals were obtained from the records of the Meteorological Division.

Unfortunately, these data are given without reference to cloudiness conditions during the day. However, Fritz has devised a relatively simple graphical technique for obtaining the "observed average insolation on cloudless days" at the various radiation stations. He examined several years of insolation data for Washington, D.C., and Albuquerque, N.M. The dates were listed for days during which no clouds had been observed at any of the regular hourly meteorological observations at these two stations, and the insolation data for those dates were plotted on time charts similar to the one in Fig. 2 (one chart per year per station). In addition, the radiation data for the same years were plotted for all days (cloudiness conditions considered unknown) on which the observed radiation had been high. It was found that the smooth annual curve drawn through the cloudless day data fell just below the very highest points.

Using this graphical technique, annual curves were drawn for each station for each year of insolation data. The values for the 15th day of each month were taken from the smoothed curves and averaged, over the years of record. The resulting average represents Q, the observed cloudless day insolation. Values of "$-D$" may now be obtained from equation [5] for each of the radiation stations. These values of "$-D$" were plotted on maps covering Canada, eastern Alaska, and the northern United States and smooth isolines of "$-D$" were drawn. Because of the sparsity of radiation stations there is no unique way to draw these isolines. Following Fritz, isolines around extreme values of "$-D$" were restricted to small geographical areas. From these isolines and from the values of F obtained for the radiosonde stations, values of Q were obtained for each station and are plotted on Figs. 3–14, inclusive.

In some parts of Western Canada, where the ground is considerably above sea level, additional computations were carried out for non-radiosonde stations. The pressures at the ground and the total precipitable water vapor were obtained by appropriate interpolation. The computations for these elevated regions are included in Figs. 3–14. The isolines of Q on these charts are drawn to account only for the major changes of elevation in the mountainous areas.

4. DISCUSSION OF INSOLATION MAPS

During the winter, the insolation isolines follow the parallels of latitude fairly closely with only minor changes to account for changes in elevation and areas of high humidity and/or atmospheric pollution. There is a strong latitudinal gradient of insolation owing to the greater solar elevation and longer days in the south as opposed to the north.

In the summer, insolation is about the same over most of Canada with areas of maximum occurring in the regions of greatest elevation and areas of

minimum in regions of high atmospheric pollution. The latitudinal effect observed in winter has disappeared because the lower solar altitudes in the north are compensated for by the longer daylight period.

Large negative values of "$-D$" are observed in the Lower Lakes region throughout the year. These are probably due to the generally greater haziness in the vicinity of the lakes and also to the heavy industrial activity in that area.

Positive values of "$-D$" occur occasionally and are most widespread on the charts for the spring months. There are several factors which may contribute to this effect. First, the errors inherent in the method of computation of F may be responsible. One second possibility, which may be applicable where snow cover exists, is that the effect is partially due to the high albedo of the snow cover. With about 85% of incoming insolation reflected by the snow surface, some of this reflected radiation will be scattered in the atmosphere and that portion scattered downward will tend to make the observed insolation greater than the computed. Other possibilities are mentioned in section 5.

Negative values of "$-D$" occur at most stations in the fall because of the greater haziness of the atmosphere in that season.

In using the insolation charts, consideration should be given to the particular location for which values are desired. In parts of the country where the radiation instrument is located in a city where there is considerable industrial activity, the cloudless day insolation in the adjacent rural areas will likely be somewhat higher than is indicated by the charts. The studies of Church (1) at Seattle suggest that these areas of high depletion of insolation due to excessive atmospheric pollution are likely of very limited size. For example, he found that the average insolation at the Seattle–Tacoma airport was about 120 ly./day greater than at the Federal Supply Laboratory during June 1951. In December, the difference was about 30 ly./day. The Federal Supply Laboratory is located in the most industrialized section of Seattle and is only nine miles from the airport.

5. SOURCES OF ERROR

Errors in the insolation charts may be classified under two headings: (1) errors in the observed cloudless day insolation values, and (2) errors due to the method of construction of the charts.

Errors in Observed Cloudless Day Insolation

Instrumental Errors

It is known from the work of MacDonald (9) that the Eppley pyrheliometer has an ambient temperature error—the instrument reads relatively higher

---

FIGS. 3–14. Average cloudless day insolation (in ly./day) at the ground for the 15th day of each month. For the radiation stations (solid square dots on the charts), the average observed insolation is plotted at the right of the station symbol, the "$-D$" correction appears at the upper left, and the number of years of observations used in the determination of the average is plotted at the lower left. For the radiosonde stations (solid round dots) and for the elevated stations (circular station symbol) only the final insolation value is plotted.

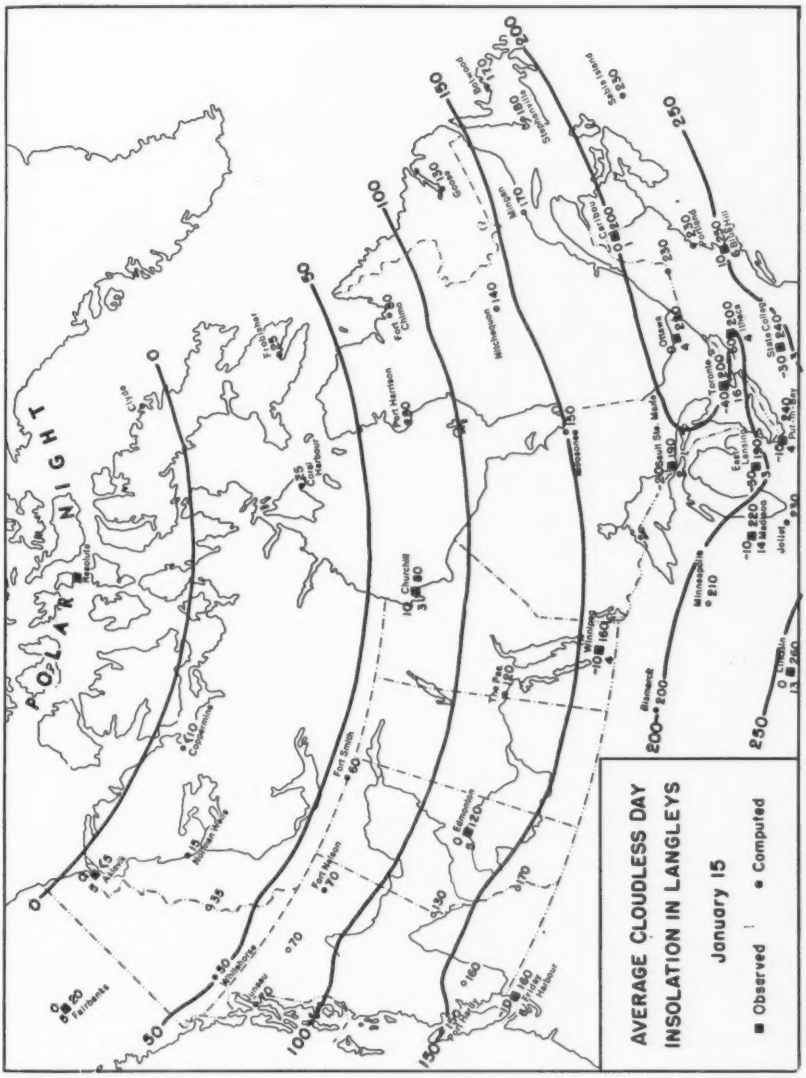
POLAR NIGHT
AVERAGE CLOUDLESS DAY
INSOLATION IN LANGLEYS
January 15
■ Observed • Computed

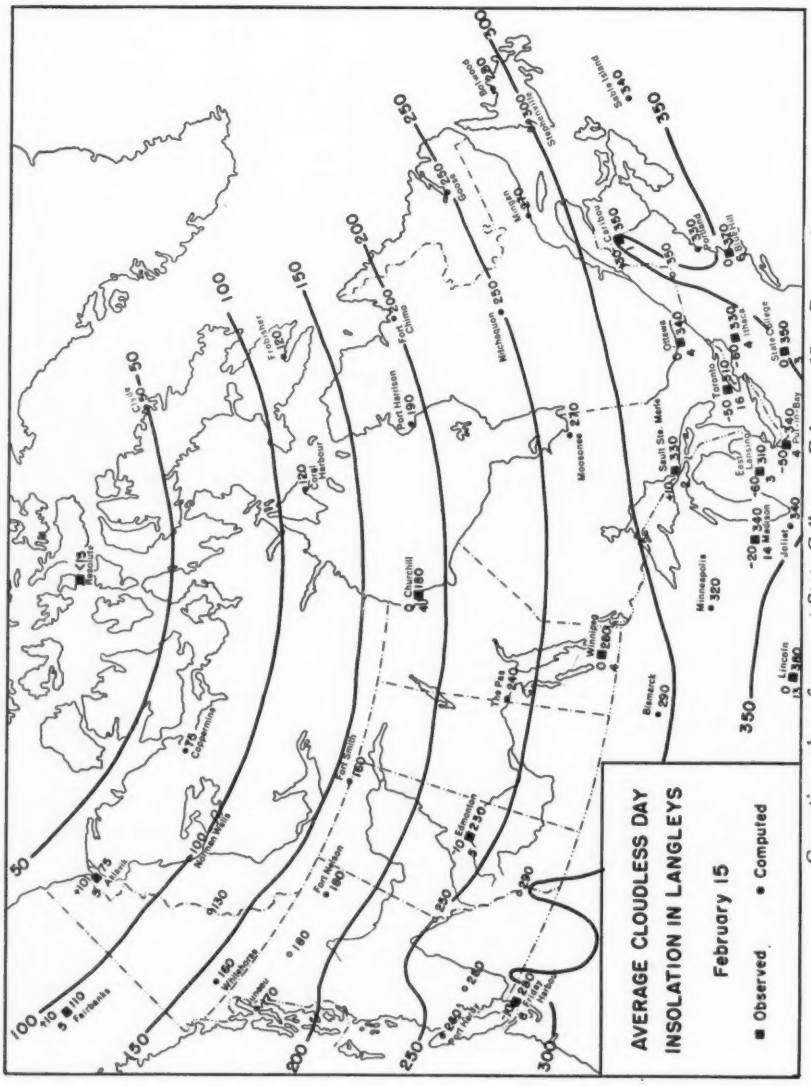

Correction: above figure—at State College on February 15, $-D = -50$.

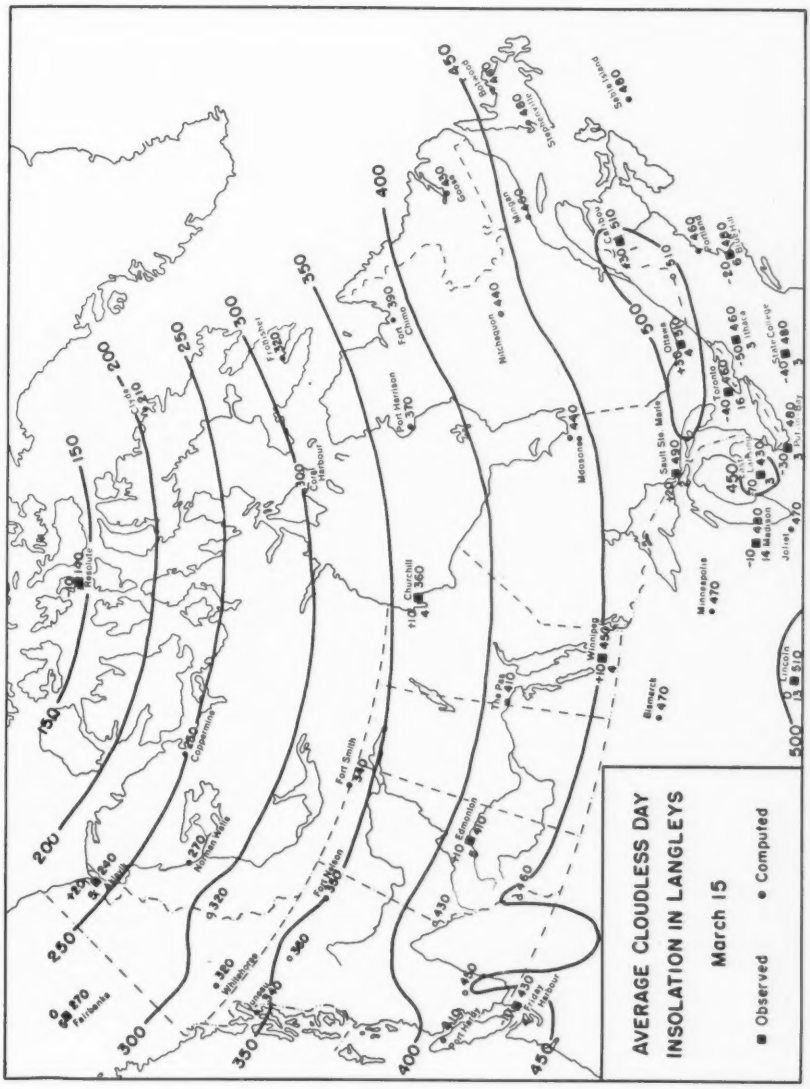
AVERAGE CLOUDLESS DAY
INSOLATION IN LANGLEYS
March 15
■ Observed • Computed
Fairbanks
Aklavik
Resolute
Coppermine
Norman Wells
Whitehorse
Fort Nelson
Fort Smith
Fort Chimo
Fort Harrison
Churchill
Moosonee
Edmonton
The Pas
Winnipeg
Bismarck
Minneapolis
Sault Ste Marie
Ottawa
Toronto
Kingston
Montreal
Jolliet
Lincoln
Sherbrooke
Grand Falls
Goose Bay
Nain
Port Harrison
Port Hardy
Prince Rupert
Victoria
Seattle
Spokane
Glasgow
Sable Island
Stair Corner
Thunder Bay

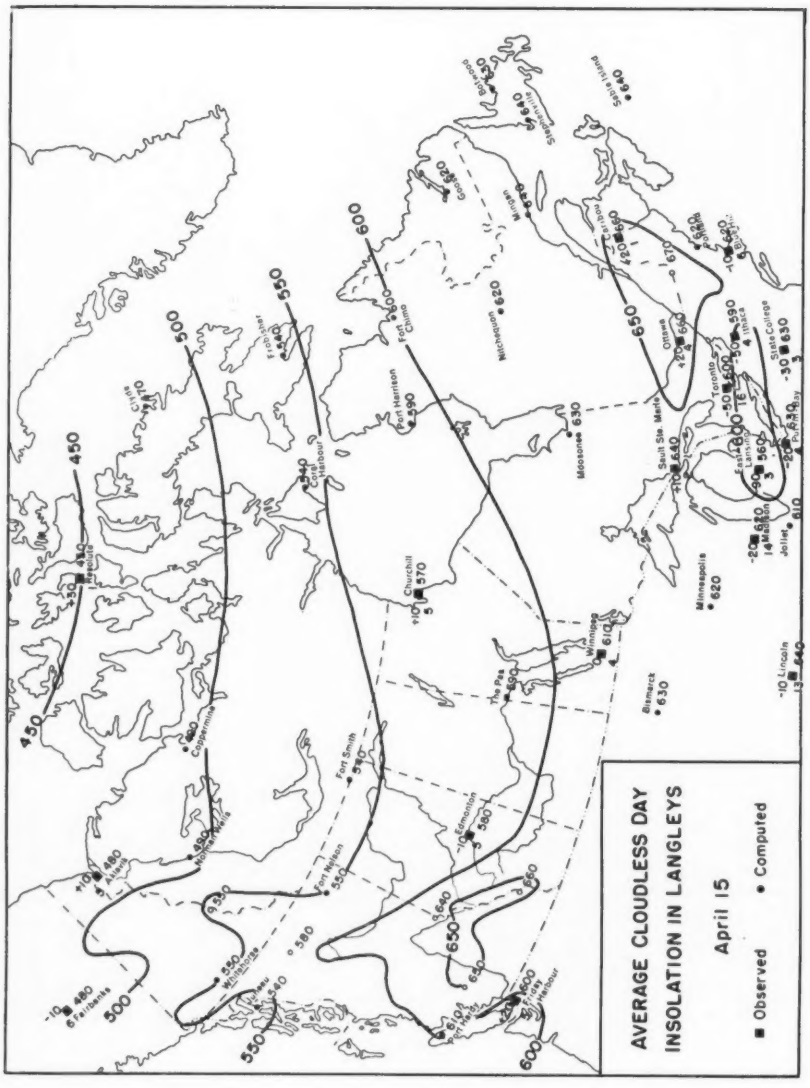
AVERAGE CLOUDLESS DAY
INSOLATION IN LANGLEYS
April 15
Observed
Computed
Fairbanks
Aklavik
Coppermine
Whitehorse
Watson Lake
Fort Nelson
Fort Smith
Edmonton
Prince George
Prince Rupert
Vancouver
Victoria
Cape Hope Island
Sandspit
Alert
Resolute
Clyde
Cape Dorset
Fort Chimo
Nitchequon
Goose
Mingan
Sept Iles
Fort Harrison
Moosonee
Churchill
Cross Lake
The Pas
Winnipeg
Sault Ste. Marie
Ottawa
Toronto
Kingston
Fort Wayne
Lansing
Minneapolis
Bismarck
Jolliet
Lincoln
State College
Buffalo
Rochester
Boston
Portland
Caribou
Moncton
Sydney
Halifax
Yarmouth
Charlottetown
Fredericton
Saint John
Gaspe
Quebec
Baie Comeau
Seven Islands
Goose Bay
Stephenville
Port aux Basques
Argentia
St. John's

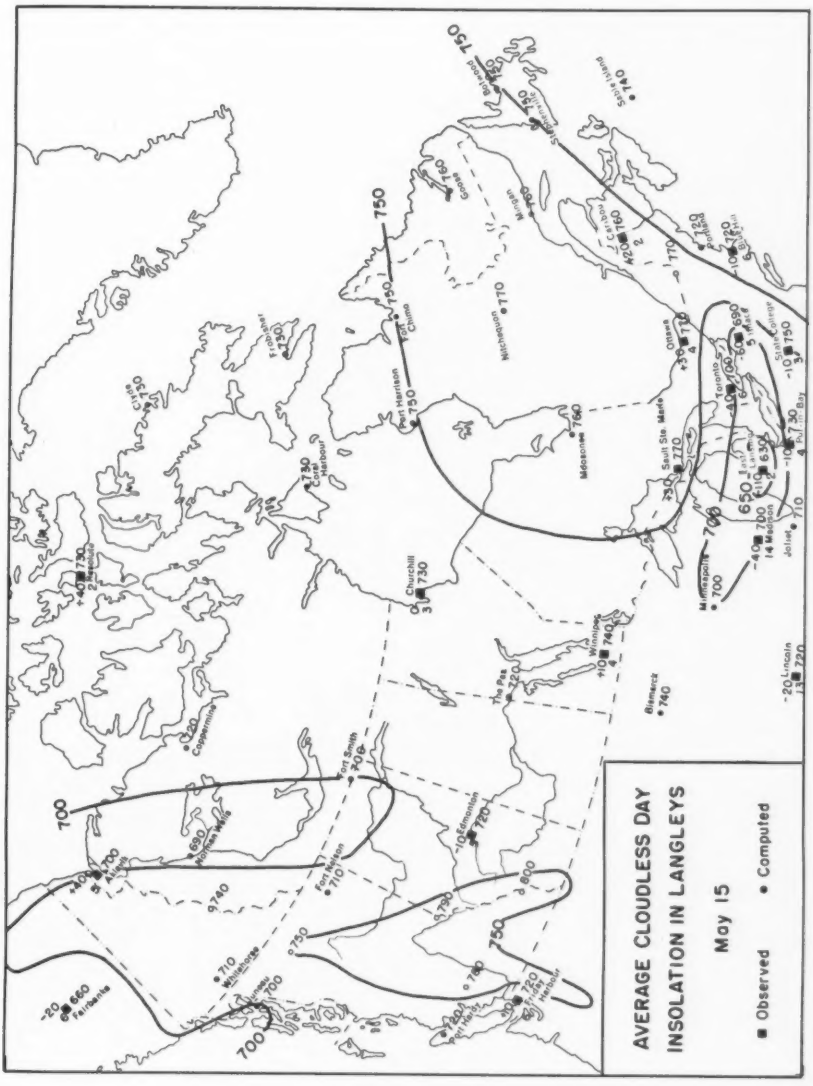
AVERAGE CLOUDLESS DAY
INSOLATION IN LANGLEYS
May 15
■ Observed • Computed

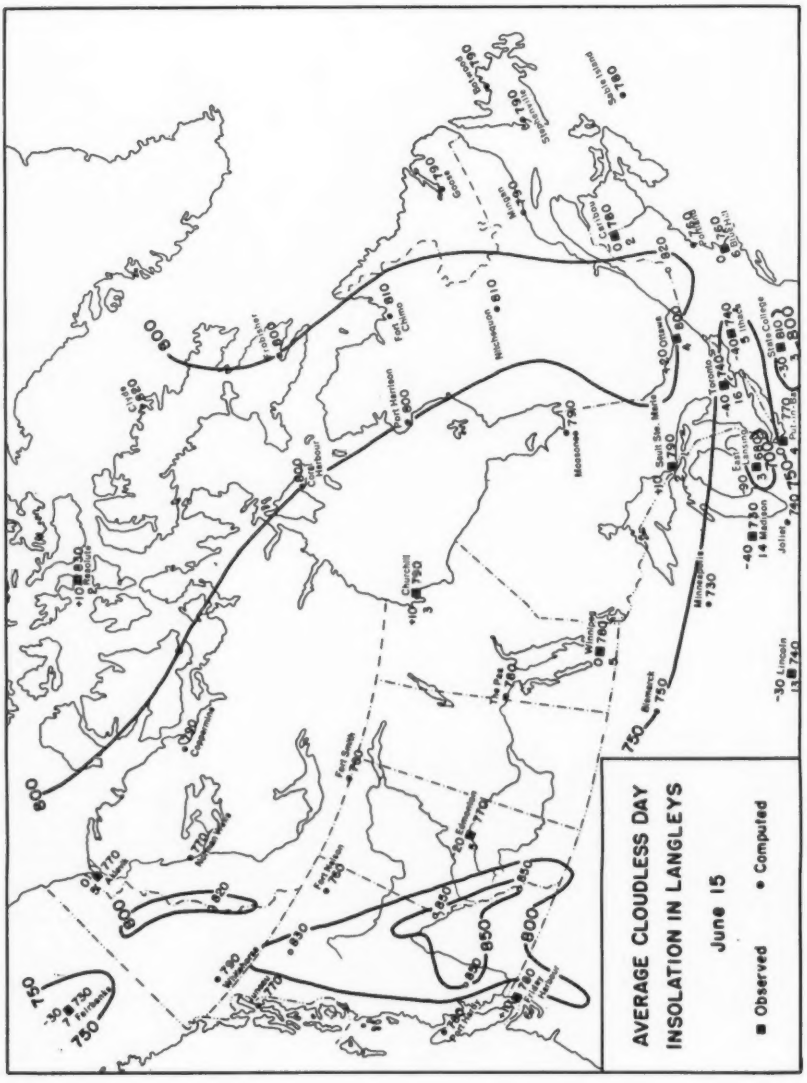
AVERAGE CLOUDLESS DAY
INSOLATION IN LANGLEYS
June 15
■ Observed • Computed

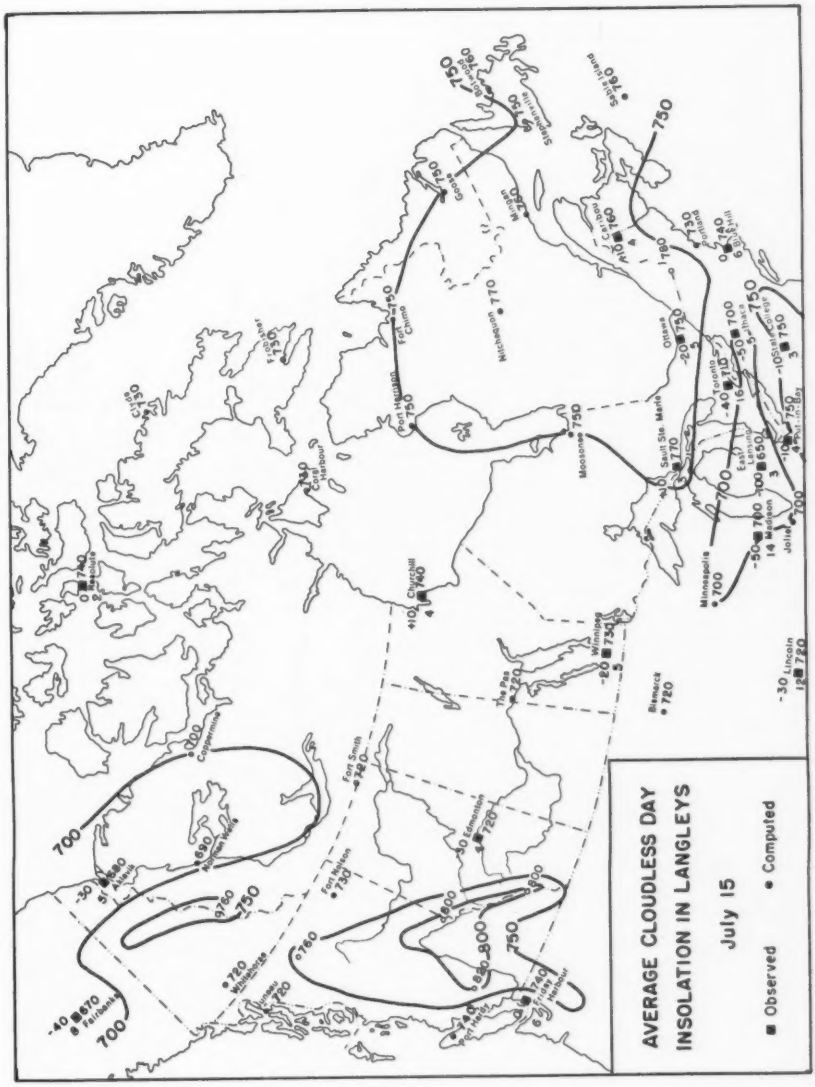
AVERAGE CLOUDLESS DAY
INSOLATION IN LANGLEYS
July 15
■ Observed • Computed

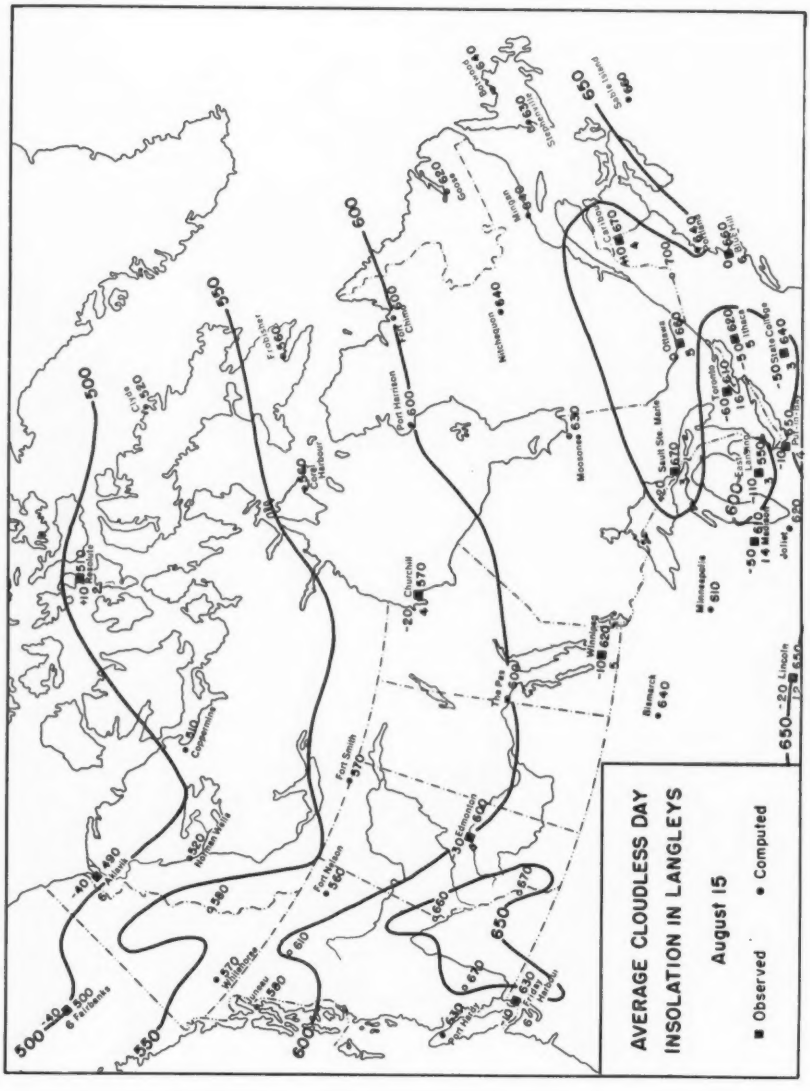
AVERAGE CLOUDLESS DAY
INSOLATION IN LANGLEYS
August 15
■ Observed • Computed

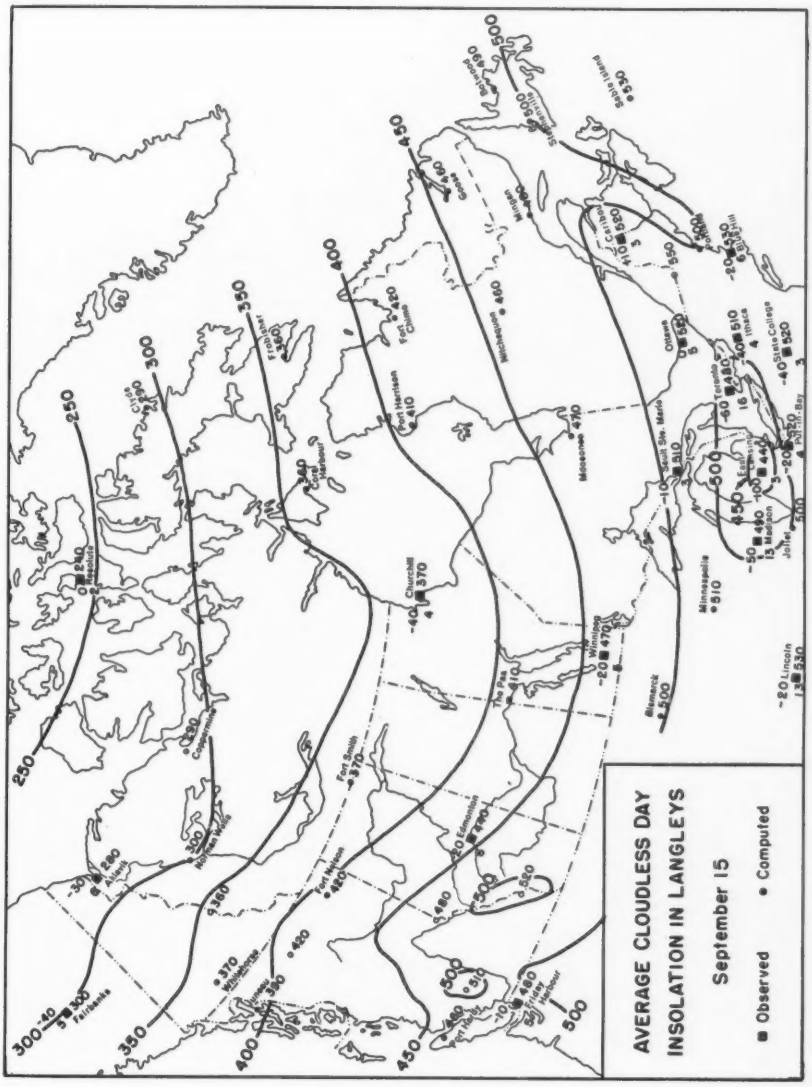
AVERAGE CLOUDLESS DAY
INSOLATION IN LANGLEYS
September 15
■ Observed • Computed

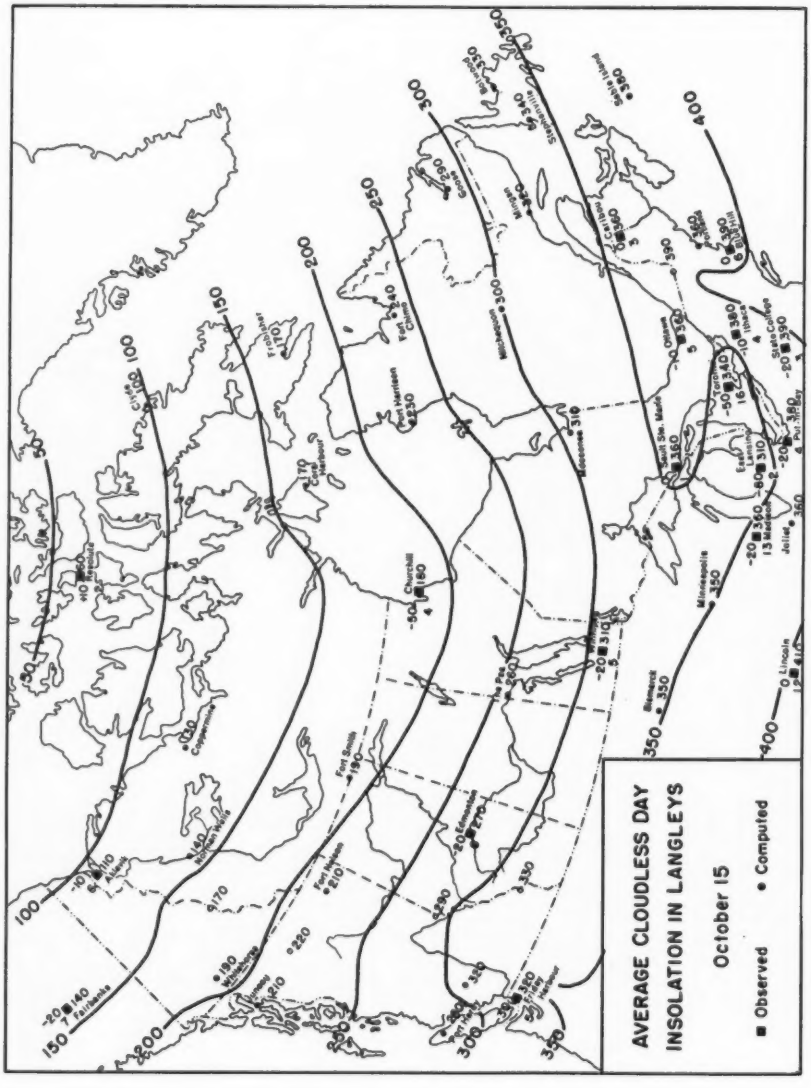
AVERAGE CLOUDLESS DAY
INSOLATION IN LANGLEYS
October 15
■ Observed • Computed

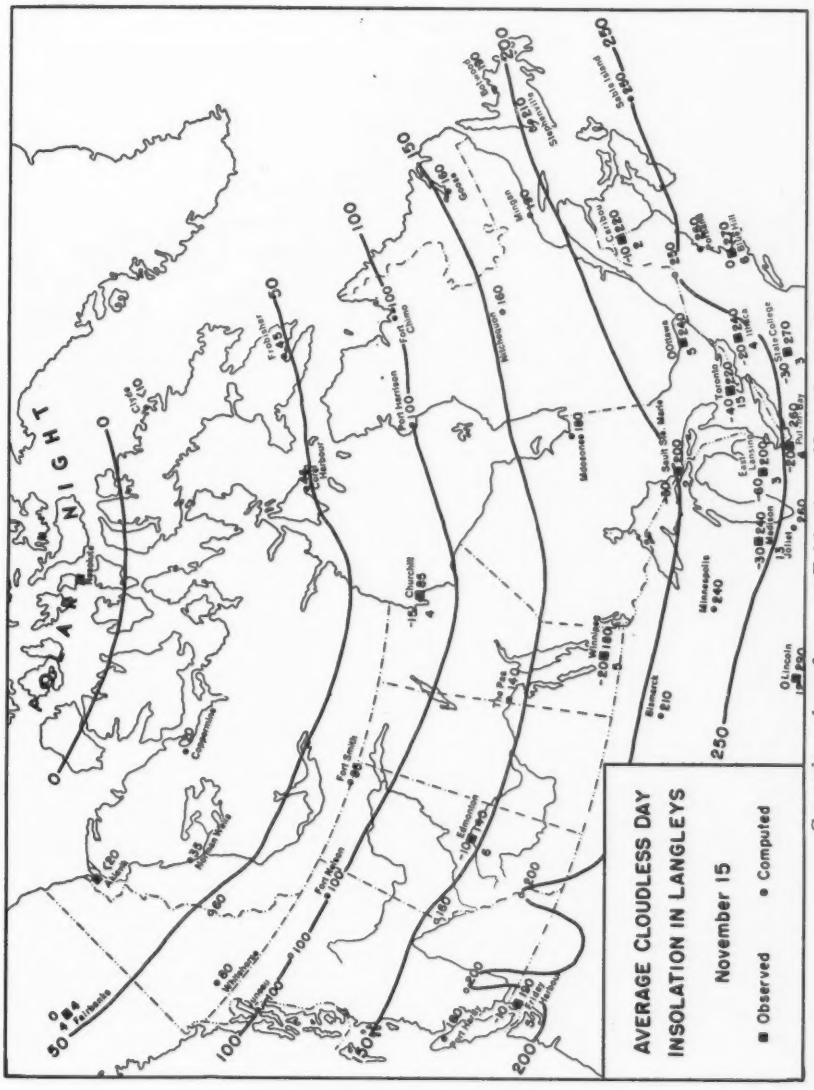

Correction: above figure—at Fairbanks on November 15, $Q = 40$.

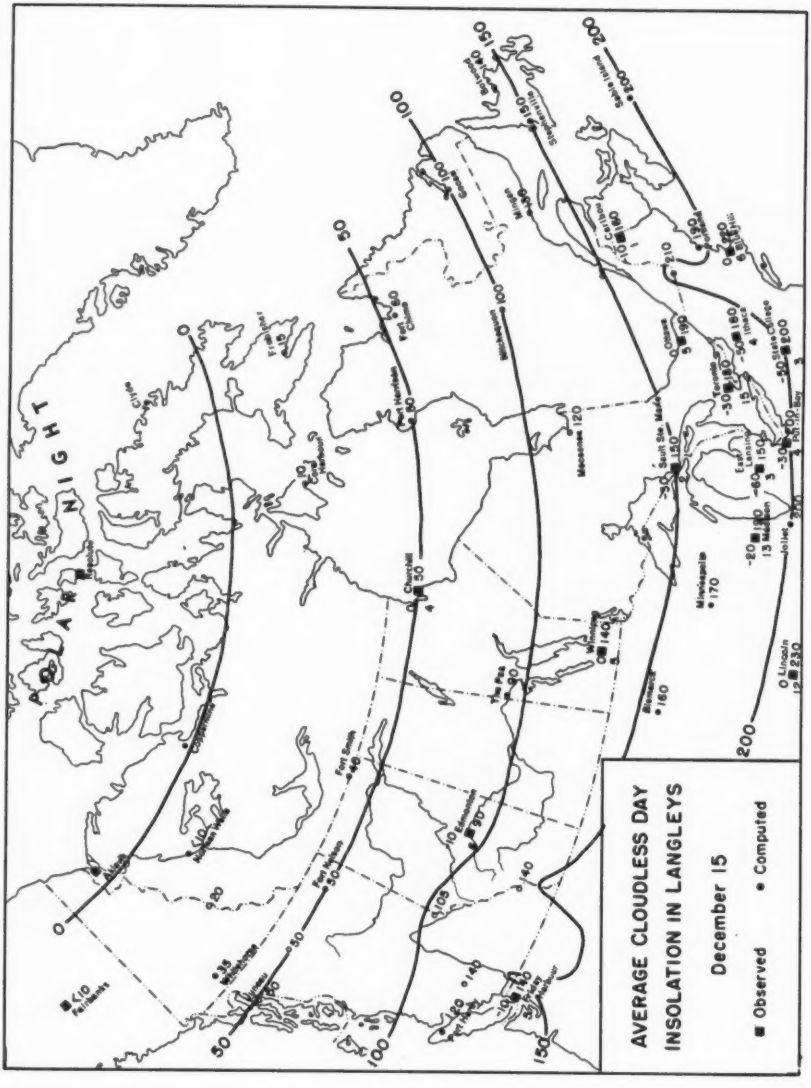
POLAR NIGHT
AVERAGE CLOUDLESS DAY
INSOLATION IN LANGLEYS
December 15
Observed
Computed

at lower temperatures. According to MacDonald's data, this would not be important where the annual temperature range is not excessive. However, in Canada, where the Eppley is frequently operating at temperatures considerably below that at which the instrument was calibrated, this effect may result in the observed winter insolation being some 5% too high. However, this error will likely be compensated for by the "cosine" error at the low solar altitudes in Canada during the winter months. In addition to the above, there may be some drift in the calibration factor of the Eppleys.

Errors due to the accretion of ice or frost on the glass bulb of the pyrheliometer occur occasionally in winter. Such a difficulty appears to result in insolation values that are too high. For example, in one instance at Resolute, the recorder reading dropped from 10 to 2 after the removal of ice from the pyrheliometer bulb. This may account for some of the positive values of "$-D$" observed.

Further errors in the observed cloudless day insolation may result from: errors in the reduction of instrument records; errors due to the approximate method of analysis of the insolation data to obtain the average cloudless day insolation; and errors because of the non-representative nature of the short period of record at most Canadian stations.

Errors Due to Method of Computation and Construction of Charts

Errors in the computation of F arise from limitations in the basic equation [1] and from the use of Kimball's chart as well as from the extrapolation of this chart. Houghton (4) has recently pointed out that there were errors in Kimball's interpretation of the original Smithsonian data used for his chart. The atmospheric transmission given by this chart is too high. Using Houghton's interpretation of the Smithsonian data, the value of F for Aklavik was computed for June 15. The result was 745 ly./day as opposed to 770 ly./day using the Kimball chart. For February 15, the values were 59 and 66 ly./day, respectively. These differences are not large and are not too important because the computation of F simply provides a *uniform* method of determining an approximate value of the insolation for every station. These F values are corrected, by the "$-D$" factor, to the observed insolation values and, therefore, the final insolation values on the charts are based essentially on the observational data.

As mentioned previously in section 3, there are many ways to draw the "$-D$" isolines. For example, at Port Harrison on August 15, "$-D$" was taken equal to zero. However, the isolines could have been drawn so that $-D = -20$ ly./day or $-D = 10$ ly./day. On any individual map, an examination of the "$-D$" values plotted for the radiation stations will give some idea of the possible variations in this quantity at a particular station.

ACKNOWLEDGMENTS

The author wishes to acknowledge the permission of Dr. Sigmund Fritz, U.S. Weather Bureau, and *Heating and Ventilating* to reproduce Fig. 1 and

the data plotted on Figs. 3–14, inclusive, for the following stations: Portland, Maine; Blue Hill, Massachusetts; Elevated station in New Hampshire; Ithaca, New York; State College, Pennsylvania; Put-in-Bay, Ohio; East Lansing, Michigan; Joliet, Illinois; Madison, Wisconsin; Minneapolis, Minnesota; Lincoln, Nebraska; and Friday Harbor, Washington.

The author also wishes to acknowledge the considerable assistance of Mr. D. U. MacKenzie, formerly of the Meteorological Division, in the preparation of this paper.

REFERENCES

1. CHURCH, P. E. Proc. Natl. Air Pollution 2nd Symposium, Pasadena, Calif. p. 47. 1952.
2. FRITZ, S. Heating and Ventilating, 46: 69. 1949.
3. HENRY, T. J. G. and ARMSTRONG, G. R. Aerological data for northern Canada. Meteorol. Div., Toronto. 1949.
4. HOUGHTON, H. G. J. Meteorol. 11: 1. 1954.
5. HUMPHREYS, W. J. Bull. Mount Weather Observatory, 4: 121. 1911.
6. KIMBALL, H. H. Monthly Weather Rev. 47: 769. 1919.
7. KIMBALL, H. H. Monthly Weather Rev. 58: 43. 1930.
8. KLEIN, W. H. J. Meteorol. 5: 119. 1948.
9. MACDONALD, T. H. Monthly Weather Rev. 79: 153. 1951.
10. RATNER, B. Upper air average values of temperature, pressure, and relative humidity over the United States and Alaska. U.S. Weather Bur., Tech. Paper No. 6. 1945.
11. SHANDS, A. L. Mean precipitable water in the United States. U.S. Weather Bur., Tech. Paper No. 10. 1949.
12. Summaries of radiosonde observations in southern Canada. Meteorol. Div., Toronto. 1952.

SEPARATION OF STARCH AND GLUTEN

VII. THE APPLICATION OF BACTERIAL PENTOSANASES TO THE RECOVERY OF STARCH FROM WHEAT FLOURS[1]

By F. J. Simpson

ABSTRACT

Culture supernatants containing pentosanases from *Bacillus licheniformis*, *B. polymyxa*, *B. pumilus*, and *B. subtilis* were used to hydrolyze pentosans present in starch slurries prepared from wheat flour. The treatment increased the rate at which starch settled and reduced the amount of starch sludge or "squeegee" starch. Recovery of starch from 75-lb. lots of flour was increased by enzyme treatment from 76% to 87–93%, and the protein content of the starch reduced from 1.1 to 0.5%.

INTRODUCTION

Although wheat was the principal source of commercial starch in America until about the middle of the nineteenth century, it lost its dominance to corn because of the higher cost of the raw material and technical difficulties of processing wheat. In addition to trouble encountered in removing the tenacious gluten, about 30% of the starch is lost in a slimy sludge known in the trade as "squeegee" starch (1). This fraction consists of strongly hydrated pentosan masses in which starch granules, nitrogenous materials, and fiber are embedded (5). When starch is recovered by allowing a slurry to flow slowly over tables, the "squeegee" starch passes into the tailings while the prime quality starch settles to form a hard cake. When the starch is recovered in a solid bowl centrifuge, the prime quality starch and some of the "squeegee" material are packed together to give a low quality product.

Clendenning and Wright tried unsuccessfully to eliminate the "squeegee" fraction by encouraging spontaneous fermentation; by briefly treating with dilute acid or alkaline solutions; and by fractional precipitation with C_2 to C_{12} monohydric alcohols (5). Although they were able to reduce the pentosan and protein content of starch slurries to acceptable levels by holding for 24–48 hr. at pH 2.0, the paste viscosity of the recovered starch was greatly reduced. In modern plants part of the starch in the "squeegee" material is recovered by recycling several times through continuous centrifuges.

If the pentosans causing the "squeegee" fraction could be rapidly hydrolyzed by an enzyme, the embedded starch granules should be released. This should simplify starch recovery. A number of bacteria and molds produce extracellular enzymes which attack both the water soluble pentosans of wheat flour and the relatively water insoluble pentosans of "squeegee" starch (7). Such enzymes produced by four bacilli were tested in the laboratory and pilot plant for their effect on the rate of starch settling and recovery.

[1]*Manuscript received September 7, 1954.*
Contribution from the National Research Council of Canada, Prairie Regional Laboratory, Saskatoon, Saskatchewan. Issued as Paper No. 173 on the Uses of Plant Products and as N.R.C. No. 3442.

MATERIALS AND METHODS

Production of Pentosanases

Four bacilli, *Bacillus licheniformis*, B479; *B. polymyxa*, B507; *B. pumilus*, B12; and *B. subtilis*, B92 that had previously been found to produce extracellular pentosanases (7) were used to produce the enzymes in 30-liter stainless steel fermentors. The basal medium consisted of 0.5% distillers' dried solubles, 0.4% $(NH_4)_2HPO_4$, 0.1% $MgSO_4.7H_2O$, 0.2% $CaCO_3$, and 0.5 to 1.0% carbohydrate. The carbohydrate for *B. licheniformis* and *B. subtilis* was sucrose whereas for *B. polymyxa* and *B. pumilus* it was xylose. The sugars were sterilized separately and added aseptically to the basal medium just before inoculation.

Fifty milliliters of a culture grown in a 500-ml. Erlenmeyer flask for 24 hr. at 30° C. on a rotatory shaker was used to inoculate 18 to 20 liters of medium in the fermentors. Sterile lard oil (50 ml.) was also added as an antifoam agent. The medium in the fermentor was maintained at 30° C., agitated with an impeller at 400 r.p.m., and aerated at one-half volume per volume of medium per minute. After 36 hr. of fermentation samples were withdrawn periodically from the fermentor and assayed for units of pentosanase by the method previously described (7). Maximum activity was obtained after 48 to 60 hr. incubation. The fermented liquor was then removed from the fermentor and the pH adjusted to 6.5. Suspended material and bacterial cells were removed in a Sharples' supercentrifuge. The supernatant was used without further treatment as the enzyme source in laboratory and pilot plant studies. All laboratory studies were made with an enzyme preparation (1100 units of pentosanase per ml.) obtained from a fermentation with *B. pumilus*. The preparations from *B. pumilus*, *B. polymyxa*, *B. subtilis*, and *B. licheniformis* used in pilot plant trials contained 970, 850, 550, and 300 units of pentosanase per ml. respectively.

Separation of Starch

Straight-run, unbleached flours to which no improvers had been added were used. The flours contained from 63 to 67% starch, 12 to 14% protein, 1.5 to 3% pentosan, and 10 to 12% moisture. Starch and gluten were separated by the method of Shewfelt and Adams (6). In the pilot plant (Fig. 1) dough was prepared by mixing 75 lb. of flour with 6.5 to 7 gal. of water at 30° C. in a stainless steel tank equipped with horizontal paddles and stationary intermeshing fingers. Twenty-nine gallons of water was added to form a slurry. Gluten was removed on a rotex screen and washed once by shredding in a power meat grinder, suspending in approximately five gallons of water, and rescreening.

The starch milk passed through the screen and was collected in a holding tank equipped with an impeller type agitator. Starch was recovered in a suspended basket centrifuge (R.C.F. 570 at the free surface of the liquid). The bulk of the "squeegee" fraction lay on top of the hard starch and collected

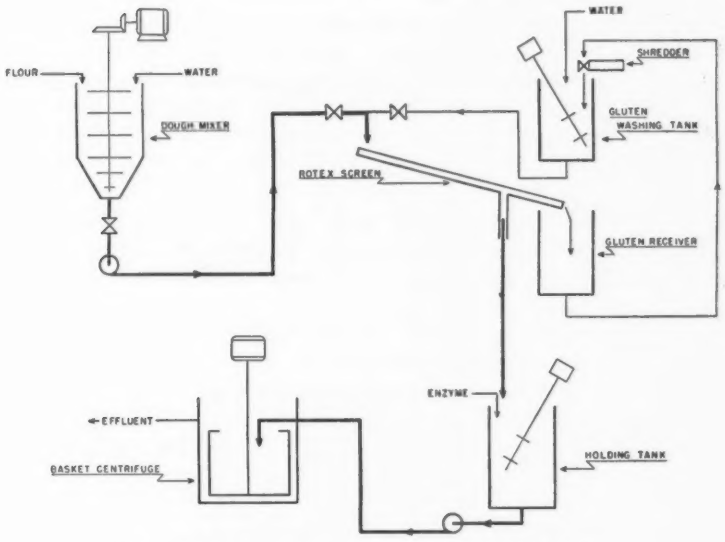

FIG. 1. Flow sheet for separation of starch and gluten.

in the upper part of the bowl. Eventually it would spill over with the tailings. The centrifuge was stopped before this happened and the "squeegee" material removed.

Analytical Methods

The water content of the flour, gluten, starch, "squeegee" starch, and tailing fractions was obtained by drying three samples at 110° C. in shallow dishes. Dry weights were then calculated. Kjeldahl nitrogen was determined by the semimicro method with a copper–selenium catalyst. The factor 5.7 was used to calculate protein. Pentosans were determined by the method of Adams and Castagne (2) and starch by the polarimetric method of Clendenning (3, 4) on lyophilized samples. Results are expressed on a dry basis.

EXPERIMENTAL

The Effect of Pentosanases on the Settling Rates of Starch Slurries

To 500-ml. aliquots of freshly prepared starch milk, 125 ml. of water plus pentosanase preparation from *B. pumilus* were added to give various concentrations of enzyme. The mixtures were held at 30° C. for 30 min. and stirred occasionally. The pH of each mixture was then adjusted to 9 with dilute sodium hydroxide to inhibit enzyme action and bacterial growth. A 500-ml. aliquot of each was poured into a graduated cylinder and the starch allowed to settle at 2° C. to further inhibit enzyme action and bacterial growth. Cylinders of the same diameter were selected so that results would be com-

parable. The rates of settling were determined by hourly readings of the volume of settled starch.

There was considerable variation between batches of starch milk in the final volumes of settled starch, but the effect of adding pentosanases was consistent. Addition of the enzymes increased the rate of settling (Fig. 2) and

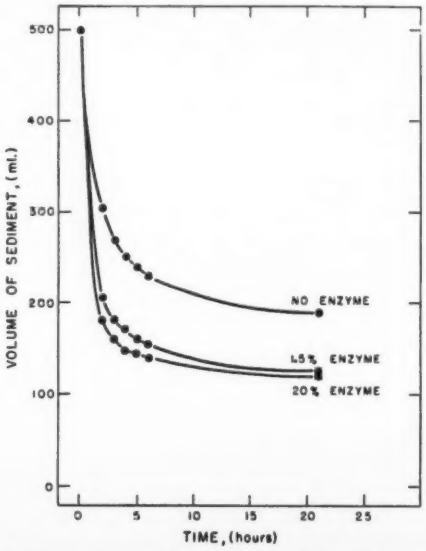

FIG. 2. Effect of pentosanases of *B. pumilus* on the settling of starch slurries.

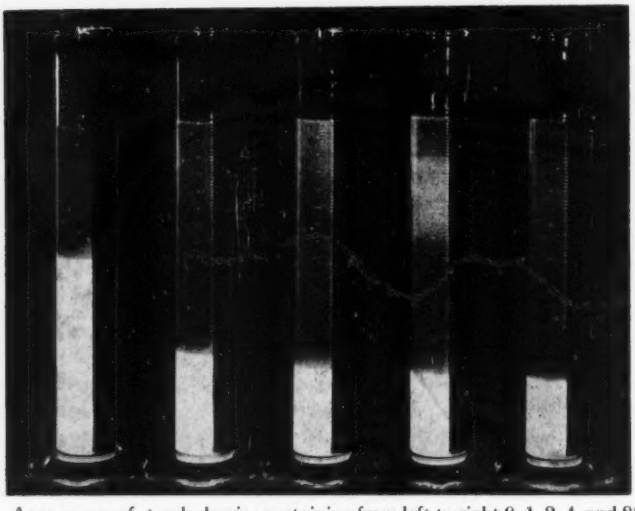

FIG. 3. Appearance of starch slurries containing from left to right 0, 1, 2, 4, and 8% enzyme after a settling period of 12 hr.

reduced the amount of "squeegee" starch. The latter is evident from the low final readings of the treated samples as compared with the control. The appearance of cylinders in a similar trial after a 12 hr. settling period is shown in Fig. 3.

Effect of Enzyme Treatment on Protein and Pentosan Contents of the Recovered Starch

The protein and pentosan contents of the starch recovered from some of the settling experiments described above were determined. After a settling period of 21 hr. the opalescent supernatant water was removed and replaced with distilled water. The contents were stirred and transferred to plastic centrifuge tubes. The supernatant was removed as completely as possible and the solids dried. Not only was the pentosan content of the treated starch considerably reduced, but there was also a reduction in protein (Table I). The crude enzyme preparation contained nitrogen equivalent to 0.4% protein, but apparently this was not absorbed by the starch.

TABLE I

THE EFFECT OF PENTOSANASE TREATMENT ON THE PROTEIN AND PENTOSAN CONTENTS OF SETTLED STARCH

Flour	Enzyme, % by volume*	Composition of starch	
		Protein, %	Pentosan, %
A	0	1.6	1.33
	1.5	1.1	0.25
	4	1.5	0.22
	20	1.0	0.25
B	0	3.2	1.36
	1.5	1.9	0.28
	4	1.6	0.25
	20	1.2	0.25

**Enzyme preparation from B. pumilus contained 1100 units of pentosanase per ml.*

Effect of Adding Enzyme at the Dough or Slurry Stages

The earlier the addition of enzyme in the separation process, the longer the enzyme would be in contact with its substrate. Although the crude preparation contained proteolytic enzymes, their action on gluten was not known. Degradation of the gluten would be undesirable, particularly in the production of vital gluten. One-kilogram lots of flour were processed in the laboratory. In the first run no enzyme was added; in the second 80 ml. of the water used to prepare the dough was replaced with 80 ml. of enzyme preparation; in the third run a similar replacement was made with 80 ml. of slurry water. Both the dough and the slurry were mixed for 10 min. Aliquots of the starch milk were placed in cylinders and the rates of settling determined as before, except that the pH was not adjusted to 9.

The settling rates were the same for addition of enzyme at either the dough or slurry stage. Addition at the dough stage, however, raised the protein content of the starch (Table II). The slurry stage thus appeared to be the earliest point at which crude pentosanase preparations might be added. In the pilot plant even this was impractical. The gluten towards the end of the

TABLE II

THE EFFECT OF ADDING PENTOSANASE AT THE DOUGH AND SLURRY STAGE ON THE COMPOSITION OF THE SETTLED STARCH

Addition of enzyme at	Composition of settled starch	
	Protein, %	Pentosan, %
Dough stage	5.1	0.32
Slurry stage	1.1	0.38
Control	1.4	1.6

screening process was pumped from the slurry tank in a semifluid condition. After the gluten had stood at room temperature for a few hours, liquefaction had proceeded to such an extent that the gluten could be stirred with a glass rod. The crude pentosanase preparations were therefore added to the starch milk after the gluten had been removed.

Effect of Washing Starch Recovered after Treatment with Pentosanases

The effect of washing on the protein and pentosan contents of starch treated with pentosanase was studied. A composite starch prepared from several separations treated with various enzyme preparations was used. One hundred-gram lots were suspended in 400 ml. of 0.01 *M* sodium citrate – phosphate solution and adjusted to various pH values with dilute hydrochloric acid or sodium hydroxide. The suspensions were stirred for 10 min. The solid material was recovered by centrifuging and drying. Such treatment, particularly at pH 1 and 11, removed considerable protein and a small amount of pentosan (Table III).

TABLE III

THE PROTEIN AND PENTOSAN CONTENT OF STARCH TREATED WITH PENTOSANASES AFTER WASHING AT VARIOUS pH VALUES

Treatment	Composition of starch	
	Protein, %	Pentosan, %
None	0.86	0.46
Washed, pH 1	0.33	0.36
Washed, pH 3	0.43	0.39
Washed, pH 5	0.48	0.36
Washed, pH 6	0.56	0.42
Washed, pH 7	0.52	0.37
Washed, pH 9	0.35	0.34
Washed, pH 11	0.25	0.35

The crude enzyme preparations were brown and some of this color was absorbed by the starch. Much was removed by washing, but none of the starches had quite the same degree of brightness as untreated prime starch.

Application of Pentosanases to Recovery of Starch in the Pilot Plant

Seventy-five-pound lots of flour were processed in the pilot plant. The starch milk was collected in the holding tank and treated with 3 gal. of crude pentosanase preparation. Preparations obtained from *B. pumilus* and *B. polymyxa* were allowed to act for 30 min. at the natural pH (6.0–6.8) of the starch milk and preparations obtained from *B. licheniformis* and *B. subtilis* were allowed to act for 60 min. The temperature of the mixture by this time was about 25°–28° C. The optimum for the pentosanases lies between 40° and 45° C. No provision was made for controlling the temperature, or for inactivating the enzyme after treatment.

The enzyme treatment with all four preparations reduced the amount of "squeegee" material and increased the yield of starch (Table IV). As previously noted in laboratory trials, the quality of the starch was improved (Table V). In addition, the treated starch was drier and easier to remove from the centrifuge bowl than the untreated starch.

TABLE IV

THE EFFECT OF PENTOSANASES PRODUCED BY DIFFERENT BACILLI ON THE RECOVERY OF STARCH FROM WHEAT FLOUR

Source of pentosanase	Starch recovery, % of that in the flour			
	Starch	Gluten	"Squeegee"	Total
Control	76	3	16	95
B. pumilus	89	7	2	98
B. polymyxa	93	2	3	98
B. subtilis	87	5	3	95
B. licheniformis	87	4	5	96

TABLE V

EFFECT OF PENTOSANASES ON QUALITY OF STARCH RECOVERED

Component	Amount in starch fraction, %				
	Control	*B. polymyxa*	*B. pumilus*	*B. subtilis*	*B. licheniformis*
Starch	92.0	95.7	96.0	96.0	94.2
Protein	1.1	0.5	0.4	0.4	0.9
Pentosan	1.0	0.3	0.3	0.4	0.4

DISCUSSION

The troublesome sludge formed during the recovery of starch from wheat can be eliminated by the use of microbial pentosanases. In addition to increasing the yields obtained when starch is recovered in a basket centrifuge

or on a starch table, the enzyme treatment should eliminate the necessity of recycling the starch sludge through continuous centrifuges to obtain good yields. This would reduce the amount of physical equipment and power required. Since the treatment accelerates the rate of settling, shorter tables, or slightly faster flow rates may be possible when the starch is recovered by sedimentation.

If the proteolytic enzymes could be selectively inhibited or removed from the crude pentosanase preparation, addition of enzyme at the dough or slurry stage should be possible. This would eliminate the holding period in the present procedure. The objectionable color of the crude enzyme preparation could be reduced by careful selection of ingredients for the production medium or by partial purification of the enzyme.

As yet no detailed information has been obtained whether these enzyme preparations affected the properties of the starch. The viscosities of hot pastes (2.5%) of starches treated with enzyme preparations from *B. pumilus* and *B. subtilis* did not differ from a similarly prepared starch not treated with enzyme. It is thus doubtful if significant changes have occurred.

No provision was made in these experiments to inactivate the enzymes added to the starch slurries. Some would pass into the effluent during recovery and subsequent washings. The pentosanases of these bacilli are quickly inactivated at pH values below 4.5 and above 8.5. An acid or alkaline rinse would thus be effective, and also would remove additional protein from the starch. The enzymes are sensitive to temperatures above 45° C., and therefore would be destroyed at the temperatures used to gelatinize starch.

The effectiveness of these crude pentosanase preparations in reducing the starch sludge adds additional support to the conclusions of Clendenning and Wright (5) that the "squeegee" fraction consists of strongly hydrated pentosan masses in which starch granules are embedded.

ACKNOWLEDGMENTS

Mr. K. L. Phillips and Dr. H. R. Sallans generously assisted in the pilot plant operations. The author is also indebted to them and to Dr. G. A. Ledingham for helpful discussions on the problem. It is a pleasure to acknowledge the technical assistance of Mr. H. R. Rainer and Mr. A. S. Sieben.

REFERENCES

1. Adams, G. A. Can. J. Technol. 29: 217. 1951.
2. Adams, G. A. and Castagne, A. E. Can. J. Research, B, 26: 314. 1948.
3. Clendenning, K. A. Can. J. Research, C, 20: 403. 1942.
4. Clendenning, K. A. Can. J. Research, B, 23: 239. 1945.
5. Clendenning, K. A. and Wright, D. E. Can. J. Research, F, 28: 390. 1950.
6. Shewfelt, A. L. and Adams, G. A. Can. J. Research, F, 23: 373. 1945.
7. Simpson, F. J. Can. J. Microbiol. 1: 131. 1954.

FRACTIONAL FREQUENCY GENERATION BY REGENERATIVE MODULATION[1]

By D. Makow

ABSTRACT

Circuits are described by which the generation of fractional frequencies can be achieved by means of regenerative modulation. A separation between the odd and even fractional frequency components on two different output terminals is realized. The amplitudes of the generated frequency components do not differ appreciably from each other. The ability of these circuits to produce the various fractional frequency components is to a large extent independent of the variation of the input, filament, and plate voltages. In addition, phase shift in the feedback loop, which is troublesome in many regenerative circuits, is of little consequence.

A. INTRODUCTION

Recent progress in radio techniques, carrier telephony, television, and other allied fields has made the problem of increasing the number of available channels an urgent matter. Methods of generating precision standards of frequency and development of reliable circuits to divide, multiply, and transfer frequencies into the desired frequency spectra are tasks of prime importance closely associated with the fast growing field of radio communication.

A considerable amount of published material exists regarding production of fractional frequencies by means of synchronization of an oscillator of the relaxation or other type to a desired submultiple of the frequency of the applied wave. In a large number of cases, this method has the serious disadvantage that there is a possibility that the oscillator may lock on an incorrect submultiple or simply drift when the values of circuit elements or the input and power supply voltages change, or when the synchronizing voltage fails.

Fractional frequency generators utilizing the principle of regenerative modulation eliminate the above limitations, and have a number of characteristics which make them particularly suitable for the mentioned applications. The basic idea has been described by Horton (1), and a detailed description of some circuit types has been given by Miller (3).

The regenerative modulation circuits described below retain the desirable characteristics of the circuits known to date and offer additional advantages. It has been found that oscillation can be maintained in a suitably designed circuit when the feedback voltage contains several different frequencies. The amplitudes of the useful frequency components do not differ from each other appreciably. Also, it is possible to obtain only the odd fractional frequencies in one branch of the feedback loop and only the even fractional frequencies in the other branch. Thus, the required Q of the filter elements employed to make the desired frequency components available can be reduced, which is

[1]*Manuscript received September 23, 1954.*
Contribution from the Radio and Electrical Engineering Division, National Research Council, Ottawa, Canada. Issued as N.R.C. No. 3444.

of particular value in low frequency applications. In an attempt to answer the question whether it is possible to design regenerative modulation systems in which a further reduction of Q would be realized, circuits were investigated where the various generated fractional frequency components are distributed over more than two outputs.

B. THEORY

(*a*) *Conditions of Operation*

A block diagram of four interconnected circuit elements is shown in Fig. 1. It consists of two mixers MI and MII and two amplifier–filter units V' and V''.

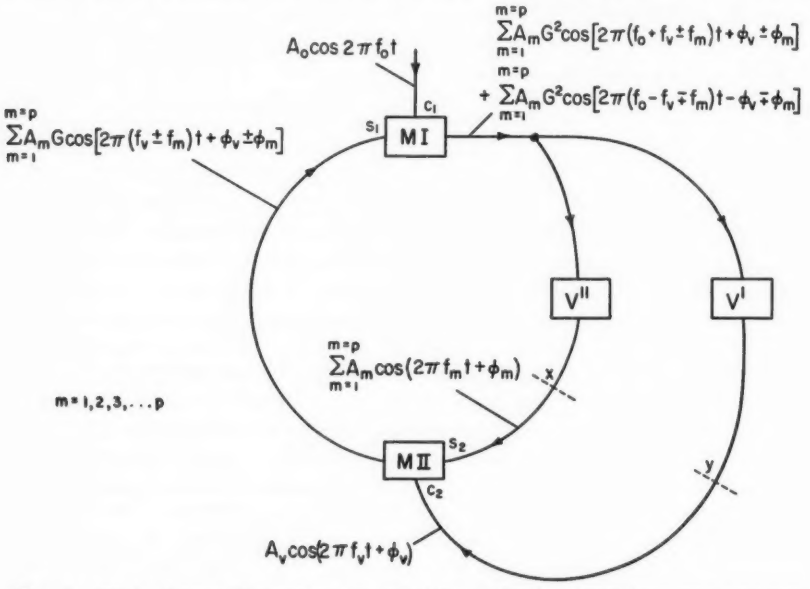

FIG. 1. Block diagram illustrating the principle of the fractional frequency generator employing regenerative modulation.

Assume that each mixer adds to or subtracts from the frequency of the carrier voltage at input c the frequencies of the signal voltages at the input s.

In case of mixer MII, the signal voltage at s_2 is

$$[1] \qquad \sum_{m=1}^{m=p} A_m \cos(2\pi f_m t + \phi_m), \qquad m = 1, 2, 3, \ldots p,$$

and the carrier voltage at c_2 is

$$[2] \qquad A_v \cos(2\pi f_v t + \phi_v)$$

where ϕ_m and ϕ_v are the relative phases. The frequencies are such that

$$[3] \qquad f_1 < f_2 < f_3 \ldots < f_m \ldots < f_p < f_v < f_0$$

where f_0 is the frequency of the carrier voltage at c_1 input of MI.

The signal voltage at the s_1 input of MI is (higher order modulation products are neglected)

$$[4] \qquad \sum_{m=1}^{m=p} A_m G \cos[2\pi(f_v \pm f_m)t + \phi_v \pm \phi_m];$$

G is the conversion gain of the mixer referred to a side-band frequency of the first order, and is assumed to be the same for MI and MII. The carrier voltage at c_1 input of MI, $A_0 \cos 2\pi f_0 t$, is applied to the system from an outside source.

The output voltage of MI is then

$$[5] \qquad \sum_{m=1}^{m=p} A_m G^2 \cos[2\pi(f_0 + f_v \pm f_m)t + \phi_v \pm \phi_m] + \sum_{m=1}^{m=p} A_m G^2 \cos[2\pi(f_0 - f_v \mp f_m)t - \phi_v \mp \phi_m].$$

Assume that the filter in V' is a band-pass filter designed to pass the highest difference frequency only, $f_0 - f_v + f_p$, and the filter in V'' is a low-pass filter designed to pass all frequencies smaller than $f_0 - f_v + f_p$.

Let the filter–amplifier unit V' introduce a gain μ_v' and a phase shift a_v' for the frequency f_v. Likewise, let V'' introduce gains $\mu''_{0-v\pm m}$ and phase shifts $a''_{0-v\pm m}$ for the frequencies $f_0 - f_v \pm f_m$.

If the loop is to be closed at x and y and the system to oscillate, the series of voltage components passed by the filters V' and V'' must equal the series of voltage components assumed at c_2 and s_2 in frequency, amplitude, and relative phase. Also, the frequencies of the series of voltage components must be rationally related to one another in order to maintain a periodic wave form.

As a simple example consider the case where $p = 2$. Then the conditions of oscillation can be expressed by (see equation [5])

$$[6] \qquad \mu'_{0-v+2} A_2 G^2 \cos[2\pi(f_0 - f_v + f_2)t - \phi_v + \phi_2 + a'_{0-v+2}] = A_v \cos(2\pi f_v t + \phi_v)$$

and

$$[7] \qquad \mu''_{0-v-1} A_1 G^2 \cos[2\pi(f_0 - f_v - f_1)t - \phi_v - \phi_1 + a''_{0-v-1}] + \mu''_{0-v+1} A_1 G^2 \cos[2\pi(f_0 - f_v + f_1)t - \phi_v + \phi_1 + a''_{0-v+1}] + \mu''_{0-v-2} A_2 G^2 \cos[2\pi(f_0 - f_v - f_2)t - \phi_v - \phi_2 + a''_{0-v-2}] = A_1 \cos(2\pi f_1 t + \phi_1) + A_2 \cos(2\pi f_2 t + \phi_2).$$

Since there are three voltage components on the left side of equation [7], the frequency of two of them must be equal. Because $f_1 < f_2 < f_v < f_0$, the only possible equality is

$$[8] \qquad f_0 - f_v - f_1 = -(f_0 - f_v - f_2) \text{ or } 2f_0 - 2f_v - f_1 - f_2 = 0.$$

If the parts of the phase which are time dependent are equated in equation [6] and in the remaining components of equation [7] (see equations [9] and [10])

$$[9] \qquad f_0 - f_v + f_2 = f_v,$$

$$[10] \qquad f_0 - f_v + f_1 = f_2,$$

and equation [8] considered, the values of frequencies which can be maintained are found from [8], [9], and [10] to be

$$[11] \qquad \begin{aligned} f_1 &= (1/7)f_0, \\ f_2 &= (3/7)f_0, \\ f_v &= (5/7)f_0. \end{aligned}$$

Then the outputs of MI and MII contain voltage components of the following fractional frequencies:

[12] Output MI: $(1/7)f_0$, $(3/7)f_0$, $(5/7)f_0$, $(9/7)f_0$, $(11/7)f_0$, $(13/7)f_0$, $(15/7)f_0$;
Output MII: $(2/7)f_0$, $(4/7)f_0$, $(6/7)f_0$, $(8/7)f_0$.

In the general case $p = p$, the following values of frequencies can be maintained:

[13] Output MI: $\frac{1}{2p+3}f_0, \frac{3}{2p+3}f_0, \frac{5}{2p+3}f_0, \ldots \frac{6p+3}{2p+3}f_0$ (f_0 excluded);

Output MII: $\frac{2}{2p+3}f_0, \frac{4}{2p+3}f_0, \frac{6}{2p+3}f_0, \ldots \frac{4p}{2p+3}f_0$;

[14] Input c_2 of MII: $\frac{2p+1}{2p+3}f_0$.

The higher order modulation products found at the output of MI or MII will not deliver any new frequency components, because they will be either rejected by the low-pass filter in V'', or they will coincide with the useful frequencies, since the output frequencies of a balanced ring-modulator (4) are

$$kf_c \pm f_s,$$

where f_c is the carrier frequency, f_s the signal frequency, and k an odd integer. Also in this case f_s is rationally related to f_c. For modulator MI, f_s is an even fractional frequency and converts into an odd one for any value of k. Likewise, for modulator MII, f_s and f_c are both odd fractional frequencies and convert into even ones for any value of k.

Equations [6] and [7] can be simplified, observing that $\mu''_{0-v\pm1} = \mu''_{0-v-2} = \mu''$, since the low-pass filter in V'' is flat and introduces equal attenuation to all frequencies in its acceptance band, and that $\mu'_{0-v+2} = \mu_v'$. Also the values of frequencies given by [11] can be inserted into equations [6] and [7], and the corresponding indices of A, ϕ, μ, and a substituted. In order to avoid fractional numbers in the notations, it is assumed that the input frequency f_0 has the value $7f$.

Then, equating voltage components of equal frequencies, equations [6] and [7] take the form

$$[15] \qquad \mu_5' A_3 G^2 \cos(10\pi ft - \phi_5 + \phi_3 + a_5') = A_5 \cos(10\pi ft + \phi_5),$$

$$[16] \quad \mu'' A_1 G^2 \cos(2\pi ft - \phi_5 - \phi_1 + a_1'') + \mu'' A_3 G^2 \cos(2\pi ft + \phi_5 + \phi_3 - a_1'')$$
$$= \mu'' A_1 G^2 \sqrt{1 + (A_3/A_1)^2 + 2(A_3/A_1)\cos(2\phi_5 + \phi_3 + \phi_1 - 2a_1'')}$$
$$\times \cos\left[2\pi ft - \phi_5 - \phi_1 + a_1'' + \tan^{-1}\left(\frac{(A_3/A_1)\sin(2\phi_5 + \phi_3 + \phi_1 - 2a_1'')}{1 + (A_3/A_1)\cos(2\phi_5 + \phi_3 + \phi_1 - 2a_1'')}\right)\right]$$
$$= A_1 \cos(2\pi ft + \phi_1),$$

$$[17] \qquad \mu'' A_1 G^2 \cos(6\pi ft - \phi_5 + \phi_1 + a_3'') = A_3 \cos(6\pi ft + \phi_3).$$

The amplitude conditions are

$$(A_3/A_5)\mu_5' G^2 = 1, \tag{18}$$

$$G^2\mu''\sqrt{1+(A_3/A_1)^2+2(A_3/A_1)\cos(2\phi_5+\phi_3+\phi_1-2a_1'')} = 1, \tag{19}$$

$$(A_1/A_3)\mu'' G^2 = 1. \tag{20}$$

The phase conditions are

$$2\phi_5-\phi_3-a_5' = 0, \tag{21}$$

$$2\phi_1+\phi_5-a_1''-\tan^{-1}\left(\frac{(A_3/A_1)\sin(2\phi_5+\phi_3+\phi_1-2a_1'')}{1+(A_3/A_1)\cos(2\phi_5+\phi_3+\phi_1-2a_1'')}\right) = 0, \tag{22}$$

$$\phi_3+\phi_5-\phi_1-a_3'' = 0. \tag{23}$$

ϕ_1 and ϕ_3 can be expressed in terms of ϕ_5 from relations [21] and [23] and inserted into equations [19] and [22], which can be written then as

$$1 = D\sqrt{1+K^2+2K\cos C}, \tag{24}$$

$$0 = B+C-\tan^{-1}\left(\frac{K\sin C}{1+K\cos C}\right), \tag{25}$$

where

$$\begin{cases} B = a_1''-a_3'', \\ C = 7\phi_5-2a_5'-a_3''-2a_1'', \\ D = G^2\mu'', \\ K = A_3/A_1. \end{cases} \tag{26}$$

A_3/A_1 and ϕ_5 can be found by solving equations [24] and [25] for K and C. The significant values for A_3/A_1 and ϕ_5 are

$$\frac{A_3}{A_1} = \frac{\cos(a_1''-a_3'')\overset{(+)}{-}\sqrt{G^4\mu''^2-\sin^2(a_1''-a_3'')}}{G^2\mu''}, \tag{27}$$

$$\phi_5 = \overset{+}{(-)}\frac{1}{7}\left[\sin^{-1}\left(\frac{\sin(a_3''-a_1'')}{G^2\mu''}\right)\right]+\frac{2}{7}a_5'+\frac{1}{7}a_3''+\frac{2}{7}a_1''. \tag{28}$$

Also ϕ_1 and ϕ_3 are found from relations [21] and [23]

$$\phi_1 = \overset{+}{(-)}\frac{3}{7}\left[\sin^{-1}\left(\frac{\sin(a_3''-a_1'')}{G^2\mu''}\right)\right]-\frac{1}{7}a_5'-\frac{4}{7}a_3''+\frac{6}{7}a_1'', \tag{29}$$

$$\phi_3 = \overset{+}{(-)}\frac{2}{7}\left[\sin^{-1}\left(\frac{\sin(a_3''-a_1'')}{G^2\mu''}\right)\right]-\frac{3}{7}a_5'+\frac{2}{7}a_3''+\frac{4}{7}a_1''. \tag{30}$$

Substituting A_3/A_1 from equation [20] in [27] it is found that

$$A_3/A_1 = G^2\mu'' = \sqrt{\tfrac{1}{2}\{1+2\cos(a_1''-a_3'')\}\overset{(+)}{-}\sqrt{[(\tfrac{1}{2})^2\{1+2\cos(a_1''-a_3'')\}^2-1]}}. \tag{31}$$

Inspection of equation [31] shows that real values for A_3/A_1 are possible only for

$$-60° < (a_1''-a_3'') < 60°. \tag{32}$$

a_1'' and a_3'' are phase shifts through the same amplifier–filter unit and in practice the difference between them is small. Hence $\cos(a_1''-a_3'')$ is nearly equal to unity and $\sin(a_1''-a_3'')$ is equal to the angle in radians, the amplitude condition [31] reduces to

$$[33] \qquad A_3/A_1 = G^2\mu'' = \sqrt{\tfrac{1}{2}(3-\sqrt{5})} = \tfrac{1}{2}(\sqrt{5}-1) \cong 0.618.$$

The expressions [28], [29], and [30] for the relative phases reduce to

$$[34] \qquad \phi_5 \cong (1/7)a_1''+(2/7)a_3''+(2/7)a_5',$$

$$[35] \qquad \phi_1 \cong (3/7)a_1''-(1/7)a_3''-(1/7)a_5',$$

$$[36] \qquad \phi_3 \cong (2/7)a_1''+(4/7)a_3''-(3/7)a_5'.$$

The conversion gain G of a balanced ring modulator increases with increasing carrier voltage to a constant value, approximately equal to $2/\pi$ (4). At the same time the amplification factor μ'' eventually decreases with increasing grid voltage. Then equation [33] is satisfied when the amplitude of oscillation is great enough to balance the losses in the modulator MII with gain in the amplifiers.

Since the carrier voltage of a ring modulator should be N-times greater than the signal voltage (3 to 10 times for satisfactory operation), the required amplification in the V' amplifier–filter unit follows from equation [18] as

$$[37] \qquad \mu_5' = N/G^2 = N\pi^2/4.$$

The phase conditions [34], [35], and [36] are met under all conditions, since ϕ_5, ϕ_1, and ϕ_3 are simply functions of the phase shifts in the amplifier–filter units. Thus no phase adjustment is necessary, either by automatic shift in frequency or by deliberate design.

(*b*) *Relationship Between Amplitude of Oscillation and Input Frequency*

Next the relationship between the amplitudes of the fractional frequencies and the input frequency will be considered. The relative phase ϕ_5 of the carrier voltage at the c_2 input of MII is (see equation [28])

$$[38] \qquad \phi_5 = \frac{2}{7}a_5'+\frac{1}{7}\left[\sin^{-1}\left(\frac{\sin(a_1'-a_3'')}{G^2\mu''}\right)+a_3''+2a_1''\right]$$
$$= \frac{2}{7}a_5'+\lambda,$$

and its amplitude is determined by the response characteristic of V' (see Fig. 2). As the input frequency decreases, a_5' will increase, and to the lower frequency side, the amplitude of the carrier voltage will decrease until the conversion gain G of MII is too small to satisfy the gain condition [33], where the operation of the circuit stops. As the input frequency increases, a_5' decreases to the point where ϕ_5 goes through zero and becomes negative. Then the modulator MII introduces a phase shift of 180°, due to the reversal of the carrier voltage, and it can be seen from equations [31] and [32] that then no real output is possible.

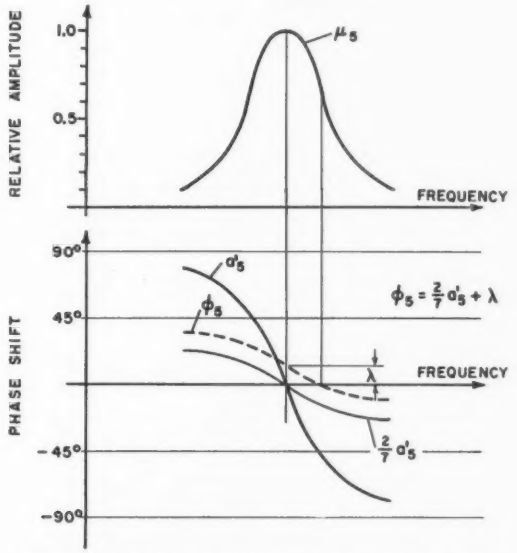

FIG. 2. Amplitude and phase relationship of the amplifier–filter unit V'.

When λ is zero (see Fig. 2 and equation [38]), the point where ϕ_5 equals zero coincides with maximum carrier amplitude where the operation of the circuit stops. For values of λ other than zero, stopping of operation takes place before or after the frequency where the carrier amplitude is a maximum.

C. DISCUSSION OF THE CIRCUIT TYPES $n = (2p+1)/(2p+1+t)$, $t = 2$, $p \geqslant 1$

The circuits investigated above theoretically can be characterized by a value $n = (2p+1)/(2p+1+t)$, $t = 2$, n being the ratio of the carrier frequency of MII to the input frequency and t their difference divided by f.

It was found that in such circuits the odd and the even fractional frequencies are separated, and are available at the output of MI or MII respectively (see voltage components in [12] and [13]). Also for the circuit example $p = 2$ it is seen that the output of MII contains a pair of voltage components having different frequencies and relative phases, which are converted in MI into a modulation component of the same frequency. As a result, the amplitudes of the various fractional frequency components, generated by the circuit, depend on the phase shift in the loop (see equation [31]).

In circuits with $p > 2$ there are $(p-1)$ pairs of voltage components of that type. Hence, in this case also the amplitude of the voltage components is dependent on the phase shift in the loop.

In the circuit case $p = 1$, there are no pairs of voltage components of that type, and hence the amplitude of the fractional frequency components is independent of the phase shift in the loop.

Fig. 3 graphs (*a*), (*b*), and (*c*) show the closed loop systems formed by the flow of energy contained in the various fractional frequency voltage compo-

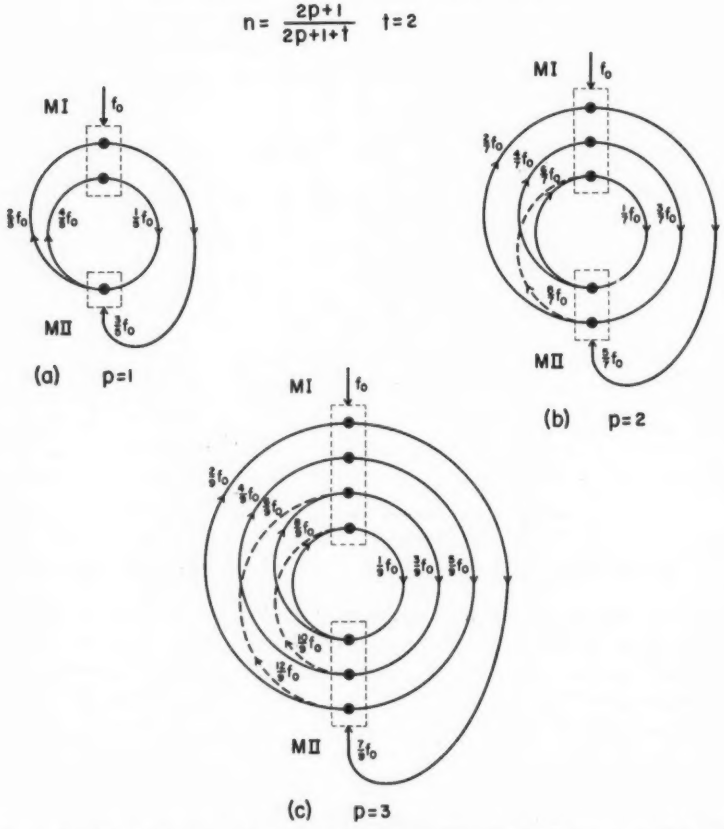

FIG. 3. Graphical representation of the closed loop system formed by the flow of energy contained in the various frequency components of the fractional frequency generator circuits for the circuit types $n = (2p+1)/(2p+1+t)$, $t = 2$, (*a*) $p = 1$, (*b*) $p = 2$, and (*c*) $p = 3$.

nents for the circuit cases $p = 1$, $p = 2$, and $p = 3$ respectively. The dots indicate frequency conversion taking place in *M*I or *M*II.

Simpler, spiral-like loop systems could be obtained if the voltage component paths indicated by dashed lines in Fig. 3, graphs (*b*) and (*c*), were rejected by a low-pass filter cutting off at f_0 and placed at the output of *M*II. Such systems are simpler to study theoretically, and it is found that they have similar properties to the circuit case $p = 1$. However, they are difficult to investigate experimentally as they do not start readily.

D. DISCUSSION OF THE CIRCUIT TYPES $n = (2p+1)/(2p+1+t)$, $t = 4, 6, 8, \ldots 2p$, $p > 1$

In circuits discussed in B and C, the carrier frequency of *M*II is the highest difference frequency of the *M*I inputs, and the difference of the input fre-

quency to the carrier frequency of MII, divided by f, is given by the value $t = 2$. It is found that some circuits are possible for values of $t = 4, 6, 8, \ldots 2p$ and $p > 1$, where the low-pass filter V'' is designed to pass all frequencies smaller than the carrier frequency of MII.

The properties of these circuit types are found to be similar to a large extent to the circuit type $t = 2$. The even and odd fractional frequencies are separated. Also, the number of pairs of voltage components of different frequencies and relative phase, which are converted in MI into the same modulation component, is proportional to p. Fig. 4 shows the closed loop system formed by the flow of energy contained in the various fractional frequency voltage components for the circuit case $t = 4$ and $p = 4$.

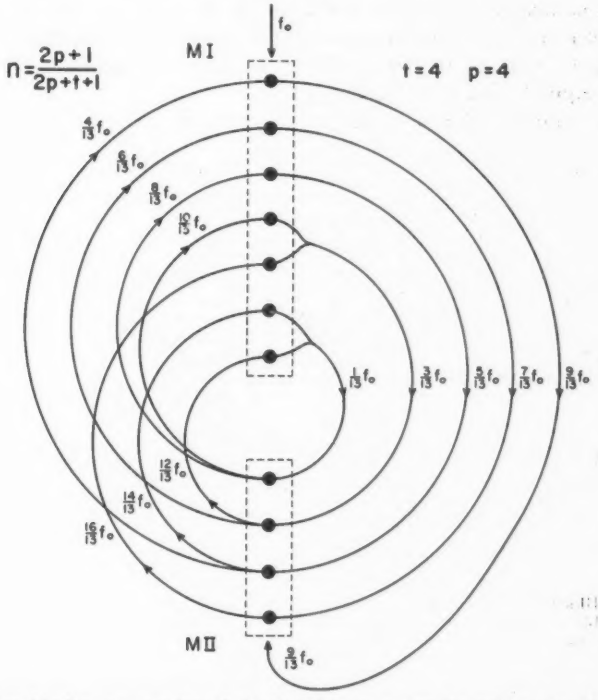

FIG. 4. Graphical representation of the closed loop system formed by the flow of energy contained in the various frequency components of the fractional frequency generator circuit of the type $n = (2p+1)/(2p+1+t)$, $t = 4$, $p = 4$.

Circuits of the types $t = 4, 6, 8, \ldots 2p$ can be useful in certain cases, where it is of advantage to employ low Q resonant elements. The relative separation of the adjacent frequency components from the carrier frequency of MII or from the cutoff frequency of the low-pass filter in V'' increases with t, and therefore the required value of Q, for the resonant circuits in V' and V'', decreases correspondingly.

E. FURTHER CIRCUIT POSSIBILITIES

Up to this point, circuits capable of producing the odd and even fractional frequency components at separate outputs have been investigated. The question now arises whether circuits exist which are capable of generating fractional frequencies distributed on more than two outputs, or where the relative separation of the fractional frequency components from each other, found at one output, is greater than by the factor $s = 2$. Such circuits would require correspondingly less selective filter elements to make the generated frequency components available and could be of value in low frequency applications.

It has been found that such circuits are theoretically possible, if the number of mixers is increased to equal the value of the relative separation factor s. A study of possible circuit arrangements revealed that only very few of them are practical, and in some cases the input voltage must be applied to more than one input terminal of the circuit.

Fig. 5, graph (*a*), shows an example of a circuit arrangement where sepa-

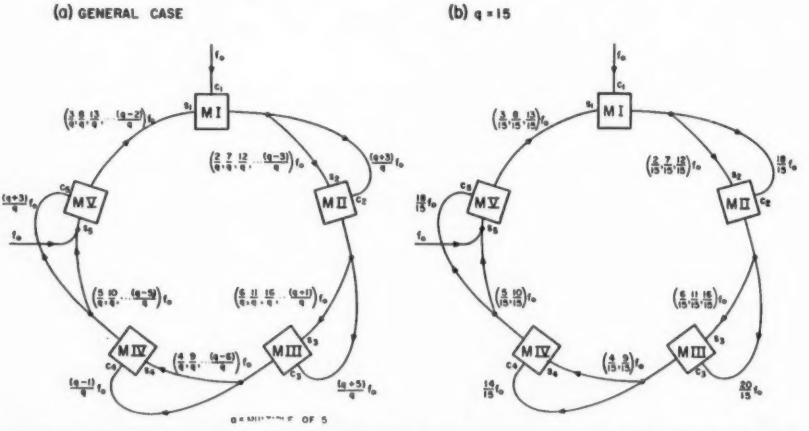

FIG. 5. Block diagram of a fractional frequency generator circuit employing five modulators capable of distributing the various frequency components on five separate outputs; (*a*) general case, (*b*) $q = 15$.

ration of the fractional frequency components by the factor $s = 5$ is realized. It consists of five mixers *M*I, *M*II, *M*III, *M*IV, and *M*V suitably interconnected. Amplifiers and filters are assumed to be inserted in some of the branches to provide loop gain and enough power for the c inputs of the mixers, and to reject the undesired frequencies, respectively. The amplifiers and filters are not shown in Fig. 5. A voltage of frequency f_0 is applied to the c_1 input of *M*I and s_5 input of *M*V at the same time. It can be shown that fractional frequencies of the form $(v/q)f_0$, $v = 2, 3, 4, \ldots (q-1), (q+1)$, $q =$ multiple of 5, are possible in this circuit, and they are distributed in such a way that only certain consecutive fractional frequencies, separated by the factor $s = 5$,

can be maintained in each of the five branches of the main regenerative loop. In Fig. 5, graph (*b*), the fractional frequencies which can be maintained in the circuit are shown for the example $q = 15$.

F. EXPERIMENTAL WORK

(*a*) *Experimental Check of the Theory for the Circuit Type* $n = (2p+1)/(2p+1+t)$, $t = 2$, $p = 2$

Experiments were carried out to verify the results of the theory for the circuit type $n = (2p+1)/(2p+1+t)$, $t = 2$, $p = 2$.

Fig. 6 shows the details of the circuit. The amplifier–filter units in V' and V'' are made up respectively of a 6AG7 pentode tuned stage and a 6SF5 triode

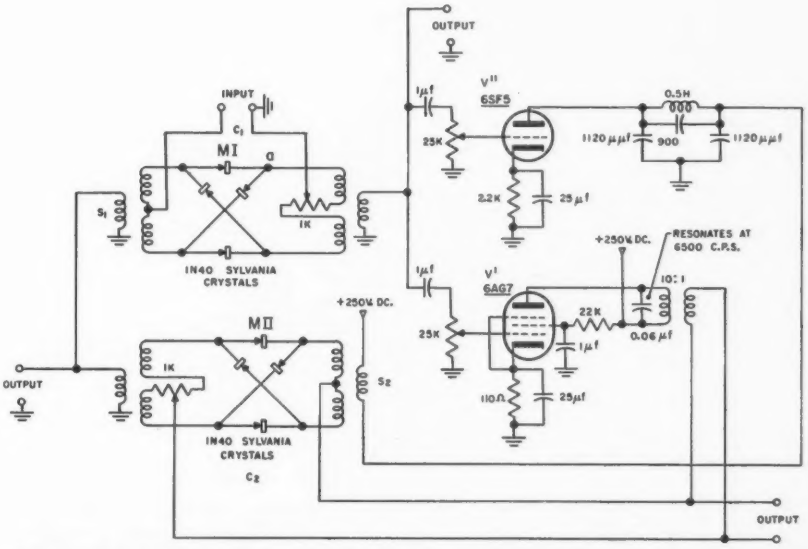

FIG. 6. Circuit diagram of a fractional frequency generator employing regenerative modulations.

with a low-pass filter in the plate circuit. The tuned stage in V' employs a ferroxcube pot-core and has a Q of 35 at the frequency of 6500 c.p.s. The low-pass filter passes all frequencies smaller than 6500 c.p.s.

It was found that the circuit is self-starting when there is sufficient gain in the loop, or when the input voltage is large. As the gain in the loop or the input voltage is reduced, there is a range where starting of operation could be accomplished by shorting to ground the terminal '*a*' of *M*I, thus momentarily introducing useful frequency components into the loop. A slight unbalance of *M*I also improves the starting ability of the circuit. As the gain in the loop or the input voltage is further reduced, starting of operation is impossible.

When the input voltage is increased from its minimum starting value, the amplitude of the fractional frequency $(5/7)f_0$ is found to increase (see left-hand graph (*a*), Fig. 7) and then to remain approximately constant between 1 v. and 6 v. input. Similar behavior is found for the remaining fractional frequencies. The circuit operates in the range 180 v. to 300 v. on the plate for 6.3 v. on the filament and between 4.5 v. to 8.5 v. on the filament for 250 v. on the plate.

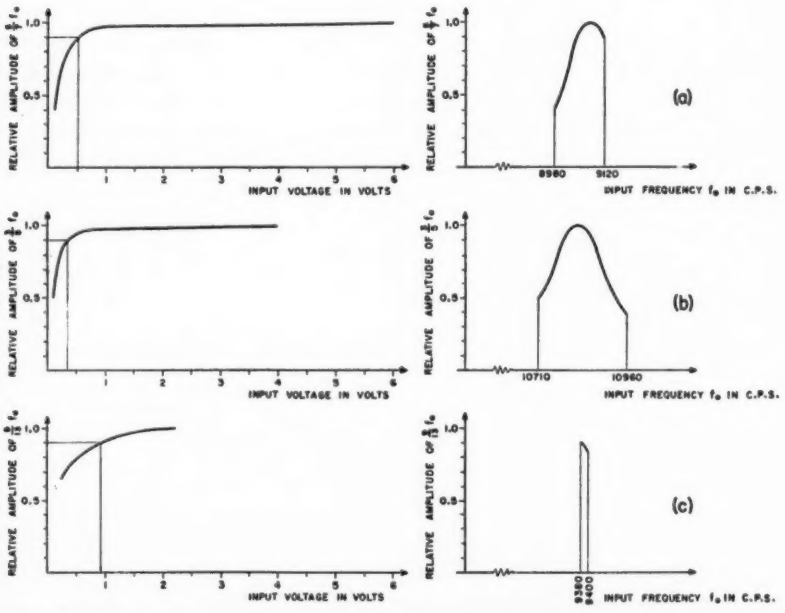

FIG. 7. Relationship between the amplitude of the frequency components, produced in the fractional frequency generator circuit, and input voltage or input frequency respectively. $n = (2p+1)/(2p+1+t)$, (*a*) $t = 2$, $p = 2$; (*b*) $t = 2$, $p = 1$; (*c*) $t = 4$, $p = 4$.

The relationship between the amplitude of the fractional frequency $(5/7)f_0$ and the input frequency f_0 is shown in the right-hand graph (*a*), Fig. 7. The graph of this relationship has the same shape as the resonance curve of the tuned stage in V'. A region of operation was obtained as predicted in the theory, bounded by frequencies 8980 c.p.s. to 9120 c.p.s.

The fractions of the input frequency $f_0 = 9100$ c.p.s. found at the output of MI and MII were measured with a wave analyzer and are shown in graph (*a*) of Fig. 8. It can be seen that the relation [33] is approximately fulfilled, good discrimination between the odd and even fractional frequencies is realized, and the values are in accordance with those given in [12].

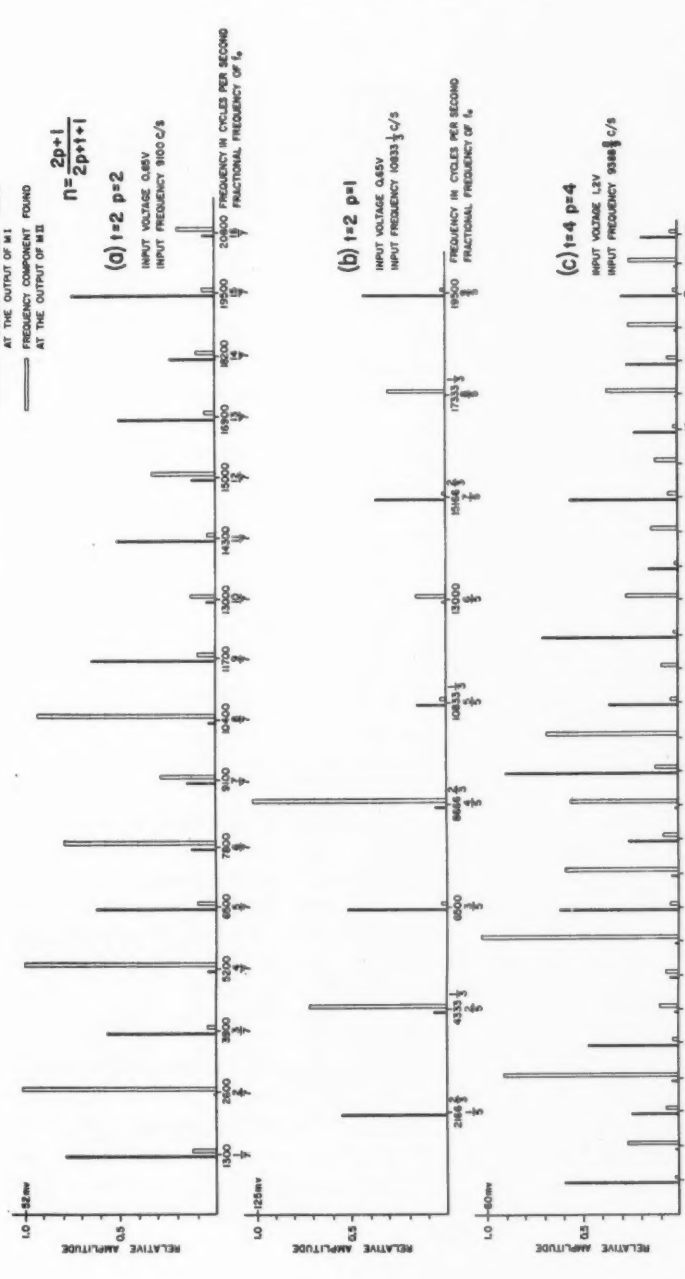

FIG. 8. Frequency spectra of the output voltages of the mixers MI and MII in the fractional frequency generator circuit measured with a wave analyzer. $n = (2p+1)/(2p+1+t)$, (*a*) $t = 2$, $p = 2$; (*b*) $t = 2$, $p = 1$; (*c*) $t = 4$, $p = 4$.

(*b*) *Experimental Results for the Circuit Type*

$$n = (2p+1)/(2p+1+t),\ t = 2,\ p = 1$$

Further circuit types can be investigated experimentally by modifying the band-pass and low-pass filter in the V' and V'' units respectively to pass different frequency spectra, the frequency of the input voltage being left unchanged. The same qualitative results can also be obtained using the original circuit and changing the input frequency correspondingly. For a frequency of about 10,830 c.p.s., applied to the input of the circuit in Fig. 6, an oscillation can be maintained to correspond to the case $t = 2$, $p = 1$.

Starting properties and the relationship between the amplitude of the fractional frequency component $\frac{3}{5}f_0$ and others and the input voltage, for this case, are found to be similar to the case $t = 2$, $p = 2$ (see left-hand graph (*b*), Fig. 7). The circuit operates in the range from 100 v. to 300 v. on the plate for 6.3 v. on the filament, and from 3.5 v. to 8.5 v. on the filament for 250 v. on the plate.

The relationship between the amplitude of the fractional frequency component $\frac{3}{5}f_0$ and the input frequency f_0 is shown in the right-hand graph (*b*) in Fig. 7. Unlike the case $t = 2$, $p = 2$, the discontinuities at 10,710 c.p.s. and 10,960 c.p.s. are both believed to be caused by loop gain smaller than unity at these frequencies.

The fractions of the input frequency f_0 of about 10,830 c.p.s. found at the output of *M*I and *M*II are shown in graph (*b*), Fig. 8.

(*c*) *Experimental Results for the Circuit Type*

$$n = (2p+1)/(2p+1+t),\ t = 4,\ p = 4$$

At the input frequency of about 9390 c.p.s., oscillation can be maintained in the mode $t = 4$, $p = 4$. The relationships between the amplitude of the fractional frequency component $(9/13)f_0$ and the input voltage and input frequency respectively are found to be similar to the cases above, but the input voltage and input frequency ranges for which operation of the circuit is possible are reduced (see graph (*c*), Fig. 7). The circuit operates between 150 v. and 300 v. on the plate for 6.3 v. on the filament and between 4.8 v. and 8.5 v. on the filament for 250 v. on the plate. The fractions of the input frequency f_0 of about 9390 c.p.s. found at the output of *M*I and *M*II are shown in graph (*c*), Fig. 8.

G. CONCLUSIONS

Some circuit types for generation of fractional frequencies of a given frequency using the method of regenerative modulation have been described. A theory has been developed for a circuit designed to produce six fractional frequencies smaller than the input frequency and a number of fractional frequencies larger than the input frequency, and this theory has been confirmed experimentally. In addition, other types of regenerative modulation circuits were discussed and studied experimentally.

It was found that these circuits have properties desirable in applications in multichannel radio communication, synchronization systems, and frequency standard work. The odd and the even fractional frequencies are available at separate output terminals and are of comparable amplitude; they are generated only when the input frequency is applied and they bear a fixed relationship to it. Distortion of the input wave does not influence the wave form of the output components. The generation of the fractional frequencies was found to be unimpaired to a large degree by considerable variations of the power supply and input voltages, and by phase shift in the circuit.

ACKNOWLEDGMENTS

Appreciation is extended to Prof. H. Weber from the Swiss Federal Institute of Technology in Zurich, under whose direction a frequency divider circuit of the type $n = (2p+1)/(2p+1+t)$, $t = 2$, $p = 1$ has been developed (2).

The author wishes also to express gratitude to Dr. G. J. van der Maas for solution of equations [24] and [25], and to Mr. C. F. Pattenson and Mr. J. Swail for checking the manuscript.

REFERENCES

1. HORTON, J. W. U.S. Patent No. 1,690,299. 1928.
2. MAKOW, D. and DIEWALD, H. Frequenzteilung, Diplomarbeit. Swiss Federal Institute of Technology, Zurich. 1950.
3. MILLER, R. L. Proc. I.R.E. 27: 446–457. 1939.
4. TUCKER, D. G. J. Inst. Elec. Engrs. (London), Part III, 95: 161–172. 1948.

AN EVALUATION OF THE RECOVERY THEORY OF CREEP[1]

By H. H. Bleakney[2]

ABSTRACT

The recovery theory of creep was defined by Bailey in 1926 as the balance of the rate of production of strain-hardening by distortion and its removal by thermal action. Three main objections have been raised, as follows: (1) The observation that creep-rupture tests made with light loads frequently reveal lower ductility than similar tests made with heavier loads is inconsistent with the recovery theory. (2) The equicohesive temperature concept is inconsistent with the recovery theory. (3) The experimental evidence for stress-relaxation across grain boundaries as presented by Kê is inconsistent with the recovery theory. In this paper evidence is presented to show that the phenomenon of creep-rupture embrittlement is not necessarily inconsistent with the recovery theory; that the equicohesive temperature concept may be without validity; and that Kê's conclusions are not substantiated by the evidence. It is suggested that the opposing influences of strain-hardening and thermal softening, modified by factors introduced by metallurgical instabilities, are the fundamental verities of creep.

In 1926 Bailey (1) summarized his recovery theory of creep as follows: "The author believes that a rational explanation of the phenomenon of creep is to be found in the balance of the rate of production of strain-hardening by distortion, and the rate of its removal by thermal action". Although it was the first formal written statement of the theory, Bailey's paper probably represented the independent opinions of a respectable number of those metallurgists whose interests and responsibilities had awakened them to the problems of creep. The theory was so simply logical, and followed so inexorably from the facts of work hardening and annealing that it is only reasonable to think that others had reached the same conclusion as Bailey. In discussion the theory was generally accepted as fundamentally correct, although not entirely without reservations. The reservations were mainly prompted by a judicious "wait and see" attitude, based on the wise conclusion that more data were needed, and that final acceptance would depend upon whether or not such data could be reconciled with the proposed mechanism.

As time went on, however, it was observed that many metals did not display the increased ductility in creep-rupture tests which would be a corollary to the theory. This objection was expressed by Tapsell (17) as follows: "If, during the progress of creep, thermal influence were such that it tended to balance out the hardening produced by strain it would be expected that a much greater elongation and reduction of area would be obtained by creep failure after a long period than by rapid failure as in the ordinary tensile test, but such is not usually the case." Sully (16) and Smith (15) both criticize the

[1]*Manuscript received in original form May 14, 1954, and as revised, September 27, 1954. Contribution from the Department of Mines and Technical Surveys, Mines Branch, Ottawa, Ontario. Published by permission of the Deputy Minister.*

[2]*Metallurgist, Physical Metallurgy Division, Mines Branch, Department of Mines and Technical Surveys, Ottawa, Ontario.*

theory and state that there are several objections to it. Both, however, cite only Tapsell's objection, and that is quite understandable since Tapsell's objection alone appears quite sufficient to invalidate Bailey's argument.

It is the purpose of this paper to show that the cited objection to Bailey's basic premise is not valid; to discuss other objections; and to suggest that the opposing influences of strain-hardening and thermal softening, modified by factors introduced by metallurgical instabilities, are the fundamental verities of creep.

INTERCRYSTALLINE EMBRITTLEMENT

The evidence which has accumulated since Tapsell stated his objection to Bailey's theory has shown that many metals not only do not gain ductility but actually become markedly embrittled in creep-rupture tests, and that the embrittlement is a result of fissures forming at the grain boundaries. O.F.H.C. copper, tested in tension at 350° C., will display a reduction in area of 90%, more or less. The same copper, tested in creep-rupture at the same temperature under a load which brings about failure in five hours, may display a reduction in area of only 50% or less. Under the microscope a longitudinal section of this material reveals numerous transverse fissures at the grain boundaries. A variety of hypotheses have been advanced to explain this phenomenon of which copper is merely one example. Zener (20) attributed it to stress concentration caused by stress-relaxation across grain boundaries. Carpenter and Robertson (5) expressed the view that, during recrystallization, grain boundaries are susceptible to fissuring because of the mobility of the atoms at the grain boundaries. Orowan (12) spoke of an amorphous type of plasticity of the grain boundaries. Rotherham (13) suggested that, during creep, flow took place mainly at the grain boundaries which then failed because of strain-hardening. These are just a few examples, but most of those who have written on the subject either state or infer that the mechanism of deformation during creep differs fundamentally from the mechanism in a short-time tension test; and they attribute the embrittlement to this difference. Many believe, with Rotherham, that the deformation, in creep, is confined largely to the grain boundaries. Nearly all agree that the mechanism of strain at low rates and high temperatures is fundamentally different from that occurring at faster rates and lower temperatures. If this is true, then Bailey's theory does not necessarily follow from the known effects of strain-hardening and annealing.

THE EQUICOHESIVE TEMPERATURE

The equicohesive temperature concept is in conflict with Bailey's theory. It grew out of the observation that fine-grained metals at elevated temperatures usually displayed less creep-resistance than coarse-grained metals, while at some lower temperature the reverse effect was found. The conclusion was drawn that at elevated temperatures the grain boundaries are weaker than the grains, while below some lower temperature the grain boundaries are stronger than the grains; hence there must be some intermediate temperature where the grain boundaries and the grains must have equal cohesive strength.

This was called the equicohesive temperature. The explanation for this proposed change in relative strength goes back to Rosenhain's amorphous metal hypothesis. It was argued that the grain boundary material is amorphous, or at least that since the grain boundary atoms are more or less randomly disposed, the grain boundaries behave like viscous fluids, and that they lose viscosity faster than the grains lose slip resistance. Under such conditions adjacent grains, under stress at elevated temperatures, would separate like a jam sandwich, when the two pieces of bread are separated, by flow and rupture of the jam.

The equicohesive temperature concept and the concept that creep-rupture embrittlement is a result of a changed strain mechanism are complementary. The changed strain mechanism envisaged in the latter is, in fact, the viscous grain boundary flow postulated in the former, although this basic idea has been presented in a number of different forms. One can see how each gains support from the other, and one can readily imagine that, in the absence of either phenomenon, the explanation for the other might have taken quite a different direction. Therefore if it can be shown that the viscous grain-boundary concept is untenable as an explanation for creep-rupture embrittlement, then the whole idea of an equicohesive temperature will require re-examination.

THE ROLE OF IMPURITIES

In a recently published paper (3) the author has shown that the viscous grain-boundary hypothesis for creep-rupture embrittlement is untenable. Tests on copper, silver, aluminum, lead, and iron have all contributed evidence indicating that creep-rupture embrittlement is properly attributable to specific impurities in the metal, which become increasingly effective in the course of a test by gradually concentrating at the grain boundaries. There is no evidence to conflict with this conclusion whereas there is weighty evidence opposed to the viscous grain boundary hypothesis. If intercrystalline failure in creep-rupture tests were attributable to viscous flow at grain boundaries then all metals should display this type of failure when tested at comparable strain-rates, and at temperatures which are comparable with respect to some such reference property as their melting points. No such similarity of behavior is observed. On the contrary, many examples of lead have shown completely ductile fractures after hundreds of days to failure; high purity aluminum shows no signs of embrittlement after hundreds of hours to failure; but copper and silver show intercrystalline fissuring and embrittlement in tests involving only a few hundred minutes to failure. Discrepancies of this magnitude cannot be reconciled with any hypothesis which postulates that absolutely pure metals will display intercrystalline embrittlement in creep-rupture tests. On the contrary, the only explanation as yet proposed which agrees with all the facts is that which attributes the embrittlement to the gradual concentration of impurities at the grain boundaries in the course of the test, since it has been shown that the ductility is higher the purer the metal (3).

It can be argued that even though the powerful influence of impurities be

admitted, other factors may also be operating. This argument may be valid, but in the absence of other explanations consistent with all the facts, the impurity concept is the only one which may rationally be adopted, at least as a working hypothesis. Therefore the phenomenon of creep-rupture embrittlement is not a valid objection to Bailey's theory of creep. The change in the disposition of impurities in the course of a test is a metallurgical change for which allowance must be made, but which does not impair the basic soundness of the theory. Under these circumstances, the equicohesive temperature concept loses much of its plausibility. It seems more likely that the so-called equicohesive temperature is, in reality, the temperature at which grain boundary migration becomes appreciable, and this temperature will be lower the finer the grain size. The accelerating influence of recrystallization on creep is now well recognized and it is probably the growth component of recrystallization rather than nucleation which influences the creep rate. Hence boundary migration alone should bring about an increased rate of strain, probably by the mechanism suggested, as follows, by Hanson (9):

"No doubt there is a continual interchange of atoms between neighboring crystals, even if the mean position of the boundary does not greatly change. When atomic movements of this kind take place under the influence of a stress they will, on the average, be most frequent in the direction tending to relieve the stress."

VISCOUS FLOW AT GRAIN BOUNDARIES

Of the other objections to Bailey's hypothesis Kê's work is the most plausible, and is that which appears to have had most influence on metallurgical thought. The essentials of Kê's hypothesis of creep are contained in his paper (10) on "Experimental Evidence of the Viscous Behaviour of Grain Boundaries in Metals". Where Tapsell's objection was of a negative variety, based on the fact that Bailey's theory appeared to be inconsistent with the creep-rupture behavior of metals, Kê's work represents a positive approach. He presented evidence from carefully conducted experiments, the results of which appeared to be quantitatively consistent with the concept of viscous flow at grain boundaries. Proof of such a mechanism would, of course, invalidate Bailey's hypothesis.

The essential features of his work are presented and discussed as follows:

1. The internal friction of high purity polycrystalline aluminum increases rapidly as the testing temperature is raised from 200° C. to 285° C. Above 285° C. the internal friction drops quite rapidly to a position between the minimum and maximum values. Tests on a single crystal of aluminum showed no such maximum in the internal friction but only a very gradual rise with increasing temperatures. Kê explains the occurrence of the maximum in these words, "The internal friction is determined by the product of the distance slipped and the resistance to slip along the grain boundaries. At low temperatures the viscous slip along the grain boundaries is small and therefore the internal friction is small. At high temperatures the resistance to slip along the grain boundaries is small, so again the internal friction is small. Only in an

intermediate temperature range, when both the slip distance and the resistance to slip are appreciable, will the internal friction be appreciable."

2. The second point which Kê advances in support of a viscous grain-boundary concept involves an explanation for the difference in the modulus of rigidity of single-crystal and polycrystalline aluminum at elevated temperatures. Zener (19) has proposed that, in metals under stress, there is a state of stress across grain boundaries, and that this stress gradually relaxes as a result of viscous flow of the grain-boundary atoms. He has evolved an equation $E_R/E_u = \frac{1}{2}(7+5\sigma)/(7+\sigma-5\sigma^2)$, in which E_R is Young's modulus when complete stress relaxation has occurred across grain boundaries, E_u is Young's modulus where no relaxation has occurred, and σ is Poisson's ratio. Kê has converted the ratio into terms of rigidity moduli and has shown it to be 0.636, taking Poisson's ratio for aluminum to be 0.355 at 30° C.

From data obtained during measurements of internal friction, Kê constructed curves relating with temperature the rigidity moduli of single crystal and polycrystalline aluminum. At 450° C. he found that the ratio of the rigidity modulus of the polycrystalline metal to that of the single crystal was 0.67 which is in remarkably good agreement with the ratio of 0.636 forecast by Zener's theoretical calculation, assuming complete stress relaxation across grain boundaries at the temperature used.

3. Kê's third point is based upon determinations of the creep of high-purity aluminum under a constant stress of low magnitude, applied in torsion. The argument appears to be that if viscous flow is the creep mechanism, then the observed creep is characterized by an activation energy. Kê then shows that the observed creep is, in fact, associated with an activation energy of 34,000 calories per mole.

4. The fourth point upon which Kê based his reasoning was derived from experiments on stress relaxation in high-purity aluminum as a function of time at constant strain. The results obtained showing an activation energy of 34,500 cal./mole reflect the influence of the same factors observed in creep at constant stress, but projected on a different plane.

On first reading, the author found considerable plausibility in Kê's conclusions, but after more careful study they appeared to be very much less convincing. In the first place his explanation for the peak in the internal friction curve is based upon premises which can neither be proved nor disproved but which border on the sheerly speculative. On the other hand there is evidence for an alternative explanation. After passing the peak, the curve levels off at a value of the internal friction which is about one third of the maximum. Kê explains this levelling-off as follows: "It has been found that the high temperature side of the internal friction curve is quite sensitive to the amount of pre-anneal cold work, indicating that some other effects connected with the cold work come in at very high temperatures." However, there is reason to believe that plastic flow taking place during the test may be the major influence in the whole experiment. The longitudinal load on the wire was 54.5 gm./mm.^{2}, and later in this discussion it will be shown that a

load of that magnitude is above the elastic limit of some of the grains. The fact that a load three times as great as that applied yielded approximately the same results is an indication that the metal has been plastically deformed by the smaller load rather than the reverse since the greater load is well above the elastic limit.

With respect to the second point, outlined above, the figures shown in Table I are quite irreconcilable with Kê's explanation for the sharp drop in the modulus of rigidity of polycrystalline aluminum at temperatures above about 200° C.

TABLE I

99.99% ALUMINUM, 0.033 IN. DIAMETER, TESTED AT 450° C. BY THE METHOD USED BY KÊ TO OBTAIN FIG. 1

Time from application of load	Deflection (cm.) of light beam on scale
0	0.80
30 sec.	1.08
60 sec.	1.20
2 min.	1.32
5 min.	1.52
10 min.	1.72
20 min.	1.93

According to Kê the creep recorded in Table I is due to stress-relaxation across grain boundaries, just the same as the creep at constant stress and stress-relaxation at constant strain discussed in his paper; and this is the same stress-relaxation to which he attributes the peak in the internal friction curve and the drop in the modulus curve. His curve of modulus of rigidity versus temperature was obtained by the same kind of experiment employed in the internal friction determinations. In these experiments the wires were oscillated with a frequency of about one cycle per second. From this fact it follows that if there were such a thing as stress-relaxation across grain boundaries, it would have to take place in less than half a second, since in about half a second the stress rises from zero to a maximum and back to zero again. Kê pointed out that Zener's equation $G_r/G_u = 2(7+5\sigma)/5(7-4\sigma)$ requires that stress relaxation be complete, and he believes that in his experiments on the modulus, stress relaxation was complete, even in the short time available, at 450° C. Table I shows that this presumed stress-relaxation was only beginning after half a second and was still going quite rapidly after 20 min.

Another point occurs in connection with the creep and relaxation experiments. The indications that the processes are associated with activation energies of 34,000 and 34,500 cal./mole respectively are consistent with the viscous flow concept but not uniquely so. Chang and Grant (6) have demonstrated that grain boundary migration is a very important factor in creep, and Turnbull (18) reports an activation energy for grain-boundary migration in high-purity aluminum of 19,700 cal./mole between 400 and 500° C.

Burke (4) has shown that it would be considerably higher at the lower temperatures involved in Kê's work. Therefore in the complete absence of viscous flow the same activation energy might well have been observed.

EVIDENCE OF PLASTIC FLOW

The major criticism of Kê's work springs from the doubt that his experiments were carried out under the conditions which he himself laid down as necessary to the validity of his conclusions. These conditions are quoted as follows:

"1. There should be no permanent set after the stress is removed and all the effects should be recoverable after a sufficiently long period of time.

2. The observed anelastic effects should be linear with the applied stress or prior strain. Thus the internal friction and the dynamic rigidity should be independent of the amplitude of vibration; the creep per unit elastic strain (or instantaneous strain) should be independent of the magnitude of the elastic strain; and the stress relaxation per unit initial stress should be independent of the magnitude of the initial stress."

The stringency of the requirement that an author must establish the validity of his experimental method is nowhere more exacting than when, as in the present case, his conclusions depend upon highly circumstantial evidence. Kê's only claim that he fulfilled the first condition, quoted above, is the evidence reproduced in Fig. 1 which he discussed in a brief paragraph at the bottom of page 540 of his paper. This evidence is so far from proving the reliability of the method that it might equally well, or better, be used to argue that the stresses used were not entirely in the elastic range. Both the creep curve and the recovery curve are what would be expected if the applied stress was just above the yield stress of the small percentage of the grains most favorably

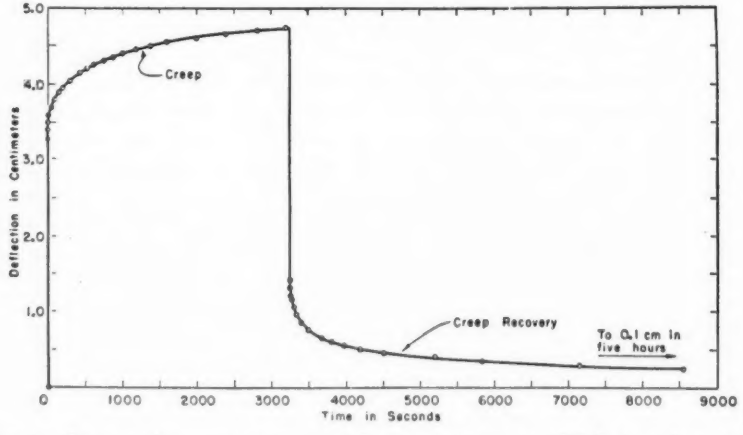

FIG. 1. Creep under constant stress, and creep recovery at 175° C. in polycrystalline aluminum. Reproduced from Kê's paper.

oriented for crystalline slip (14). The stress relief resulting from minute slip in these grains would be counterbalanced by stress intensification in the rest of the sample. The resulting elastic strain-increment would lead to further plastic flow and so the whole process would be consistent with the shape of the creep curve shown in the figure. Upon removal of the load, the plastically distorted grains would be placed under compression while residual tensile stresses would remain in the rest of the sample. The over-all result would be a reversal of the creep curve, creep recovery occurring as shown with a small but finite permanent set. Kê implies that somewhere between five hours and infinity the curve joins the time axis. From its appearance one would be more inclined to believe that the curve is approaching a constant finite value of residual strain, and this conclusion is supported in a recent paper by Betteridge (2). The evidence contained in Fig. 2 shows that in all the experiments,

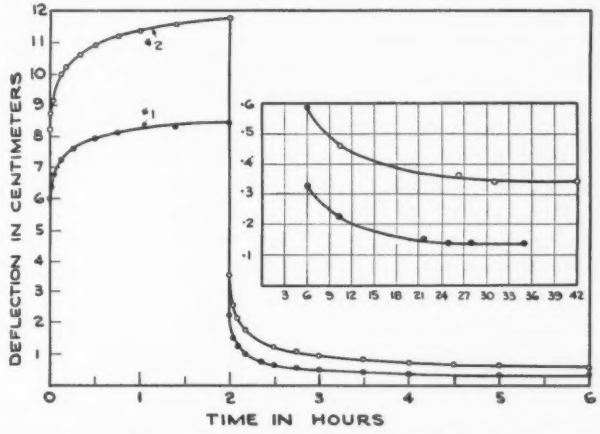

FIG. 2. Curves obtained in the author's laboratory duplicating the experiment illustrated in Fig. 1, except for the higher stresses employed. Note that the curves are continued in the inset portion of the figure, with greatly expanded deflection axis and contracted time axis.

including Kê's (Fig. 1), the metal did, in fact, take a permanent set. Therefore Kê's experiments were conducted in the plastic range of the material and his results cannot properly be attributed to anelasticity.

Some available data furnish additional evidence which suggests that the experiments under discussion did not meet the specified conditions. The highest instantaneous deflection used in any of the experiments was reported to be just under 8 cm., and the lowest is the 3.2 cm. shown in Fig. 1. From the figures given in the paper, these deflections correspond with strains of 2×10^{-5} and 8×10^{-6} respectively. Taking the modulus of rigidity of aluminum as 2700 kgm./mm.^{2}, these strains would result from stresses of 0.054 kgm./mm.^{2} and 0.022 kgm./mm.^{2} respectively. Miller and Milligan (11) have determined the critical shear stress on single crystals of 99.90 and 99.95% pure aluminum. They reported the results shown in Table II.

TABLE II

Temp., °C.	Purity, %	Critical shear stress, kgm./mm.²
24	99.90	0.113
23	99.95	0.050

The great influence of impurities shown in Table II cannot, of course, be safely extrapolated to lower values, but it is clear that metal containing less than 0.01% impurities would have a critical shear stress much lower than 0.050 kgm./mm². Two other considerations indicate the probability that a strain of 8×10^{-6} does not reflect a stress less than the yield stress for those crystals in the aggregate most favorably oriented for slip. There is no doubt that the apparatus used by Miller and Milligan was highly sensitive and their experiments impeccably conducted, but Kê's apparatus was the most exquisitely sensitive yet devised; and it is a platitude that the determination of elastic limits is a function of the sensitivity of the apparatus used. A second consideration has to do with the influence of temperature on the critical shear stress. Miller and Milligan (11) have shown an increase of the critical shear stress of 99.90% pure aluminum, with rising temperature from atmospheric up to about 250° C.; but for 99.95% pure aluminum, the effect is negligible within that temperature range. It is not unreasonable to conclude that the critical shear stress of the 99.991% aluminum used by Kê would decrease with rising temperature.

The second major criticism of Kê's work is related to the first and arises from his use of 99.2% aluminum in his single crystal experiments. It might be argued that the effect of impurities could be neglected so long as the experiments are carried out within the elastic range of the material. Even on this assumption, however, it is clearly injudicious to introduce, deliberately, an unnecessary variable. When, as in the present case, such an assumption is highly questionable, failure to use identical materials in the comparison is inexcusable. Had 99.991% aluminum been used for the single crystal experiments the area of doubt, which embraces all the experiments, would have been reduced to very small dimensions. As it is, the fact that Kê undertook the much more difficult job of making single crystals from impure aluminum very greatly enlarges the area of doubt.

CONCLUSION

After surveying all the evidence, one must conclude that Kê's data are of great value and importance, and that they can be put to excellent use; but one must also conclude that the inferences which he draws have not been substantiated. On the other hand, it is a corollary to the viscous grain boundary hypothesis that all metals must disintegrate by the formation of fissures at the grain boundaries when strained at low rates and elevated temperatures. It has been shown that all metals do not behave in this way.

Virtually all the objections to Bailey's theory are comprehended by Tapsell's observation on creep-rupture embrittlement, Kê's evidence of viscous flow, and a critique by Orowan (12) which was answered by Cottrell and Aytekin (7). Since these objections have been shown to be without foundation, little reason now exists to deny the validity of the concept that the fundamental influence at work in creep is the balance between strain-hardening and thermal softening. Not only is there little reason to deny it, there is now good reason to assert it. A paper by Cottrell and Aytekin (7) on the creep of pure zinc very elegantly confirms the theory for steady-state flow. Digges (8) concluded a discussion of their paper as follows:

"The results of numerous experiments appear to agree fairly closely with the proposed theory, and the theoretical and experimental evidence presented in this paper justifies the well-known assumption that steady-state flow is a result of a balance between strain-hardening and thermal softening."

Cottrell and Aytekin point out that primary creep appears to be complicated by an energy barrier, which is dependent on both strain-hardening and thermal softening. With this modification, then, Bailey's theory applies also to primary creep.

Bailey's theory, by itself, cannot very usefully be applied to any practical problem. As Cottrell and Aytekin point out in the introduction to their paper, creep is usually made up of several distinct mechanisms of flow, one or more of which may operate either simultaneously or consecutively and which include such effects as slipping, twinning, recovery, recrystallization, grain-boundary, and constitutional changes. The recovery theory is directly applicable only to metallurgically stable materials; and this restriction strictly applied would confine the application to single crystals of pure metals. The effects of alloys, grain boundaries, and undissolved constituents so far overshadow the influence of strain-hardening alone that control of creep depends upon research on and increased knowledge about such factors as those mentioned. At the present moment, in the author's laboratory, a creep test on 99.98% silver has just been completed in which the creep-rate was only one tenth that of a previous test on the same material. The only difference between the two was that the former was annealed at 1275° F. and the latter at 600° F. This striking result must be attributable to the action of impurities, grain boundaries, or both, and emphasizes the need for information on such factors. However, if research on such lines is to be profitable, it must be based on a foundation established by knowledge of the fundamental facts. Otherwise no end of time and money may be dissipated through groping in blind alleys. It is the author's belief that Bailey's theory is the proper foundation on which an understanding of the controlling mechanism of creep may be erected.

REFERENCES

1. Bailey, R. W. J. Inst. Metals, 35: 27–40. 1926.
2. Betteridge, W. J. Inst. Metals, 82(4): 155. 1953.
3. Bleakney, H. H. Can. J. Technol. 30: 340–351. 1952.
4. Burke, J. E. Atom movements. American Society for Metals, Cleveland. 1951. p. 220.

5. CARPENTER, H. and ROBERTSON, J. M. Metals. Oxford University Press, London. 1939. pp. 193–194.
6. CHANG, H. C. and GRANT, N. J. J. Metals, 5(2): 305–312. 1953.
7. COTTRELL, A. H. and AYTEKIN, V. J. Inst. Metals, 77: 389–421. 1950.
8. DIGGES, T. G. Metal Progr. 59(2): 294. 1951.
9. HANSON, D. Trans. Am. Inst. Mining Met. Engrs. 133: 49. 1939.
10. KÊ, T. S. Phys. Rev. 71: 533–546. 1947.
11. MILLER, R. F. and MILLIGAN, W. E. Trans. Am. Inst. Mining Met. Engrs. 124: 235. 1937.
12. OROWAN, E. J. West Scot. Iron Steel Inst. 54: 60. 1946–47.
13. ROTHERHAM, L. A. Creep of metals. Institute of Physics, London. 1951. p. 68.
14. SCHMID, E. and BOAS, W. Plasticity of crystals. F. H. Hughes & Co., Ltd., London. 1950. p. 111.
15. SMITH, G. V. Properties of metals at elevated temperatures. McGraw-Hill Book Company, Inc., New York. 1950. p. 100.
16. SULLY, A. H. Metallic creep and creep resistant alloys. Butterworth's Scientific Publications, London. 1949. p. 79.
17. TAPSELL, H. J. Creep of metals. Oxford University Press, London. 1931. p. 59.
18. TURNBULL, D. Trans. Am. Inst. Mining Met. Engrs. 191: 662. 1951.
19. ZENER, C. Phys. Rev. 60: 906–908. 1941.
20. ZENER, C. Elasticity and anelasticity of metals. University of Chicago Press, Chicago. 1948. p. 158.

THE BLISTERING OF PAINT IN THE PRESENCE OF WATER[1]

By J. M. Kuzmak and P. J. Sereda

ABSTRACT

Experiments on the blistering of paint on wood in the presence of water were carried out. It was found that the paints which blistered when subjected to a temperature gradient blistered also when placed in water kept at a constant temperature. Experiments using fluid pressures were carried out also. With each paint, whether or not it blistered when subjected to a temperature gradient, the presence of water at the wood–paint interface was found to have reduced the fluid pressure necessary to produce blisters.

INTRODUCTION

Although it has been known for some time that the blistering of paint on wood is in some way associated with the presence of moisture, neither the mechanism by which the moisture is transferred through the wood nor the mechanism by which the blisters are formed is known. Adhesion measurements show that it takes a pressure of 200 to 500 p.s.i. to pull a dry paint film away from the substrate. To account for pressures of this magnitude during blistering, Dunn (3) has suggested that osmosis and osmotic pressure may be involved. Hopkins and Smart (4) state that, in addition to moisture, a temperature gradient is necessary. One of their experiments consisted of fastening a wooden panel, painted with ordinary linseed oil house paint, to the open side of a container which was then filled with water so that the unpainted back of the panel was in continuous contact with water under a slight head. There was no sign of blistering during a period of 13 days. A temperature gradient applied across a similar panel in a somewhat similar apparatus readily produced blisters. Hopkins and Smart state, "No matter how wet the back of the siding, blistering does not occur unless there is a temperature differential." On the basis of this observation, Babbitt (1) suggests a mechanism which will lead to a transfer of moisture similar to osmosis and which will give rise to pressures of the same magnitude. An equation is presented by means of which the pressures can be calculated. The theory is interesting not only because it accounts for the large pressures thought necessary to produce blistering but also because it may represent an advance in the understanding of the mechanism of moisture transfer.

The present paper describes an investigation of the observation by Hopkins and Smart that blistering does not occur unless there is a temperature difference. Also, related experiments on fluid pressures necessary to produce blisters are described.

MATERIALS AND APPARATUS

Materials

The following paints which represent a wide range of susceptibility to blistering were used:

[1]*Manuscript received September 2, 1954.*
Contribution from the Division of Building Research, National Research Council, Ottawa, Canada. Issued as N.R.C. No. 3453.

No. 1—Composition: Titanium dioxide 16.7%, zinc oxide 34.2%, basic carbonate white lead 34.2%, and magnesium silicate 14.9% by weight of total pigment, in linseed oil;
No. 2—A commercial, red, floor enamel;
No. 3—Composition: Zinc oxide 86% and magnesium silicate 14% by weight of total pigment, in linseed oil;
No. 4—A commercial, black, vinyl resin paint.

White pine was used as the substrate material. In order to ensure that the pressure (described in the following section) at the wood–paint interface was equal to the applied pressure, it was necessary to select a wood which was very permeable. The wood selected permitted both air and nitrogen as well as water to pass freely through unpainted samples at a pressure of 1 p.s.i. (see Fig. 4). All the samples were taken from the same flat-sawn board.

Only distilled water was used.

Apparatus

Three main pieces of equipment were used.

(*a*) The temperature gradient apparatus is shown in Fig. 1. A circular, porous, ceramic plate, *A*, was sealed into a retaining metal ring, *B*, which supported the plate inside a large evaporating dish, *C*. The evaporating dish

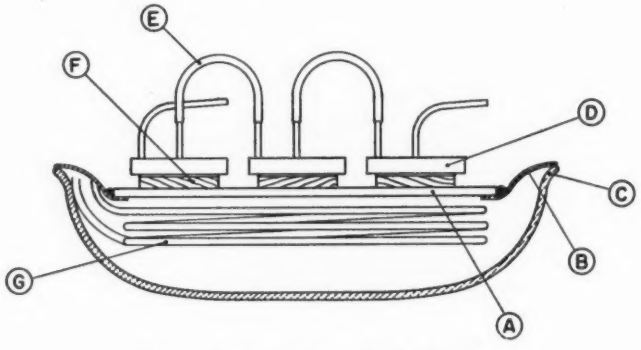

FIG. 1. Temperature gradient apparatus.

was filled with water so that there was contact between the bottom of the ceramic disk and the water. The water was heated to any given temperature by means of a copper heating coil, *G*. The temperature of the hollow cooling plates, *D*, made of brass and joined together by rubber tubing, *E*, was controlled by circulating water from a constant temperature bath. The apparatus could handle seven samples, *F*, at one time.

(*b*) The apparatus used to produce blisters, using nitrogen, is shown in Fig. 2. The unit consisted of a brass cylinder, *A*, machined to provide a compression seal against the sample, *B*, and thus serve as a pressure chamber. The samples were cut to fit closely into a rubber ring, *C*. The tightening of a

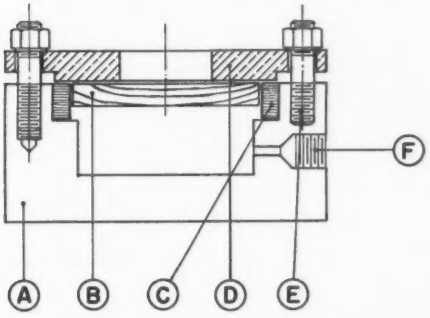

FIG. 2. Apparatus to produce blisters, using nitrogen.

brass ring, *D*, with three screws, *E*, provided an adequate edge seal to nitrogen. The brass unit was connected, at the point *F*, to a nitrogen cylinder and a pressure gauge by copper tubing and standard brass fittings.

(*c*) The apparatus to determine the pressure of water required to produce blisters is shown in Fig. 3. The sample, *A*, was sealed to a brass plate, *B*, which had a 1-in. hole at the center. An adequate seal between the sample and the plate was produced by a rubber gasket, *C*, when a brass retaining ring, *D*, was tightened against the sample by means of three screws, *E*. A seal between the brass plate and a cylindrical lucite chamber, *F*, was provided by another rubber gasket, *G*, when six screws, *H*, were tightened. The copper tube, *J*, was connected to the source of pressure.

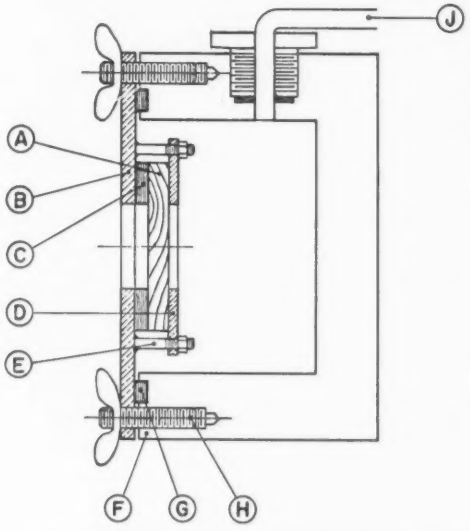

FIG. 3. Apparatus to produce blisters, using water.

EXPERIMENTS AND RESULTS

The samples were prepared in each case by brushing on three coats of the paint to a board $\frac{1}{4}$ in. thick. The thickness of the paint films when dry varied from approximately 0.003 to 0.005 in., depending on the paint. When the paint had aged for the desired length of time, the board was cut into disks 2 in. in diameter. Each disk was used for only one test.

To determine whether blisters could be produced without a temperature gradient, samples were placed in a covered vessel of water maintained at a constant temperature. Some of the samples were placed with the painted side down, others with the painted side up. The samples were kept immersed $\frac{1}{2}$ in. below the surface of the water by means of a screen which could be fixed at any chosen height. In another experiment, the samples were allowed to float. In all cases, paints No. 1 and No. 3 blistered within 24 hr. The blistering of paint No. 1 is shown in Fig. 5. Paints No. 2 and No. 4 did not blister in seven days at which time the experiment was discontinued.

In the above experiment, as in all the experiments reported in this paper, each test was carried out using five or more samples of any one paint. This was done to serve as a check and to help eliminate any spurious observations which might arise because of any local variations in the properties of the wood.

In studying the effect of temperature, the gradient across the $\frac{1}{4}$ in. sample was 50° F. (53° to 103°), each temperature being held constant within 0.5° F. as determined by copper–constantan thermocouples. The samples were placed on the porous plate of the temperature gradient apparatus with the painted side toward the cold plate. Filter paper was placed between the paint surface and the cold plate in order to allow the blisters to form properly. It was found that, without the filter paper, the blisters were flattened by the weight of the plate. As shown in Table I, paints No. 1 (see Fig. 6) and No. 3 blistered while No. 2 and No. 4 did not.

It is interesting to compare the data obtained when the samples were placed in water held at a constant temperature with those obtained when the

TABLE I

THE BLISTERING OF PAINT DUE TO A TEMPERATURE GRADIENT AND DUE TO FLUID PRESSURES

Paint	Age	Blistering due to temperature gradient	Pressure of nitrogen required to produce blisters (p.s.i.)	Pressure of water required to produce blisters (p.s.i.)
No. 1	5 months	Marked in 5 hr.	>500	20
	4–5 days	Marked in 1 hr.	60–80	15
No. 2	5 months	None in 6 days	>500	125
	4 days	None in 7 days	150–200	25
No. 3	19 days	Marked in 5 hr.	250–>450	15
No. 4	$1\frac{1}{2}$ months	None in 7 days	180–225	25
	5 days	None in 7 days	110–120	20

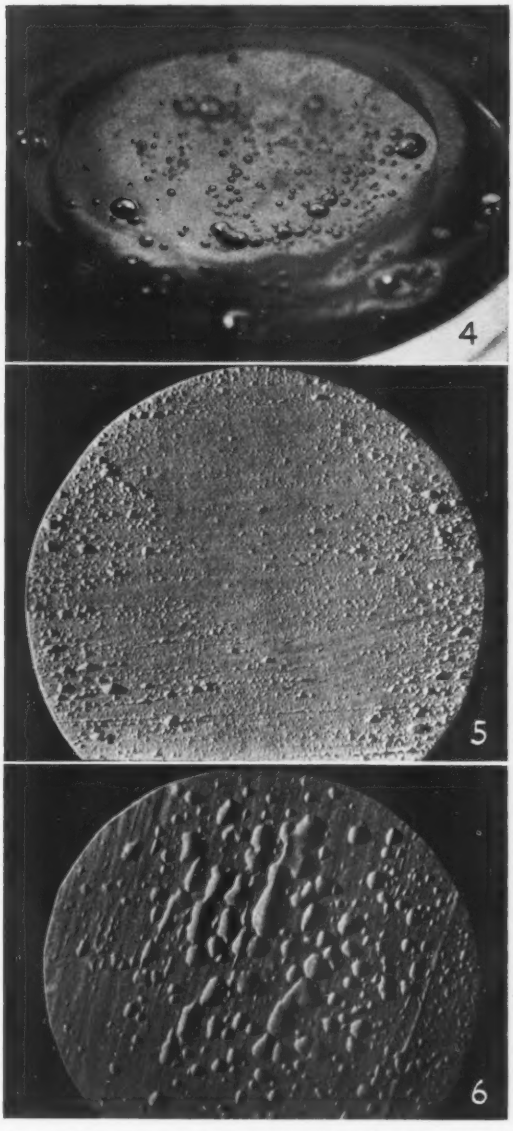

FIG. 4. Air bubbling through water after passing through a wood sample.
FIG. 5. The blistering of paint No. 1 shown by a sample placed in water at a constant temperature.
FIG. 6. The blistering of paint No. 1 shown by a sample subjected to a temperature gradient.

samples were subjected to a temperature gradient. It is seen that paints No. 1 and No. 3 which blistered in the first experiment, blistered in the second also, and that paints No. 2 and No. 4, which did not blister in the first, did not blister in the second. The conclusion, on the basis of the above evidence, would seem to be that the mere presence of water at the wood–paint interface is in some way responsible for the blistering, and that the role of the temperature gradient is probably secondary.

The fact that blistering occurred without a temperature gradient in the experiments reported here appears to contradict the observation of Hopkins and Smart reported earlier. It is possible that, in their experiments with no temperature gradient, the wood was too impervious to allow an appreciable amount of water to reach the wood–paint interface. Preliminary tests with various woods carried out during the present investigation showed that the wood underneath the paint was comparatively dry in those cases where a paint known to blister within a certain time failed to do so within that time.

In order to determine whether and to what extent the presence of water affected the strength of the bond between the wood and the paint, the pressure of nitrogen and the pressure of water required to produce blisters were measured. The pressure of nitrogen was taken as a measure of the strength of the bond before it was affected by water, and the pressure of the water as a measure of the strength after it had been affected by the water.

In the test for blistering using the pressure of nitrogen, the samples were placed in the apparatus shown in Fig. 2. Tightening down the brass ring top forced the rubber against the sample thus forming a good seal. Any small, slow leaks at the seal were not important since they did not affect the applied pressure. The applied pressure was controlled by means of a reducing valve on the nitrogen cylinder. Up to 200 p.s.i., the pressure was read on a low range helicoid gauge; beyond this, the pressure was read on the gauge mounted on the reducing valve. Pressures in excess of 500 p.s.i. could not be used because the wood began to fail at this point. The pressure was increased at the rate of approximately 1 p.s.i. per second. In the case of paints No. 1, No. 2, and No. 3, the rate was found to have no effect on the pressure needed to produce blisters. In the case of paint No. 4, when the rate was decreased by a factor of 10, blistering occurred at a slightly lower pressure. This behavior is very likely associated with plastic flow of the paint film.

To determine the pressure of water required to produce blisters, the samples were placed in the apparatus shown in Fig. 3. When the unit was assembled as already outlined, the chamber was filled with water so that the entire unpainted side of the sample was in contact with water. The air pressure applied to the water was controlled by a reducing valve and measured with a helicoid gauge. Blistering occurred within 10 min. The results of this test along with those described in the preceding paragraph are given in Table I. From this table, it is seen that the pressures required in the two different tests differ by a factor which varies from 4 to 20 or more, depending on the type and age of the paint. Paint No. 1, when pushed by nitrogen and by water, blistered as shown in Figs. 7 and 8 respectively.

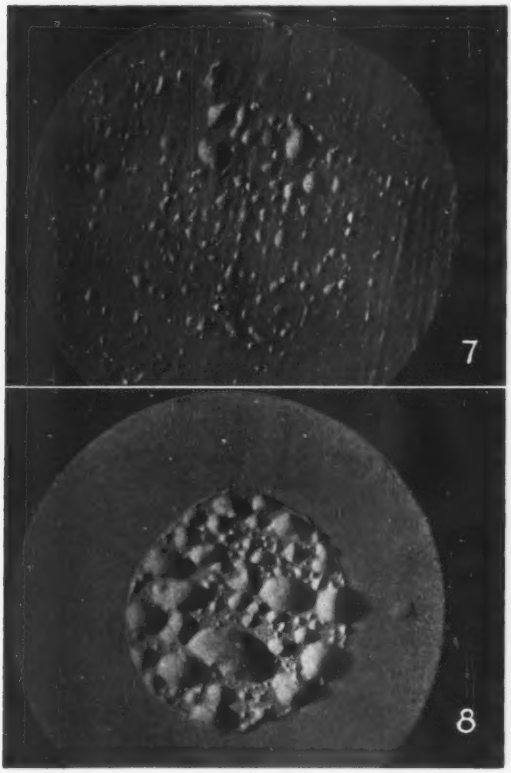

FIG. 7. The blistering of paint No. 1 shown by a sample subjected to a pressure of nitrogen.
FIG. 8. The blistering of paint No. 1 shown by a sample subjected to a pressure of water.

Tests to determine the effect of water kept in contact with the paint surface (painted side of the sample) were carried out. Paints No. 1 and No. 3 were used. The samples were mounted in the apparatus shown in Fig. 3. Water was placed on the painted surface. No water was placed in the reservoir, and an air pressure of 15 p.s.i. was applied to the unpainted side of the sample. The experiment was continued uninterrupted for three days. No blisters developed although the paint surface was affected to the extent that a few small holes developed which allowed some air to pass and bubble through the water. Water was then placed in the reservoir to cover the unpainted side, and a pressure of 15 p.s.i. was applied. Blistering occurred within 30 min. A similar test was carried out but, at the end of three days, instead of water being placed in the reservoir, the air pressure was raised to 100 p.s.i. No blistering was observed. The indication is that water on the surface of the paint did not greatly affect the bond between the paint and the wood.

DISCUSSION OF RESULTS

As already mentioned, the fact that the paints which blistered when subjected to a temperature gradient blistered also when immersed in water at constant temperature leads to the conclusion that the phenomenon is due primarily to the presence of water at the wood–paint interface and not to the existence of a temperature gradient. The results of the experiments in which the pressures required to produce blistering were measured are consistent with the above conclusion. It appears that the main effect of the temperature gradient is to bring water to the wood–paint interface. Many of the samples subjected to the temperature gradient were broken up and visually examined. A very pronounced moisture gradient was observed in all samples exposed for only a few hours. There was a color gradation across from the hot to the cold side, the color deepening toward the cold side, indicating a higher moisture content. In many instances, the water could be squeezed out of the cold side but not out of the other. With time this gradient disappeared as the whole sample approached saturation.

Assuming that the sample became saturated, it is interesting to calculate, using Babbitt's equation (1), the hydrostatic pressure that should be built up as a result of the temperature gradient. The equation is

$$\pi = \frac{RT}{V} \ln \frac{p}{p_0}$$

where, in this case,

π is the excess pressure,
R is the gas constant,
T is the absolute temperature of the cold face,
V is the molar volume of water,
p is the vapor pressure of water at the temperature of the hot face,
p_0 is the vapor pressure of water at the temperature of the cold face.

Taking the temperature gradient as 12°–39° C. (measured as 53°–103° F.), the following values were substituted into the equation: $R = 82.07$ cm.^{3} atm./degree, $T = 285°$ A., $V = 18$ cm.^{3}, $p = 52.4$ mm. Hg, $p_0 = 10.5$ mm. Hg. The value of π is then calculated as 2090 atm. This tremendous pressure could not have been exerted on the paints because even those which failed to blister as a result of the temperature gradient did blister when pushed by water at a pressure of 25 p.s.i. or less. The exception occurred with paint No. 2 which was five months old and in this case blistering occurred at a pressure of 125 p.s.i.

It should be noted that failure to detect anything like the predicted pressure does not invalidate the theory as far as potential forces are concerned. It may be that, within the wood itself, the confining forces which would be necessary to realize any build-up of pressure are either too small or non-existent under the conditions of the experiment. Though perhaps more improbable, another possible reason may be that in applying Babbitt's equation the temperature difference across only a part of the thickness should be considered.

The experiments in which water was applied to the outer surface of the paint while the wood was kept dry were carried out to investigate whether the water

sorbed by the paint affected the strength of the bond between wood and paint. Browne (2) reports that certain paints absorb an amount of water more than one and one-half times the weight of linseed oil contained in the film, and that the surface area, if the film is free, may increase by as much as 50%. When the paint is attached to wood, this increase in area is prevented to some extent and this gives rise to stresses within the coating which he suggests may have a direct bearing on the phenomenon of blistering.

The data in Browne's paper (2) indicate that, in three days, paints of the type represented by No. 1 and No. 3 in the present experiment absorb more than 75% of the total water they are capable of absorbing. Maximum absorption, according to the data, may require between 15 and 30 days. It is possible, however, that actually much less water was absorbed in the present experiment, where the paint was in contact with water on one side only, than in the case of Browne's work where the films were free and were in contact with water on both sides. The data in the present investigation, although they show that water kept on the surface of the paint for three days did not markedly affect the strength of the bond between the wood and the paint, do not necessarily answer the question concerning the effect of water absorbed by the paint. The amount of water absorbed by the paint films was not determined. It may have been considerably less than 75% of the total possible in the case of a free film. Also, a moisture gradient in the paint film could result in very little water in the paint at the wood–paint interface. The effect of water absorbed by the paint on the strength of the bond between wood and paint requires further investigation.

It is possible that the blistering may be related to the great affinity of wood for water. In the process of swelling, it is believed that water molecules disrupt hydrogen bonds between hydroxyl groups on adjacent cellulose molecules, the water molecules themselves becoming attached to the hydroxyl groups. If the nature and strength of the bond between the wood and the paint are similar in kind and in magnitude to those of the hydrogen bonds mentioned above, then this bond may well be broken by the same mechanism.

Once the bond is broken, it is possible that the actual formation of a blister may be related to the degree of swelling of the paint, the tendency to blister decreasing as the degree of swelling decreases. This view is supported by the fact that paints No. 2 and No. 4, which did not blister when subjected to a temperature gradient, were found to have a low degree of swelling.

CONCLUSIONS

In the case of paint blistering in the presence of moisture, it appears that the primary function of the temperature gradient is to bring the water to the wood–paint interface.

With certain paints, water is able to break or weaken the bond between the paint and the wood with the result that the paint blisters. Even in the case of those paints which did not blister when subjected to a temperature gradient, water was found to have weakened the bond.

ACKNOWLEDGMENTS

The writers appreciated the assistance of Mr. John Harris in selecting and preparing the paints, the assistance of Mr. P. J. Barrette in collecting the data, and the assistance of Mr. H. F. Slade in constructing the apparatus.

REFERENCES

1. BABBITT, J. D. Can. J. Technol. 32: 49–54. 1954.
2. BROWNE, F. L. J. Forest Products Research Soc. 3 (No. 5): 108–124. 1953.
3. DUNN, E. J. Conference Report No. 4, U.S. Building Research Advisory Board. 1952. pp. 38–45.
4. HOPKINS, C. Y. and SMART, B. C. Chemistry in Can. 5 (No. 9): 35(183)–40(188). 1953.

CALCULATED PATTERNS OF CIRCUMFERENTIAL SLOTS ON A CIRCULAR CONDUCTING CYLINDER[1]

By J. R. Wait and S. Kahana

ABSTRACT

Extensive computations are presented for the radiated fields of thin half-wave circumferential slots cut on a circular conducting cylinder of infinite length.

INTRODUCTION

Slotted cylinder antennas are becoming extensively utilized in microwave radiating systems. The patterns are usually calculated on the assumption that the tangential electric field in the slot is a prescribed function and the cylinder is of infinite length (1–6). The present paper deals with a narrow half-wave slot in the circumferential direction. In this case the field in the slot has an axial component only. This particular configuration has been treated by Papas (2, 3) who calculated patterns for the axial component of the radiated field by an application of the scalar Green's theorem. The results given here extend those of Papas and include patterns for the cross-polarized component of the radiation field. The case of two diametrically opposed slots is also considered.

METHOD

The cylinder of radius a containing the circumferential slot is shown in Fig. 1. With respect to a cylindrical polar co-ordinate system (ρ, ϕ, z), the slot extends from $\phi = (\pi/2)-(\pi/2ka)$ to $(\pi/2)+(\pi/2ka)$ along the circumference of the cylinder at $\rho = a$, $z = 0$. Since the slot is assumed to be thin the voltage distribution along the slot is cosinusoidal. The radiation fields expressed in terms of spherical polar co-ordinates (R, θ, ϕ) are then given by (1, 4, 6)

$$E_\theta = \frac{e^{-ikR}}{R} V P_\theta(\theta, \phi) e^{i\omega t} \tag{1}$$

and

$$E_\phi = \frac{e^{-ikR}}{R} V P_\phi(\theta, \phi) e^{i\omega t} \tag{2}$$

where V is the effective voltage at the center of the slot, $k = 2\pi/\text{wave length}$, and $\omega = \text{angular frequency}$;

$$P_\theta(\theta, \phi) = \sum_{m=0}^{\infty} \epsilon_m \frac{ka}{\pi^2 \sin\theta} \frac{e^{i(m-1)\pi/2}}{H_m^{(2)}(ka \sin\theta)} \frac{\cos(m\pi/2ka) \cos m(\phi - \frac{1}{2}\pi)}{[(ka)^2 - m^2]}, \tag{3}$$

$$P_\phi(\theta, \phi) = \sum_{m=1}^{\infty} 2 \frac{\cos\theta}{\pi^2 \sin^2\theta} \frac{e^{i(m-1)\pi/2}}{H_m^{(2)\prime}(ka \sin\theta)} \frac{m \cos(m\pi/2ka) \sin m(\phi - \frac{1}{2}\pi)}{[(ka)^2 - m^2]}, \tag{4}$$

[1]*Manuscript received September 27, 1954.*
Contribution from Radio Physics Laboratory, Defence Research Board, Ottawa, Canada.

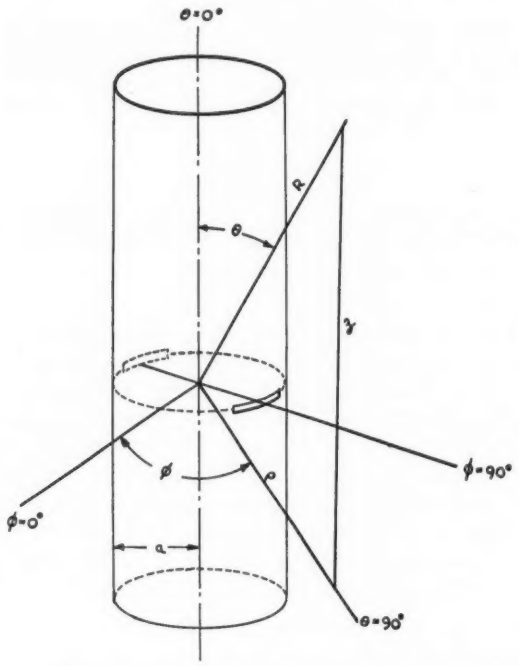

FIG. 1. Co-ordinate system for the circular conducting cylinder.

where $\epsilon_0 = 1$, $\epsilon_m = 2$ for $m \neq 0$,

$H_m^{(2)}(x)$ is the Hankel function of the second type of order m,

and $H_m^{(2)\prime}(x) = dH_m^{(2)}(x)/dx$.

The functions P_θ and P_ϕ can be called the pattern functions and they are proportional to the θ and ϕ components of the radiation field for a thin half-wave circumferential slot. These results can be extended easily to a pair of slots opposed diametrically on the surface of the cylinder as indicated in Fig. 1. When the slots are fed in antiphase the corresponding pattern function for the dual slots are given by

[5] $$P'_\theta(\theta, \phi) = P_\theta(\theta, \phi) - P_\theta(\theta, \phi + \pi),$$

[6] $$P'_\phi(\theta, \phi) = P_\phi(\theta, \phi) - P_\phi(\theta, \phi + \pi).$$

The magnitude and phase of the pattern functions have been computed and are listed in Tables I to IV. For convenience the cylinder with the single slot, excited by a voltage V, is donated as Case A and the same cylinder with the two opposing slots, excited by voltages V and $-V$, is denoted as Case B. It should be noted that P'_θ and P'_ϕ can be computed either from equations [5]

and [6] using the computed results for P_θ and P_ϕ or by summing the appropriate infinite series directly[2]. The latter method provides a good check on the computations.

RESULTS

To illustrate the nature of the results, the quantities $|P_\theta|^2$, $|P_\phi|^2$, $|P'_\theta|^2$, and $|P'_\phi|^2$ are plotted as a function of ϕ in Figs. 2 to 23 for various values of ka.

It can be seen that in all cases the cross-polarized radiated field proportional to P_ϕ is zero in the equatorial plane of the slot ($\theta = 90°$). For all other angles, however, the field is elliptically polarized. The patterns plotted in this form lend themselves readily to the calculation of the power radiated in a given direction (θ, ϕ) from the slot. For example, the time average power flux S is given by

[7] $$S = \tfrac{1}{2} \text{ real part of } [\mathbf{E} \times \mathbf{H}^*]_R$$

which in the far field is simply given by

[8] $$S = \frac{1}{240\pi} [|E_\theta|^2 + |E_\phi|^2],$$

[9] $$S = \frac{V^2}{240\pi R^2} [|P_\theta|^2 + |P_\phi|^2].$$

The power radiated as a function of θ and ϕ is then easily computed by adding the appropriate values of $|P_\theta|^2$ and $|P_\phi|^2$ in the figures.

ACKNOWLEDGMENT

We would like to thank Mr. E. Lowry for his assistance with the computations.

REFERENCES

1. BAILIN, L. L. Tech. Mem. No. 309. Hughes Aircraft Co., Culver City, Calif. July, 1953.
2. PAPAS, C. H. Cruft Lab. Tech. Rept., Harvard Univ. No. 61 (ONR. Contract N5-ori-76) Oct. 1948.
3. PAPAS, C. H. J. Math. and Phys. 28: 227–237. 1950.
4. SILVER, S. and SAUNDERS, W. K. J. Appl. Phys. 21: 153–159 and 745–749. 1950.
5. WAIT, J. R. Field produced by an arbitrary slot on an elliptic cylinder. Radio Phys. Project Rept. 19-0-8. June, 1954.
6. WAIT, J. R. and KAHANA, S. H. Can. J. Phys. 32: 714–721. 1954.

See pages 80–86 for Tables I–IV and 87–97 for Figs. 2–23.

[2]*The series formula for P'_θ and P'_ϕ is the same as equations [3] and [4] if cos $m(\phi - \pi/2)$ is replaced by 2 sin $m\phi$ sin $m\pi/2$ and if sin $m(\phi - \pi/2)$ is replaced by -2 cos $m\phi$ sin $m\pi/2$. The summation is then over the odd values of m only. This is a special case of a more general analysis (6) for slots radiating from cylindrical and wedge-shaped surfaces.*

NOTE: *Mr. R. Mittra of the Department of Electrical Engineering at the University of Toronto has recently checked some of these patterns by measurements at a wave length of 3 cm. This work will be reported at a later date.*

TABLE I

CASE A: $P_\theta = |P_\theta| e^{i \text{ phase } P_\theta}$

ka	θ (degrees)	ϕ (degrees)	$\lvert P_\theta \rvert$	Phase P_θ (degrees)
2	90.00	−90.00	0.14×10^{-2}	20.60
		−78.75	0.14	31.96
		−67.50	0.14	64.99
		−56.25	1.73	−254.39
		−45.00	3.00	−223.65
		−33.75	4.00	−185.47
		−22.75	5.48	−162.00
		−11.25	8.00	−109.27
		0.00	9.59	−105.82
		11.25	12.29×10^{-2}	− 90.03
		22.75	15.59	− 58.75
		33.75	19.44	− 39.91
		45.00	23.26	− 23.90
		56.25	26.73	− 10.38
		67.50	29.98	− 0.92
		78.75	31.75	4.77
		90.00	32.43	6.71
2	58.21	−90.00	1.87×10^{-2}	23.17
		−67.50	1.61	78.30
		−45.00	3.52	−212.61
		−22.50	6.62	−160.43
		0.00		
		22.50	17.33×10^{-2}	− 69.12
		45.00	24.58	− 37.51
		67.50	30.70	− 17.67
		90.00	33.16	− 10.90
2	30.00	−90.00	7.61×10^{-2}	85.25
		−67.50	6.32	−257.58
		−45.00	5.83	−194.78
		−22.50	11.62	−143.86
		22.50	24.92	− 93.81
		45.00	29.00	− 71.68
		67.50	32.06	− 55.96
		90.00	33.44	− 49.94
3	30.00	−90.00	2.51×10^{-2}	21.53
		−67.50	2.30	65.19
		−45.00	4.53	138.48
		−22.50	8.44	−170.26
		0.00	13.56	−121.81
		22.50	20.17	− 79.61
		45.00	27.13	− 47.29
		67.50	32.54	− 26.86
		90.00	34.73	− 19.78
3	3.82	−90.00	24.35×10^{-2}	−194.78
		−67.50	24.66	−189.62
		−45.00	26.21	−175.04
		−22.50	32.05	−156.91
		0.00	36.70	−140.51
		22.50	44.15	−128.95
		45.00	50.89	−119.24
		67.50	55.53	−114.08
		90.00	57.19	−112.37
5	90.00	−90.00	0.32×10^{-2}	1.64
		−78.75	0.89	89.74
		−67.50	0.45	−176.50
		−56.25	0.71	−111.66
		−45.00	1.10	− 27.93
		−33.75	1.98	38.75
		−22.50	3.15	110.45
		−11.25	4.69	−179.53
		11.25	9.72	− 49.75
		22.50	13.16	8.33
		33.75	17.32	60.06
		45.00	21.19	104.48
		56.25	25.46	150.47
		67.50	28.95	166.87
		78.75	31.36	184.56
		90.00	32.02	188.30

2	5.74	−90.00	24.50×10^{-2}	−192.90
		−67.50	24.74	−187.33
		−45.00	26.27	−173.50
		−22.50	30.17	−155.99
		22.50	43.68	−129.84
		45.00	50.30	−119.65
		67.50	54.86	−114.72
		90.00	56.49	−113.09
3	90.00	−90.00	0.32×10^{-2}	−179.02
		−78.75	0.55	− 94.11
		−67.50	0.71	− 19.76
		−56.25	1.37	31.05
		−45.00	2.61	84.94
		−33.75	2.93	120.73
		−22.50	4.22	167.18
		−11.25	5.97	−150.10
		0.00	8.46	−102.92
		11.25	11.01	− 71.15
		22.50	14.36	− 36.34
		33.75	18.19	− 5.79
		45.00	22.22	20.24
		56.25	26.11	41.34
		67.50	29.41	56.78
		78.75	31.58	66.07
		90.00	32.36	69.22
3	60.07	−90.00	1.00×10^{-2}	− 83.64
		−78.75	0.84	− 62.85
		−67.50	1.00	3.28
		−56.25	2.97	65.98
		−45.00	2.05	90.75
		−33.75	4.80	119.14
		−22.50	4.98	171.89
		−11.25	6.90	−140.95
		11.25	12.28	− 78.72
		22.50	15.68	− 47.83
		33.75	19.00	− 16.50
		45.00	23.35	1.40
		56.25	27.00	21.30
		67.50	30.02	34.93
		78.75	31.98	43.15
		90.00	32.68	45.94
5	66.93	−90.00	1.00×10^{-2}	65.30
		−67.50	2.23	3.92
		−45.00	1.27	2.26
		−22.50	3.48	118.70
		22.50	13.82	− 1.68
		45.00	21.40	87.37
		67.50	28.65	144.57
		78.75	31.45	160.36
		90.00	32.22	165.39
5	30.00	−90.00	1.22×10^{-2}	− 90.69
		−67.50	1.14	− 7.33
		−45.00	1.45	78.66
		−22.50	6.16	161.73
		22.50	17.94	− 54.75
		45.00	25.30	− 3.65
		67.50	31.48	32.23
		90.00	33.30	42.56

TABLE II

CASE A: $P_\phi = |P_\phi| e^{i \text{ phase } P_\phi}$

ka	θ (degrees)	ϕ (degrees)	$\lvert P_\phi \rvert$	Phase P_ϕ (degrees)
2	58.21	−90.00	0.00	
		−78.75	3.18×10^{-2}	−214.06
		−67.50	6.34	−207.98
		−56.25	7.56	−201.67
		−45.00	8.17	−188.09
		−33.75	8.16	−171.68
		−22.50	7.47	−145.57
		−11.25	8.09	−120.34
		11.25	9.69	− 73.80
		22.50	9.89	− 59.43
		33.75	9.96	− 43.05
		45.00	9.03	− 33.68
		56.25	7.42	− 22.35
		67.50	5.76	− 14.12
		78.75	2.74	− 11.26
		90.00	0.00	
2	30.00	−90.00	0.00	
		−78.75	5.81×10^{-2}	−161.21
		−67.50	10.84	−158.25
		−56.25	15.14	−154.18
		−45.00	18.04	−147.95
		−33.75	19.85	−140.66
		−22.50	20.52	−130.96
		−11.25	20.48	−120.61
		11.25	18.39	− 95.68
		22.50	16.88	− 83.50
		33.75	15.10	− 70.77
		45.00	13.08	− 60.44
		56.25	10.64	− 50.97
		67.50	7.49	− 44.99
		78.75	4.00	− 39.83
		90.00	0.00	
3	4.82	−90.00	0.00	
		−78.75	5.64×10^{-2}	−103.23
		−67.50	11.23	−102.34
		−56.25	16.68	−101.05
		−45.00	21.80	− 99.39
		−33.75	26.31	− 97.59
		−22.50	29.87	− 95.71
		−11.25	32.11	− 93.71
		11.25	32.05	− 89.80
		22.50	29.74	− 87.88
		33.75	26.15	− 86.04
		45.00	21.62	− 84.27
		56.25	16.50×10^{-2}	− 82.76
		67.50	11.09	− 81.52
		78.75	5.56	− 80.74
		90.00	0.00	
5	30.00	−90.00	0.00	
		−78.75	6.64×10^{-2}	63.50
		−67.50	11.20	71.63
		−56.25	12.61	87.75
		−45.00	11.73	117.10
		−33.75	11.80	161.45
		−22.50	14.75	−156.48
		−11.25	18.12	−124.18
		0.00	19.82	− 95.60
		11.25	19.76	− 66.82
		22.50	18.89	− 37.48
		33.75	17.78	− 10.02
		45.00	16.14	13.05
		56.25	13.47	30.73
		67.50	9.69	43.15
		78.75	5.06	50.53
		90.00	0.00	

2	5.74	−90.00	0.00	
		−78.75	6.02×10^{-2}	−100.97
		−67.50	11.80	−100.39
		−45.00	21.77	− 98.38
		−22.50	28.38	− 95.37
		22.50	28.28	− 88.25
		45.00	21.62	− 85.22
		67.50	11.70	− 83.18
		78.75	5.93	− 86.29
		90.00	0.00	
3	60.07	−90.00	0.00	
		−78.75	3.02×10^{-2}	72.92
		−67.50	5.62	84.16
		−56.25	6.14	−255.75
		−45.00	6.86	−224.13
		−33.75	8.26	−190.36
		−22.50	10.03	−161.94
		−11.25	10.97	−137.57
		11.25	8.89	− 85.72
		22.50	7.30	− 51.28
		33.75	6.58	− 14.09
		45.00	6.37	16.56
		56.25	5.80	37.88
		67.50	4.09	47.46
		78.75	2.43	59.56
		90.00	0.00	
3	30.03	−90.00	0.00	
		−78.75	0.11×10^{-2}	−205.88
		−67.50	11.35	−201.57
		−56.25	15.10	−194.23
		−45.00	17.32	−190.57
		−33.75	17.43	−167.97
		−22.50	16.99	−147.71
		−11.25	16.69	−123.57
		11.25	17.98	− 76.20
		22.50	18.48	− 57.70
		33.75	17.99	− 42.74
		45.00	17.48	− 36.95
		56.25	13.32	− 21.41
		67.50	9.43	− 14.66
		78.75	4.87	− 10.41
		90.00	0.00	
5	66.93	−90.00	0.00	
		−78.75	5.349×10^{-2}	−121.47
		−67.50	6.057	− 99.27
		−60.00	4.671	− 58.08
		−56.25	4.685	− 26.08
		−45.00	8.165	42.23
		−40.00	9.366	62.52
		−33.75	9.909	90.55
		−30.00	9.958	109.75
		−22.50	10.52	153.23
		−11.25	13.22	−145.07
		0.00	15.01	− 92.03
		11.25	15.63	− 38.82
		22.50	16.47	7.60
		30.00	16.60	42.47
		33.75	16.39	56.40
		40.00	15.67	78.33
		45.00	14.83	94.77
		56.25	12.33	127.23
		60.00	11.33	136.35
		67.50	9.023	151.23
		78.75	4.797	165.72
		90.00	0.00	

TABLE III

CASE B: $P'_\theta = |P'_\theta| e^{i \text{ phase } P'_\theta}$

ka	θ (degrees)	ϕ (degrees)	$\lvert P'_\theta \rvert$	Phase P'_θ (degrees)
2	90.00	11.25	9.80×10^{-2}	− 45.58
		22.50	17.75	− 41.57
		33.75	23.02	− 34.97
		45.00	25.90	− 25.31
		56.25	27.57	− 13.36
		67.50	29.21	− 3.04
		78.75	30.50	4.92
		90.00	30.97	5.15
2	58.21	11.25	10.15×10^{-2}	− 51.15
		22.50	18.68	− 48.39
		33.75	24.66	− 43.63
		45.00	28.08	− 36.90
		67.50	30.74	− 20.77
		90.00	31.61	− 12.77
2	30.00	22.50	19.75×10^{-2}	− 66.05
		45.00	32.56	− 62.95
		67.50	37.06	− 59.47
		90.00	39.37	− 57.80
2	8.63	22.50	21.59×10^{-2}	− 86.36
		45.00	39.48-	− 86.33
		67.50	51.06	− 86.29
		90.00	55.02	− 86.27
3	90.00	11.25	11.45×10^{-2}	− 40.51
		22.50	18.35	− 31.36
		33.75	20.05	− 12.50
		45.00	21.10	15.87
		56.25	26.08	40.17
		67.50	29.21	58.10
		78.75	31.65	66.11
		90.00	33.08	68.98
3	60.07	11.25	11.80×10^{-2}	− 45.17
		22.50	19.52	− 38.57
		33.75	22.69	− 24.94
		45.00	23.38	− 3.65
		56.25	25.55	19.30
		67.50	29.27	35.98
		78.75	32.54	44.56
		90.00	33.48	47.25
3	30.00	11.25	12.12×10^{-2}	− 58.80
		22.50	21.95	− 56.99
		33.75	28.09	− 53.69
		45.00	31.62	− 46.45
		56.25	32.59	− 38.73
		67.50	32.71	− 30.87
		78.75	32.77	− 25.06
		90.00	32.79	− 22.86
3	9.59	11.25	11.18×10^{-2}	− 81.36
		22.50	21.66	− 81.26
		33.75	30.89	− 81.10
		45.00	38.50	− 80.91
		56.25	44.30	− 80.71
		67.50	48.34	− 80.53
		78.75	50.71	− 80.42
		90.00	51.46	− 80.38

TABLE III (*Concl'd*)

ka	θ (degrees)	ϕ (degrees)	$\lvert P'_\theta \rvert$	Phase P'_θ (degrees)
5	90.00	11.25	13.19×10^{-2}	− 33.60
		22.50	14.56	− 4.06
		33.75	15.26	62.75
		45.00	22.22	106.62
		56.25	25.80	139.10
		67.50	28.21	168.14
		78.75	31.24	183.36
		90.00	32.40	188.77
5	59.91	11.25	14.00×10^{-2}	− 38.92
		22.50	17.13	− 18.35
		33.75	15.82	31.86
		45.00	22.10	78.79
		56.25	27.25	106.28
		67.50	28.97	126.51
		78.75	31.26	143.33
		90.00	32.05	148.69
		40.00	19.36	62.25
5	30.00	11.25	14.28×10^{-2}	− 52.44
		22.50	23.19	− 45.68
		33.75	25.32	− 31.99
		45.00	25.06	− 9.71
		56.25	26.63	29.10
		67.50	30.17	32.37
		78.75	33.13	41.36
		90.00	34.16	44.05
		40.00	25.24	− 20.54

TABLE IV

CASE B: $P'_\phi = \lvert P'_\phi \rvert e^{i \text{ phase } P'_\phi}$

ka	θ (degrees)	ϕ (degrees)	$\lvert P'_\phi \rvert$	Phase P'_ϕ (degrees)
2	58.21	0.00	17.90×10^{-2}	− 94.71
		11.25	16.35	− 94.84
		22.50	12.77	− 95.08
		33.75	8.02	− 95.65
		45.00	3.40	− 97.46
		56.25	0.17	178.90
		67.50	1.51	90.46
		78.75	1.27	88.64
		90.00	0.00	
2	30.00	0.00	39.13×10^{-2}	−108.63
		11.25	37.92	−108.86
		22.50	34.28	−109.67
		33.75	28.93	−111.02
		45.00	22.71	−112.85
		56.25	16.40	−114.98
		67.50	10.49	−117.09
		78.75	5.06	−118.68
		90.00	0.00	

TABLE IV (*Concl'd*)

ka	θ (degrees)	ϕ (degrees)	$\lvert P'_\phi \rvert$	Phase P'_ϕ (degrees)
2	8.63	0.00	61.54×10^{-2}	− 94.02
		22.50	56.55	− 94.03
		45.00	42.99	− 94.07
		67.50	23.02	− 94.11
		78.75	11.71	− 94.12
		90.00	0.00	
3	60.07	0.00	20.88×10^{-2}	−113.56
		11.25	17.84	−114.63
		22.50	10.11	−119.44
		33.75	1.76	−176.27
		45.00	6.71	79.53
		56.25	10.01	72.17
		67.50	9.22	68.84
		78.75	5.39	66.97
		90.00		
3	30.00	0.00	34.25×10^{-2}	− 98.56
		11.25	31.75	− 98.96
		22.50	25.08	−100.33
		33.75	16.30	−103.61
		45.00	7.94	−112.57
		56.25	2.51	−152.56
		67.50	2.30	−231.02
		78.75	1.89	−248.19
		90.00	0.00	
3	9.59	0.00	62.84×10^{-2}	−100.05
		11.25	61.40	−100.09
		22.50	57.22	−100.19
		33.75	50.70	−100.36
		45.00	42.31	−100.56
		56.25	32.60	−100.77
		67.50	22.09	−100.95
		78.75	11.14	101.08
		90.00	0.00	
5	59.32	0.00	19.85×10^{-2}	− 91.83
		10.00	13.56	− 87.68
		11.25	11.13	− 86.00
		20.00	3.217	7.97
		22.50	5.504	45.95
		30.00	13.20	66.78
		33.75	15.35	69.35
		45.00	13.94	74.07
		56.25	6.038	89.17
		67.50	2.875	−177.68
		78.75	3.254	−148.67
		90.00	0.00	
5	30.00	0.00	39.64×10^{-2}	− 95.60
		11.25	33.25	− 94.15
		22.25	17.45	− 85.20
		33.75	6.353	5.97
		45.00	17.49	53.62
		56.25	22.92	58.22
		67.50	20.25	58.45
		78.75	11.62	57.90
		90.00	0.00	

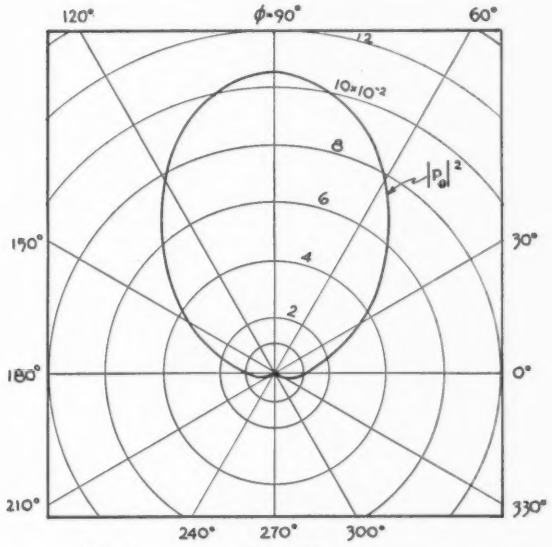

FIG. 2 CASE A
ka = 2
θ = 90°

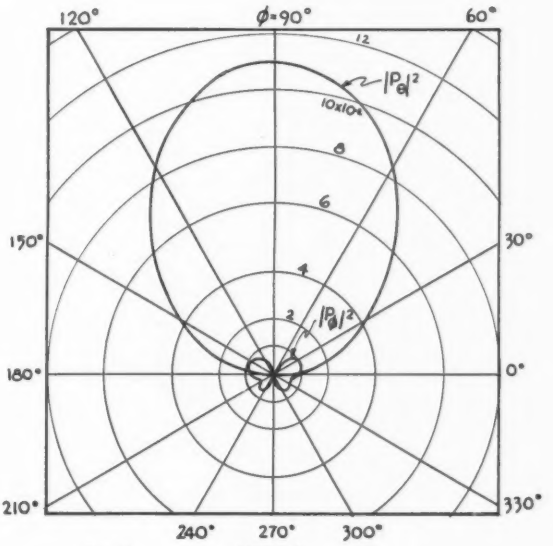

FIG. 3 CASE A
ka=2
θ=78.21°

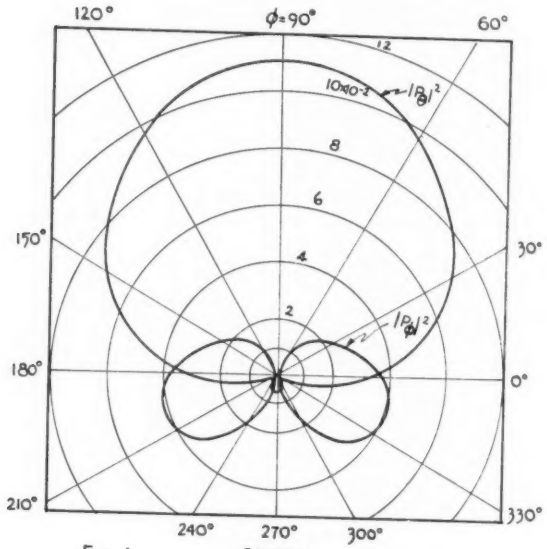

FIG. 4 CASE A
ka=2
θ=30°

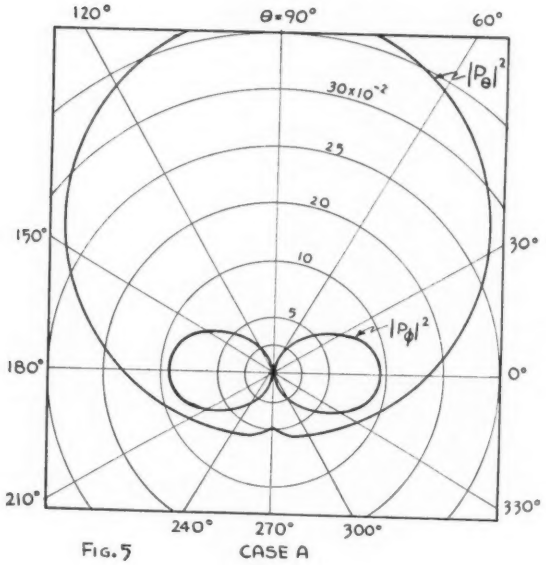

FIG. 5 CASE A
ka=2
θ=5.74°

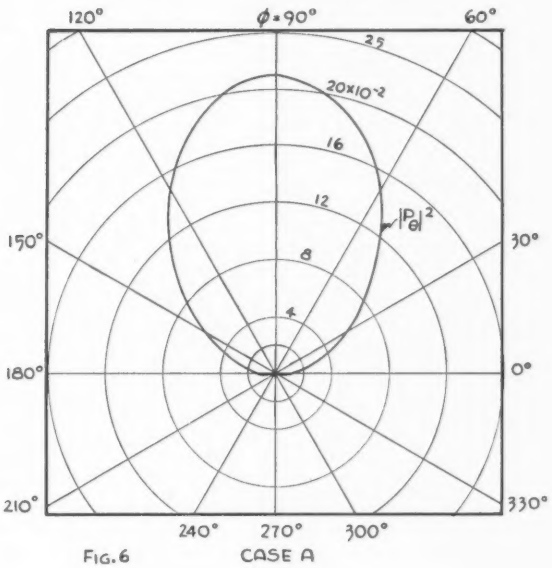

FIG. 6 CASE A
ka=3
θ=90°

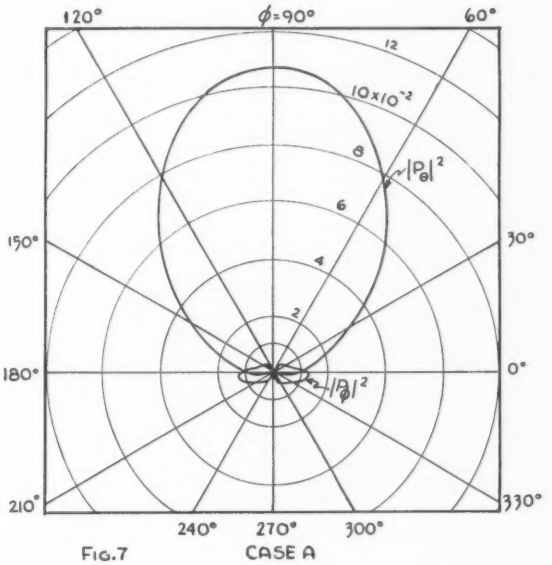

FIG. 7 CASE A
ka=3
θ=60.07°

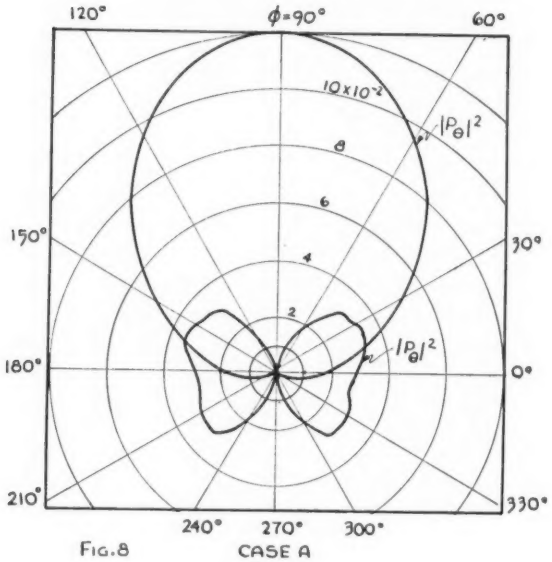

FIG. 8 CASE A
ka=3
θ=30°

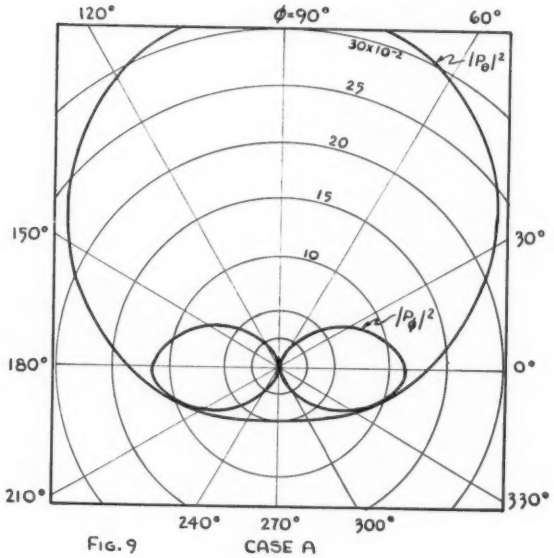

FIG. 9 CASE A
ka=3
θ=3.82°

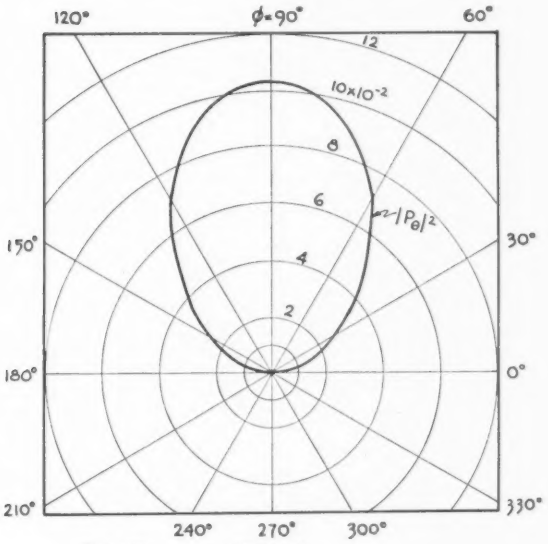

FIG. 10 CASE A
ka=7
θ=90°

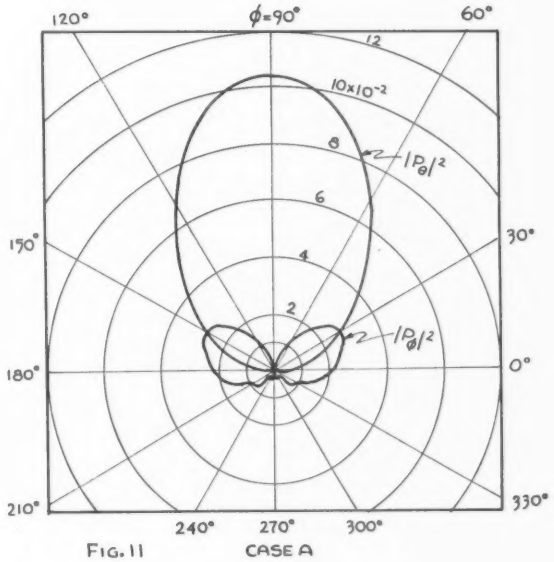

FIG. 11 CASE A
ka=7
θ=66.93°

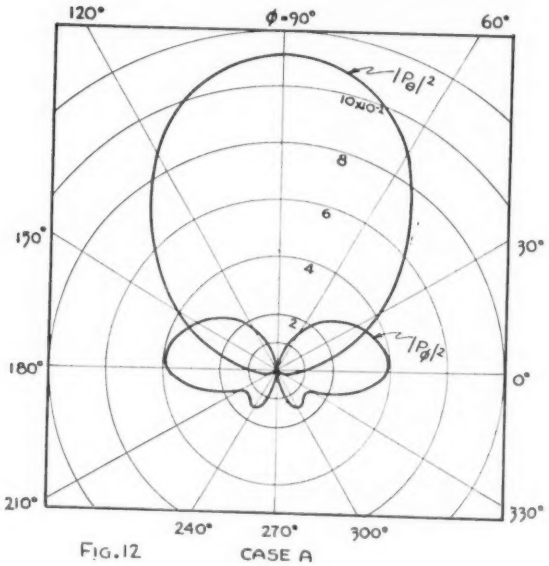

FIG. 12 CASE A
ka=5
θ=30°

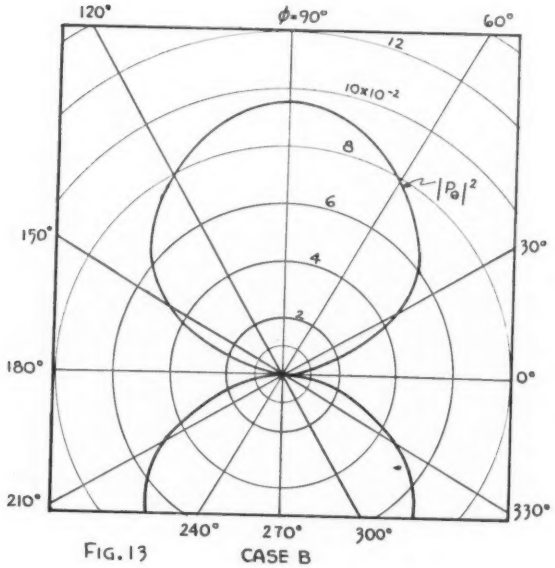

FIG. 13 CASE B
ka=2
θ=90°

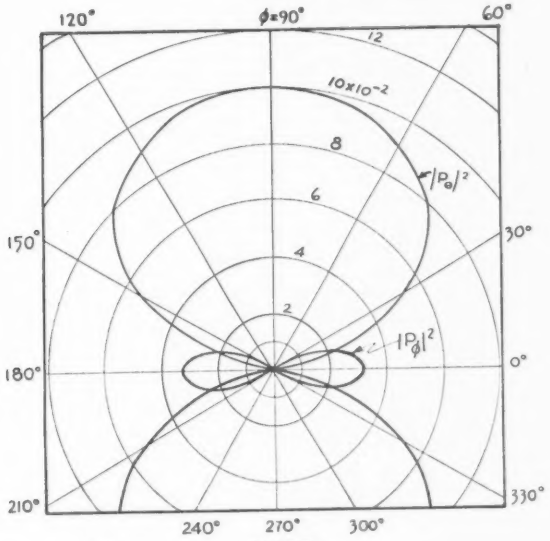

FIG. 14 CASE B
ka = 2
θ = 58.21°

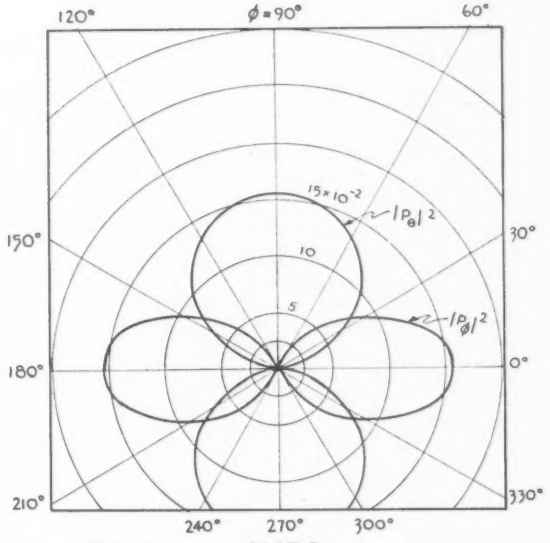

FIG. 15 CASE B
ka = 2
θ = 30°

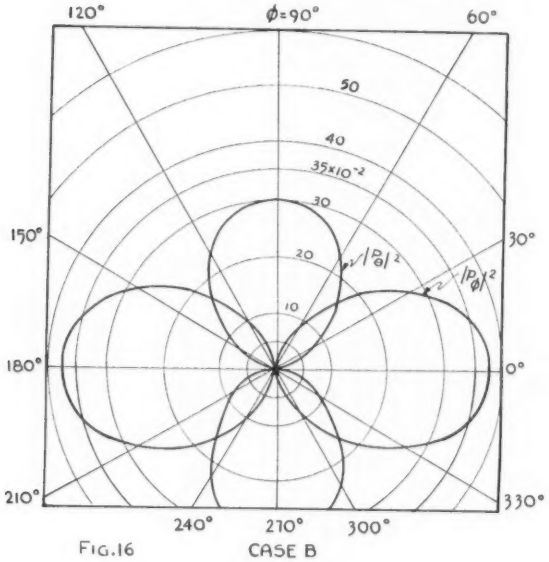

FIG.16 CASE B
ka=2
θ=8·57°

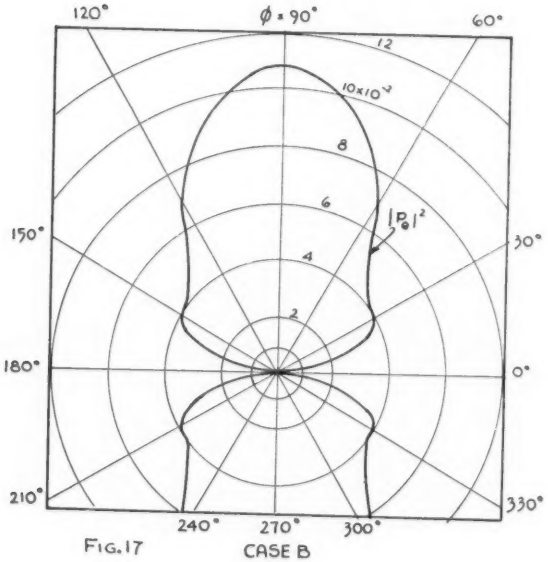

FIG.17 CASE B
ka=3
θ=90°

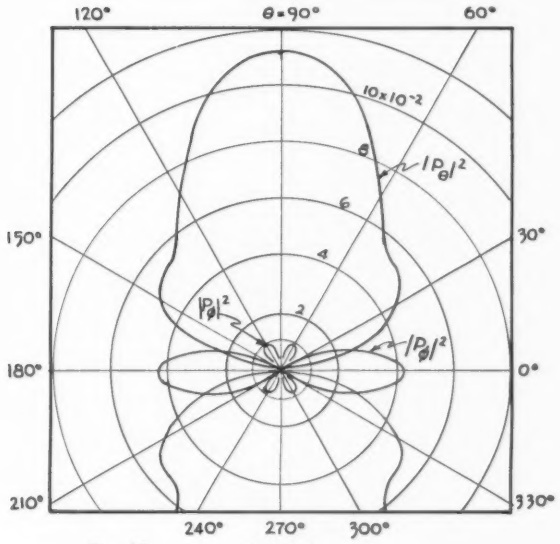

FIG. 18 CASE B
$ka = 3$
$\theta = 60.07°$

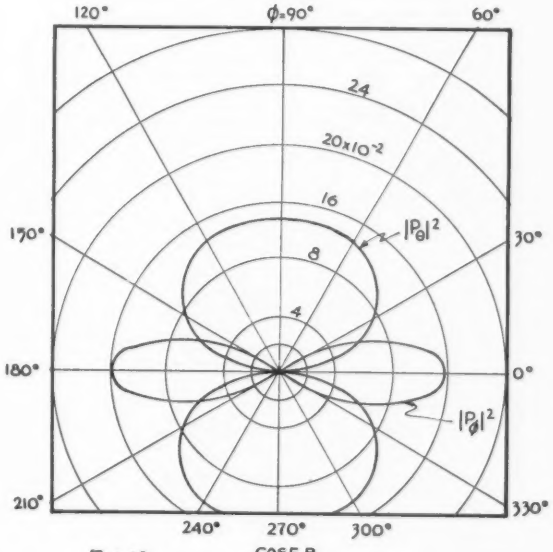

FIG. 19 CASE B
$ka = 3$
$\theta = 30°$

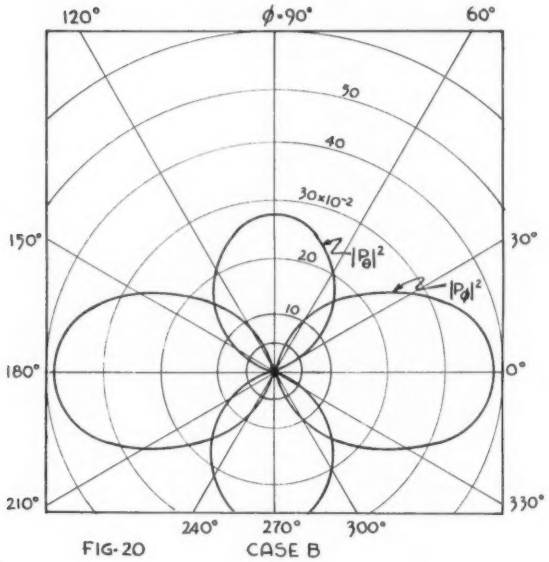

FIG. 20 CASE B

Ra=3
θ=9.59°

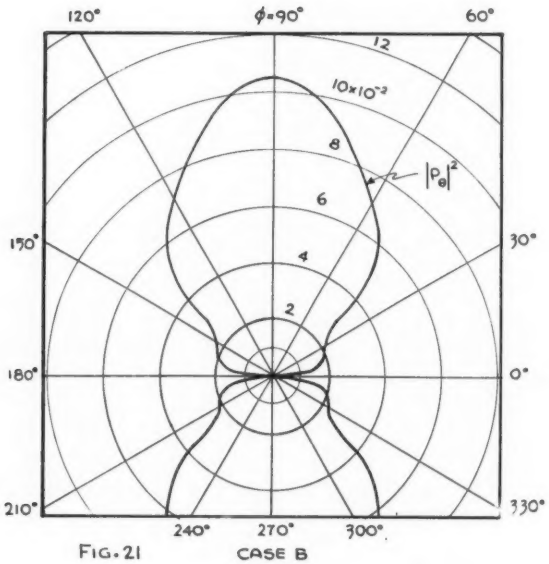

FIG. 21 CASE B

Ra=5
θ=90°

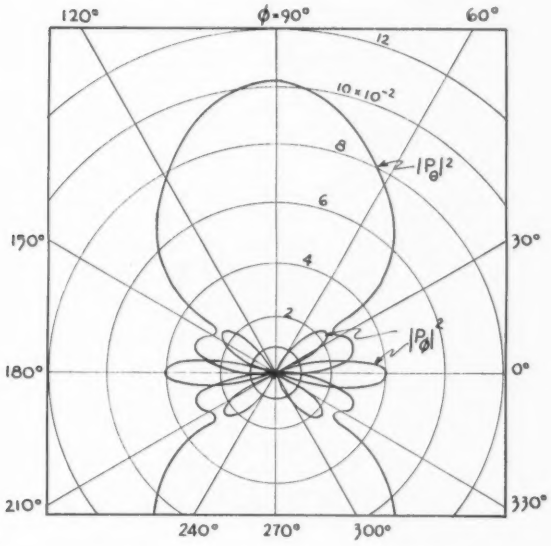

FIG. 22 CASE B
ka=5
θ=59.91°

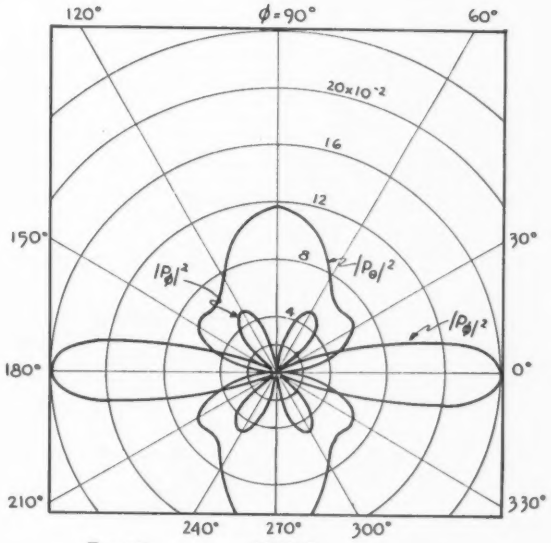

FIG. 23 CASE B
ka=5
θ=30°

PROMOTERS FOR THE REACTION OF RUBBER WITH CARBON BLACK[1]

By Kenneth W. Doak, George H. Ganzhorn, and Bernard C. Barton

ABSTRACT

Heating unvulcanized mixtures of rubber and carbon black gives increased electrical resistivity, reduced hysteresis and hardness, higher modulus, and increased abrasion resistance to the vulcanizate. This is believed to result from improved dispersion of carbon black, accompanying a chemical reaction between rubber and carbon black. Butyl rubber, with low unsaturation, reacts more slowly than Hevea rubber or butadiene–styrene copolymers (GR-S). Chemical promoters decrease the time and temperature required for the reaction. Certain quinones and aromatic nitroso compounds are effective in both Hevea and Butyl rubber. *t*-Butyl perbenzoate and cumene hydroperoxide are particularly effective in Hevea rubber and GR-S containing channel black, and when used in optimum amounts do not adversely affect tensile strength. Hexachlorocyclopentadiene and hexachlorophenol are effective in both Hevea and Butyl rubber. 1,3-Dichloro-5,5-dimethylhydantoin and hexachlorocyclopentadiene are effective in Butyl containing channel or furnace blacks. Chemical promoters are believed to initiate allylic or alkyl radicals on rubber chains, which react with active centers on carbon black, forming primary valence bonds.

INTRODUCTION: HEAT TREATMENT OF RUBBER AND CARBON BLACK IN ABSENCE OF PROMOTERS

It was discovered by Gerke *et al.* (25) and by Bradley (11) that heat treating an unvulcanized mixture of Hevea rubber and carbon black, with simultaneous or subsequent mastication, changed the physical properties of the resulting vulcanizate. The heat treated stock has increased electrical resistivity, reduced torsional hysteresis and durometer hardness, higher modulus at large deformations, and increased abrasion resistance. Heating times of 10–60 min. in the range 300–375°F. were required to obtain an extensive treatment. Typical results obtained with a mixture of Hevea rubber and channel (MPC) black are shown in Table I. Heat treatment of Hevea rubber containing 75 parts of

TABLE I

Effect of heat treatment (350°F.) of mixture of Hevea rubber and 50 parts of channel (MPC) black

Time, minutes	Log R*	T. hyst.† 280°F.	Shore durometer	300% stress
0	6.8	0.181	65	1500
3	8.2	0.093	62	1700
6	8.8	0.088	62	1725
12	11.4	0.062	60	1800
30	>13.0	0.052	58	1875

**Resistivity.*
†Torsional hysteresis.

[1]*Manuscript received September 27, 1954.*
Contribution No. 139 from the General Laboratories of the United States Rubber Company. Presented at the Canadian Institute of Chemistry, Toronto, Ontario, June 23, 1954.

black was carried out at 350°F. in a laboratory Banbury. Prior to vulcanization, additional Hevea rubber was added to give a concentration of 50 parts of black.

A mixture of Butyl rubber (GR-I) and carbon black (7, 26) also responds to heat treatment, giving similar changes in physical properties. Butadiene–styrene copolymers (GR-S) also respond to heat treatment (12). Butyl rubber, because of its low unsaturation, requires higher temperatures or longer times than Hevea rubber or GR-S. The relative reactivities can be demonstrated by a comparison of the electrical resistivities of stocks which received different times of heating at 375°F. prior to vulcanization. Table II shows the logarithm

TABLE II

EFFECT OF HEAT TREATMENT (375°F.) ON RESISTIVITY (R) OF MIXTURES OF RUBBERS AND 50 PARTS OF CHANNEL (MPC) BLACK

Time, minutes	Log R				
	Hevea	Hevea†	GR-S	GR-I-15	GR-I-25
0*	6.9	6.9	7.4	5.6	5.6
4	10.4	9.6	—	—	—
8	>13.0	11.6	12.8	—	—
15	>13.0	>13.0	>13.0	—	—
30	—	—	—	6.9	7.8
60	—	—	—	8.6	11.0
120	—	—	—	>13.0	>13.0

**At zero time log R of conventionally prepared masterbatch, prior to heat treatment, is given.*
†1.5 parts of commercial antioxidant, BLE, was added prior to heat treatment.

of resistivities (in ohm centimeters) for Hevea rubber, GR-S (containing 23.5% styrene, polymerized at 41°F.), and two types of Butyl rubber, which differ in the amount of unsaturation, GR-I-25 having higher unsaturation than GR-I-15. All stocks contained 50 parts of a medium processing channel (MPC) black. The heat treatment was carried out in a laboratory Banbury mixer.

Hevea rubber and GR-S, which are highly unsaturated, respond to the heat treatment many times more rapidly than Butyl rubber. The presence of the amine antioxidant BLE appears to retard the process slightly in Hevea rubber. GR-I-25 is somewhat more reactive than GR-I-15, because of its higher unsaturation. With Butyl rubber, as well as with Hevea, increases in log resistivity are paralleled by decreases in torsional hysteresis. Mixtures of carbon black and Vistanex, which contain no unsaturation, do not have their resistivity changed by heat treatment (7).

EFFECT OF CHEMICAL PROMOTERS ON THE HEAT TREATMENT OF HEVEA OR BUTYL RUBBER AND CARBON BLACK

Several chemicals have been reported to decrease the time or temperature required to give an extensive treatment. Howland (28, 29) used small amounts of quinones, such as *p*-quinone dioxime, and aromatic nitroso compounds, such as *p*-nitrosodiphenylamine and *p*-nitrosodimethylaniline, in Hevea rubber

containing carbon black. Some of the promoters described in Howland's patents were used by Gessler and Ford (27) in mixtures of Butyl rubber and carbon black. Thus, *p*-dinitrosobenzene (commercially known as Polyac) and *p*-quinone dioxime, as well as sulphur and certain sulphur bearing compounds were effective. Howland also used certain diprimary amines, such as *p,p'*-diaminodiphenylmethane (commercially known as Tonox) and benzidine (30). Gerke used hydrazine (24) and urea (23), while Barton used tetrachloro-*p*-quinone (5).

Since short reaction times are desirable if the process is to be used commercially, a study has been made of the relative effectiveness of a large number of chemical promoters. This included some previously reported ones, as well as many new ones for Hevea rubber, GR-S, or Butyl rubber.

The effect of several previously reported promoters in a mixture of Hevea rubber and channel (MPC) black is shown in Table III. In all experiments, a black masterbatch, containing 50 parts of black and five parts of stearic acid,

TABLE III

COMPARISON OF PROMOTERS IN MIXTURE OF HEVEA RUBBER AND 50 PARTS OF CHANNEL (MPC) BLACK*

Promoter†	Time, minutes	Log R	T. hyst. 280°F.
None	20	8.4	0.115
None	120	>13.0	0.068
p-Nitrosodiphenylamine	20	>13.0	0.057
p-Quinone dioxime	20	>13.0	0.050
p-Nitrosodimethylaniline	20	>13.0	0.060
Tetrachloro-*p*-quinone	20	>13.0	0.071
Tetrachloro-*p*-quinone	120	>13.0	0.061

**Heat treatment was static, in open steam at 300°F.*
†0.005 moles per 100 parts of rubber.

was prepared in a conventional manner. The promoters were mixed into the black masterbatch on a mill. Heat treatment was carried out statically in open steam at 300°F. The stocks were then remilled and compounded in a normal manner. Resistivity and torsional hysteresis were measured as previously described (7, 25).

The most reactive compounds are *p*-quinone dioxime and the aromatic nitroso compounds, *p*-nitrosodiphenylamine, and *p*-nitrosodimethylaniline. Tetrachloro-*p*-quinone is slightly less effective, but in 20 min. gives a result about equivalent to 120 min. in absence of a promoter.

The effect of concentration of one promoter, *p*-nitrosodimethylaniline, and time of treatment are shown graphically in Fig. 1. The heat treatment was carried out at 300°F. in a laboratory Banbury mixer for various times up to 20 min. Acceleration was adjusted to compensate for the activating effect of the promoter. As expected, the higher concentration, 1.25 parts per 100 parts of rubber, gives a faster reduction of torsional hysteresis, but after 20 min. treatment shows little advantage over 0.50 parts.

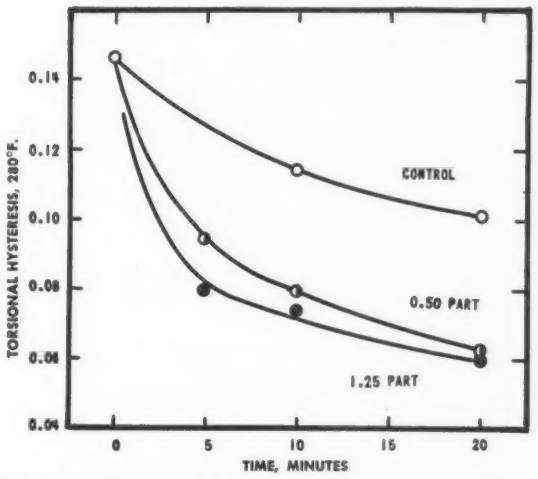

FIG. 1. Effect of *p*-nitrosodimethylaniline on heat treatment of Hevea rubber and 50 parts MPC black, in Banbury at 300°F.

Several promoters were compared in Butyl rubber (GR-I-15) containing 50 parts of channel (MPC) black and three parts of stearic acid. The promoters were mixed into the masterbatch on a mill, followed by heat treatment in the Banbury for 15 min. at 375°F. The higher temperature was used because of the relatively low reactivity of Butyl rubber. The results are shown in Table IV.

Both *p*-quinone dioxime and *p*-dinitrosobenzene are very effective. Tetrachloro-*p*-quinone is less reactive in GR-I-15. Although it increased log resistivity to 9.2 there was only a small effect on torsional hysteresis. In GR-I-25, however, it showed a larger change in log resistivity, and a characteristic reduction in torsional hysteresis. Thus, the increased unsaturation increases the reactivity of the system in the presence of promoters as well as in their absence.

TABLE IV

EFFECT OF PROMOTERS ON HEAT TREATMENT (375°F.) OF MIXTURE OF GR-I-15 AND 50 PARTS OF CHANNEL (MPC) BLACK*

Promoter	Time, minutes	Parts	Log R	T. hyst. 280°F.
None	0	—	5.6	0.300
None	15	—	6.7	0.165
p-Quinone dioxime	15	0.75	>13.0	0.065
Dinitrosobenzene (Polyac)	15	0.75	9.9	0.094
Dinitrosobenzene (Polyac)	15	1.5	>13.0	0.073
Tetrachloro-*p*-quinone	15	2.0	9.2	0.150
Tetrachloro-*p*-quinone†	15	2.0	>13.0	0.075

**Heat treatment in Banbury.*
†*In GR-I-25.*

EFFECT OF ORGANIC PEROXIDES ON HEAT TREATMENT OF MIXTURES OF HEVEA OR GR-S AND CARBON BLACK

Organic peroxides represent one of the most effective classes of promoters for Hevea rubber and butadiene–styrene copolymers (13). From a wide variety tested, *t*-butyl perbenzoate and cumene hydroperoxide (α,α-dimethylbenzyl hydroperoxide) are among the most effective.

The effect of *t*-butyl perbenzoate on a mixture of Hevea rubber and 50 parts of channel (MPC) black is shown in Table V. The peroxide was mixed into

TABLE V

EFFECT OF *t*-BUTYL PERBENZOATE ON MIXTURE OF HEVEA RUBBER AND 50 PARTS OF CHANNEL (MPC) BLACK*

Parts peroxide	ML-4 212°F.	Log R	T. hyst. 280°F.	Stress, 300%	Scott tensile
0.00	46	6.8	0.196	1525	3840
0.30	41	7.5	0.121	1650	3850
0.60	35	9.7	0.094	1800	3740
1.00	31	>13.0	0.055	1900	3530
1.60	29	>13.0	0.048	2000	2970

**Heat treatment, 5 min. at 300°F. on small mill, including control.*

the black masterbatch at a temperature below 225°F. The mixtures were then heated on a mill for five minutes, with a stock temperature of about 300°F., a time and temperature sufficient to decompose nearly all the peroxide. The control received the same heat treatment.

t-Butyl perbenzoate is extremely effective in increasing electrical resistivity and reducing torsional hysteresis. Modulus (300% stress) is progressively increased, while tensile strength is lowered less than 10% by the use of up to one part of peroxide. The stock properties thus are characteristic of the heat

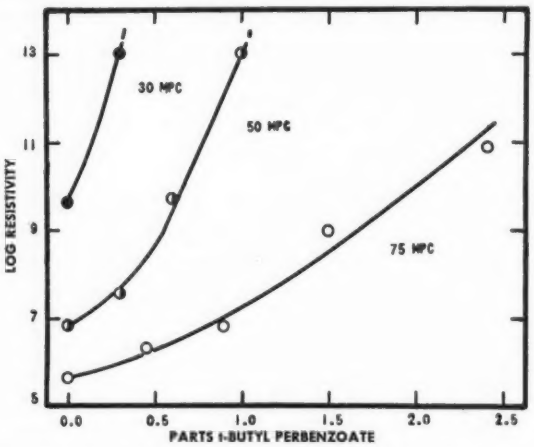

FIG. 2. Effect of *t*-butyl perbenzoate on electrical resistivity of Hevea rubber and MPC black, five minutes on mill at 300°F.

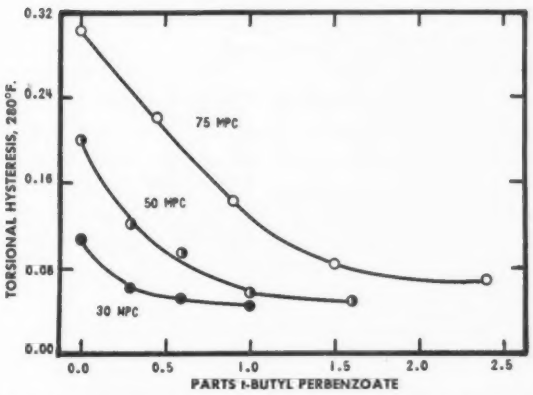

FIG. 3. Effect of *t*-butyl perbenzoate on torsional hysteresis of Hevea rubber and MPC black, five minutes on mill at 300°F.

treatment in the absence of a promoter. The peroxide progressively reduces the Mooney viscosity of the compounded stock prior to vulcanization. However, the values recorded in Table V were obtained on a laboratory mill, and are lower than normally obtained on large equipment.

The effect of *t*-butyl perbenzoate on log resistivity and torsional hysteresis of Hevea rubber containing 30, 50, and 75 parts of MPC black is shown in Figs. 2 and 3. The stock with 75 parts of black and no additional Hevea rubber has its torsional hysteresis reduced to a value less than half that normally obtained with a 50 part loading.

Peroxides are also very effective in butadiene–styrene copolymers such as GR-S containing 23.5% styrene, and polymerized at 41°F. Some representative results are shown in Table VI. In these experiments, cumene hydroperoxide was mixed into a black masterbatch, which was heat treated in a

TABLE VI

EFFECT OF CUMENE HYDROPEROXIDE ON MIXTURE OF GR-S AND 52 PARTS OF CHANNEL (MPC) BLACK*

Parts peroxide‡	ML-4 212°F.	Log R	T. hyst. 280°F.	Stress, 300%	Scott tensile	Abrasion resistance
None†	75	7.9	0.180	1100	2980	100
None	—	9.0	0.145	1275	—	—
0.6	77	10.6	0.107	1525	3130	115
1.0	81	11.4	0.102	1725	—	120
1.5	87	>13.0	0.092	1750	3050	125
2.0	92	>13.0	0.083	1925	2790	125
None§	77	11.6	0.099	1625	2900	120

**X-680 GR-S, a latex masterbatch, was used. The stocks contained six parts of hydrocarbon softener. Heat treatment was in Banbury with temperature rise from 275 to 325°F. in eight minutes.*

†Did not receive heat treatment.

‡Commercial sample, 72% peroxide.

§Heat treated for 10 min. at about 365°F.

laboratory Banbury mixer with a temperature rise from 275° to 325°F. in eight minutes. The stocks were all compounded with equivalent sulphur and accelerator level.

Cumene hydroperoxide thus increases electrical resistivity, reduces torsional hysteresis, increases stress at 300% elongation, and increases abrasion resistance; 1.0 part of cumene hydroperoxide under these conditions is about equivalent to a heat treatment of 10 min. at 365°F. Tensile strength is not reduced, except for the stock with 2.0 parts of peroxide. The peroxide causes some increase in the Mooney viscosity of the final compound, in contrast with the effect in Hevea rubber. The minimum torsional hysteresis is higher than that obtained with Hevea rubber.

EFFECT OF ACTIVE HALOGEN COMPOUNDS ON HEAT TREATMENT OF RUBBER AND CARBON BLACK

A number of active halogen compounds have been found to promote the heat treatment of rubber and carbon black. Among these are hexachlorocyclopentadiene (14), hexachlorophenol (6), and N-halogenated imides (14). Typical results obtained in Hevea rubber containing channel black are shown in Table VII. Hexachlorocyclopentadiene is very reactive at 300°F., while

TABLE VII

EFFECT OF ACTIVE HALOGEN COMPOUNDS ON MIXTURES OF HEVEA RUBBER AND 50 PARTS OF CHANNEL (MPC) BLACK*

Promoter	Parts	Log R	T. hyst. 280°F.	Stress, 300%
None	—	8.1	0.120	1500
Hexachlorocyclopentadiene	0.5	>13.0	0.061	1700
Hexachlorocyclopentadiene	1.0	>13.0	0.056	1775
Hexachlorocyclopentadiene	2.0	>13.0	0.050	1825
Hexachlorocyclopentadiene	2.7	>13.0	0.052	1950
Hexachlorophenol	0.5	9.0	0.098	1500
Hexachlorophenol	1.0	10.7	0.076	1625
Hexachlorophenol	2.0	12.6	0.063	1750
Hexachlorophenol	3.0	>13.0	0.048	1950
N-Chlorosuccinimide	1.20	9.8	0.101	1500
N-Bromosuccinimide	1.64	10.2	0.084	1500

**Heat treatment of all stocks was for 10 min. at 300°F. on mill.*

hexachlorophenol is less reactive as shown by changes in physical properties. Thus, 0.5 part of hexachlorocyclopentadiene is as effective as 2.0 parts of hexachlorophenol. N-Chloro- and N-bromosuccinimide are the least reactive. These chemicals are also effective in GR-S, although no data are presented at this time.

These active halogen compounds are also quite effective in GR-I-15 containing either channel or furnace blacks. Typical results obtained with different blacks are shown in Table VIII. Heat treatment was for 20 min. at 375°F. in a laboratory Banbury mixer.

TABLE VIII

EFFECT OF ACTIVE HALOGEN COMPOUNDS ON MIXTURES OF GR-I-15 AND 50 PARTS OF CARBON BLACK, 20 MIN. AT 375°F.

Promoter	Parts	ML-4 212°F.	Log R	T. hyst. 280°F.
Channel (MPC) Black				
None*	—	69	5.6	0.300
None†	—	64	6.9	0.170
Hexachlorocyclopentadiene	1.5	58	>13.0	0.055
Hexachlorophenol	1.5	51	>13.0	0.084
1,3-Dichloro-5,5-dimethylhydantoin	1.5	65	>13.0	0.062
N-Chlorosuccinimide	1.5	62	>13.0	0.077
N-Bromosuccinimide	1.5	57	>13.0	0.061
Dinitrosobenzene (Polyac)	1.5	66	>13.0	0.073
Furnace (HAF) Black				
None†	—	79	2.9	0.195
Hexachlorocyclopentadiene	2.0	—	>13.0	0.092
1,3-Dichloro-5,5-dimethylhydantoin	2.0	74	7.9	0.082
Furnace (ISAF) Black				
None†	—	86	2.7	0.255
Hexachlorocyclopentadiene	2.0	76	8.6	0.084
1,3-Dichloro-5,5-dimethylhydantoin	2.0	83	8.0	0.099

**No heat treatment.*
†Control received heat treatment of 20 min. at 375°F.

Hexachlorocyclopentadiene, 1,3-dichloro-5,5-dimethylhydantoin, and N-bromosuccinimide are the most reactive in channel (MPC) black stocks. Slightly less reactive (based on torsional hysteresis) are N-chlorosuccinimide and hexachlorophenol. A comparison of *p*-dinitrosobenzene (Polyac) with hexachlorocyclopentadiene and 1,3-dichloro-5,5-dimethylhydantoin at different temperatures is shown in Fig. 4. (Comparison is on equal weight basis.) The active halogen compounds are approximately equivalent in the tempera-

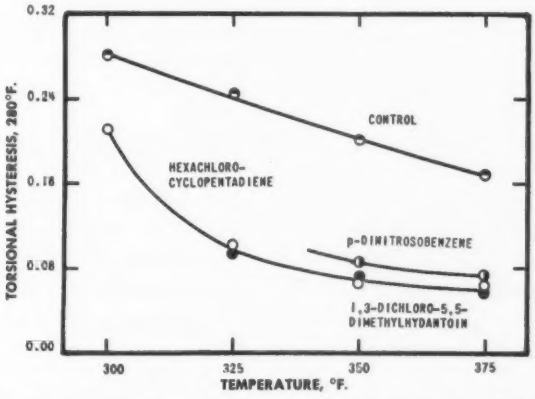

FIG. 4. Effect of promoters (1.5 parts) on torsional hysteresis of GR-I-15 and 50 parts MPC black, 20 min. in Banbury at various temperatures.

ture range 325–375°F., and appear to be slightly superior to *p*-dinitrosobenzene, although differences are small.

Both hexachlorocyclopentadiene and 1,3-dichloro-5,5-dimethylhydantoin are effective promoters for GR-I-15 containing high abrasion furnace (HAF) black and super abrasion furnace types (ISAF), also shown in Table VIII.

DISCUSSION: MECHANISM OF ACTION OF PROMOTERS

It has been suggested that the heat treatment of rubber and carbon black causes the formation of permanent chemical bonds between rubber chains and carbon black particles (7, 26, 36). Hevea rubber shows an over-all activation energy of about 18,000 calories, based on the rate of change of log resistivity (7). Butyl rubber shows an over-all activation energy of 16,000 calories, based on the increase of 300% stress (26). The rate depends on the degree of unsaturation of the rubber, and the amount of oxygen on the black (7, 47). The bound rubber content increases as the extent of the treatment increases. Although electron micrographs show no definite changes in dispersion of the carbon black (7), it has been suggested that the chemical bonding of rubber to carbon black particles, followed by mastication, improves the dispersion of carbon black sufficiently to give the marked changes in electrical resistivity and other properties (25, 34, 36).

The high efficiency of peroxides in promoting the process, and the apparent retardation by antioxidants (Table II), strongly suggests that a free radical reaction is involved. Presumably free radicals, R•, formed by decomposition of peroxides can attack α-methylene groups or double bonds in the rubber chains, forming allylic radicals A, as well as some alkyl radicals B, in a Hevea rubber chain (9, 10, 16, 18, 33).

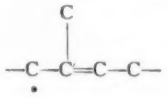

A

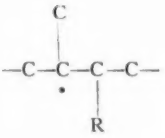

B

These radicals may undergo at least three reactions, depending on the environment:

1. Addition to a reactive center on the surface of the carbon black. Although the presence of hydroxyl, carboxyl, aldehyde, hydroperoxide, and carbonyl groups has been suggested (39, 44), the actual reaction site on the carbon black is unknown. The results of bromination reactions (40, 45) have suggested the presence of highly aromatic nuclei, to which a free radical can presumably add readily. It has been suggested that highly oxygenated blacks may have quinone groups on the surface, which are the reactive centers (7). There is evidence that free radicals can react with *p*-quinone, either by addition to oxygen or carbon (4).

2. Addition of a radical to a double bond, or coupling of two allylic radicals, to form carbon–carbon cross-links (1, 10, 15, 18, 41, 43).

3. Addition to oxygen, if present, starting an oxidation chain. Presumably alkenyl hydroperoxides such as C, will be the principal product, although there is evidence that alkyl peroxides may also be formed (9, 10, 17, 19, 33). Thermal decomposition of C is believed to break the —O—O— bond, followed by cleavage of the adjacent C—C bond, *a*, forming an allylic radical and an unsaturated aldehyde (22, 31, 43).

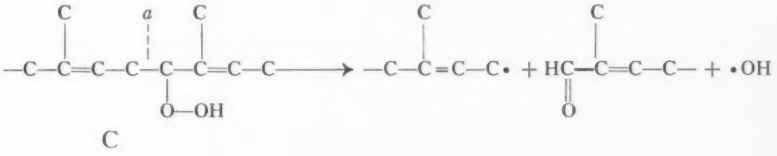

Such chain scission reactions occur readily in Hevea rubber, but less readily in butadiene–styrene copolymers.

The manner in which these different reactions compete will depend on both the molecular structure of the rubber and the reactivity of the black. Reaction of rubber free radicals with carbon black will be favored if the surface of the black is very reactive, as in the highly oxygenated channel blacks. They are thus more reactive in the heat treatment than furnace blacks, with lower oxygen content (7, 47). Channel black also suppresses gel formation during heating of GR-S (46) and retards oxidation of unvulcanized Hevea rubber and GR-S(32, 42) presumably because the carbon black competes with rubber chains for free radicals.

Peroxide treatment of Hevea rubber and carbon black causes an initial stiffening reaction, followed by fairly rapid chain scission, causing an abnormal viscosity reduction. In butadiene–styrene copolymers, cross-linking reactions compete more favorably with the carbon black reaction, and there is a viscosity increase. The different side reactions of Hevea rubber and butadiene–styrene copolymers presumably result because of the different structures of the free radicals formed on the polymer chain. Isoprene–styrene copolymers, although not reported in detail at this time, behave somewhat similarly to Hevea rubber.

N-halogenated imides conceivably can also form allylic radicals on a rubber chain, thus promoting the reaction with carbon black. Thus, N-chloro- and N-bromosuccinimide react with olefins, causing halogenation in the α-position (8, 48). Allylic radicals are believed to be formed as an intermediate. N-Bromosuccinimide and certain other active halogen compounds are known to accelerate the rate of oxidation of tetralin, apparently because they dissociate into free radicals (37).

The active halogen compounds hexachlorophenol and hexachlorocyclopentadiene conceivably can form free radicals by loss of a chlorine atom from a carbon atom adjacent to two double bonds, as in D and E. Such a chlorine atom should be quite active.

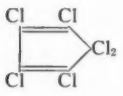

D

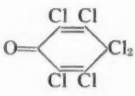

E

However, it has recently been shown that hexachlorocyclopentadiene adds to olefins (in the absence of carbon black) in a Diels-Alder reaction (20). This reaction apparently is not affected by free radicals, or phenolic inhibitors. This opens the possibility that there may also be an ionic mechanism in the reaction of rubber and carbon black.

An alternative mechanism is available for the bifunctional vulcanizing agents (21), such as *p*-dinitrosobenzene and tetrachloro-*p*-quinone. They may have one group bonded to a rubber chain and the other to a carbon black particle. When used in vulcanization at least part of these agents are chemically bonded to the rubber chain (15, 35). There is also some reduction to tetrachlorohydroquinone and *p*-quinone dioxime (3, 15, 35) suggesting that allylic rubber radicals are formed by loss of α-hydrogen atoms. *p*-Quinone dioxime may function similarly to *p*-dinitrosobenzene, since it is readily oxidized to *p*-dinitrosobenzene. Channel black renders it active, presumably because of oxygen on the surface (35).

Sulphur may also form a cross-link between rubber and carbon black (40). Sulphur is believed to cause the formation of allylic radicals in rubber (2, 15, 38), which might react with carbon black. However, there are insufficient data to decide whether these vulcanizing agents actually form cross-links between rubber and carbon black, or merely initiate rubber free radicals which then add to carbon black.

REFERENCES

1. Alfrey, T., Hendricks, J. C., Hershey, R. M., and Mark, H. F. India Rubber World, 112: 577. 1945.
2. Armstrong, R. T., Little, J. R., and Doak, K. W. Ind. Eng. Chem. 36: 628. 1944.
3. Arnold, R. T. and Collins, C. J. J. Am. Chem. Soc. 61: 1407. 1939.
4. Bartlett, P. D., Hammond, G. S., and Kwart, H. Discussions Faraday Soc. 2: 342. 1947.
5. Barton, B. C. U.S. Patent No. 2, 658,092. November, 1953.
6. Barton, B. C. U.S. Patent No. 2, 689,842. September, 1954.
7. Barton, B. C., Ganzhorn, G. H., and Smallwood, H. M. J. Polymer Sci. 12: 487. 1954.
8. Bloomfield, G. F. J. Chem. Soc. 114. 1944.
9. Bolland, J. R. and Gee, G. Trans. Faraday Soc. 42: 236, 244. 1946.
10. Braden, M., Fletcher, W. P., and McSweeney, G. P. Trans. Inst. Rubber Ind. 30: 44. 1954.
11. Bradley, H. P. U.S. Patent No. 2,239,659. April, 1941.
12. Dannenburg, E. M. Ind. Eng. Chem. 44: 813. 1952.
13. Doak, K. W. U.S. Patent No. 2,676,944. April, 1954.
14. Doak, K. W. U.S. Patents pending.
15. Farmer, E. H. Trans. Faraday Soc. 38: 340. 1942.
16. Farmer, E. H. Trans. Faraday Soc. 42: 228. 1946.
17. Farmer, E. H., Bloomfield, G. F., Sundralingam, A., and Sutton, D. A. Trans. Faraday Soc. 38: 348. 1942.
18. Farmer, E. H. and Moore, C. G. J. Chem. Soc. 131, 142, 149. 1951.
19. Farmer, E. H. and Sundralingam, A. J. Chem. Soc. 121. 1942.
20. Fields, E. K. J. Am. Chem. Soc. 76: 2709. 1954.
21. Fisher, H. L. Ind. Eng. Chem. 31: 1381. 1939.
22. George, P. and Walsh, A. D. Trans. Faraday Soc. 42: 94. 1946.

23. GERKE, R. H. U.S. Patent No. 2,315,849. April, 1943.
24. GERKE, R. H. U.S. Patent No. 2,315,850. April, 1943.
25. GERKE, R. H., GANZHORN, G. H., HOWLAND, L. H., and SMALLWOOD, H. M. U.S. Patent No. 2,118,601. May, 1938.
26. GESSLER, A. M. Rubber Age (N.Y.), 74: 59. 1953.
27. GESSLER, A. M. and FORD, F. P. Rubber Age (N.Y.), 74: 397. 1953.
28. HOWLAND, L. H. U.S. Patent No. 2,315,855. April, 1943.
29. HOWLAND, L. H. U.S. Patent No. 2,315,856. April, 1943.
30. HOWLAND, L. H. U.S. Patent No. 2,315,857. April, 1943.
31. KENDALL, C. E. Ind. Eng. Chem. 43: 452. 1951.
32. LYON, F., BURGESS, K. A., and SWEITZER, C. W. Boston Meeting of Rubber Division of Am. Chem. Soc. May, 1953.
33. MAREK, L. F. Ind. Eng. Chem. 45: 2006. 1953.
34. PARKINSON, D. and BLANCHARD, A. F. Trans. Inst. Rubber Ind. 23: 259. 1948.
35. REHNER, J., JR. and FLORY, P. J. Ind. Eng. Chem. 38: 500. 1946.
36. REHNER, J., JR. and GESSLER, A. M. Rubber Age (N.Y.), 74: 561. 1954.
37. ROBERTSON, A. and WATERS, W. A. J. Chem. Soc. 492. 1947.
38. SELKER, M. L. and KEMP, A. R. Ind. Eng. Chem. 36: 16. 1944.
39. SMITH, W. R. and SCHAEFFER, W. D. Proc. Rubber Technol. 2nd. Conf. 403. 1948.
40. STEARNS, R. S. and JOHNSON, B. L. Ind. Eng. Chem. 43: 146. 1951.
41. STURGIS, B. M., BAUM, A. A., and TREPAGNIER, J. H. Ind. Eng. Chem. 39: 64. 1947.
42. SWEITZER, C. W. and LYON, F. Ind. Eng. Chem. 44: 125. 1952.
43. TOBOLSKY, A. V. Discussions Faraday Soc. 2: 384. 1947.
44. VILLARS, D. S. J. Am. Chem. Soc. 69: 214. 1947; 70: 3655. 1948.
45. WATSON, J. W. and PARKINSON, D. Rubber Age (N.Y.), 73: 502. 1953.
46. WHITE, L. M., EBERS, E. S., SHRIVER, G. E., and BRECK, S. Ind. Eng. Chem. 37: 770. 1945.
47. ZAPP, R. L. and GESSLER, A. M. Rubber Age (N.Y.), 74: 243. 1953.
48. ZIEGLER, K., SPATH, A., SCHAAF, E., SCHUMANN, W., and WINKLEMANN, E. Ann. 551: 80. 1942.